Development and Assessment of a Coupling Force Measurement System Applied to Stationary and Vibrating Tool Handles

Mayank Kalra

A Thesis

in

The Department

of

Mechanical and Industrial Engineering

Presented in Partial Fulfillment of the Requirements

for The Degree of Masters of Applied Science (Mechanical Engineering) at

Concordia University

Montreal, Quebec, Canada

December 2014

CONCORDIA UNIVERSITY
School of Graduate Studies

This is to certify that the thesis prepared

By: Mayank Kalra

Entitled: Development and Assessment of a Coupling Force Measurement System Applied to Stationary and Vibrating Tool Handles

and submitted in partial fulfillment of the requirements for the degree of

Master of Applied Science (Mechanical Engineering)

complies with the regulations if the University and meets the accepted standards with respect to originality and quality.

Signed by the final examining committee:

_____ Chair
Dr. Muthukumaran Packirisamy

_____ Examiner
Dr. A.K. Waizuddin Ahmed

_____ Examiner
Dr. S. Samuel Li

_____ Supervisor
Dr. Subhash Rakheja

_____ Co-Supervisor
Dr. Pierre Marcotte

Approved by _____
Chair of Department

_____
Dean of Faculty

Date _____

ABSTRACT

Development and Assessment of a Coupling Force Measurement System Applied to Stationary and Vibrating Tool Handles

Mayank Kalra

Exposure to hand-transmitted vibration (HTV) arising from operating hand-held power tools has been associated with various health consequences. The magnitude of HTV is strongly affected by the hand-handle interface coupling forces, handle geometry and gripping method apart. Assessment of the HTV exposure currently does not incorporate the impact of coupling forces exerted at the hand-handle interface, mostly due to lack of reliable measurement methods for hand-handle interface forces. This dissertation seeks to develop a low cost hand-handle coupling force measurement system and methods for quantifying the hand grip and push forces applied to the tool handles.

A hand-handle interface force measurement system was developed using flexible force sensing resistors (FlexiForce). The static properties of the sensors were thoroughly characterized in terms of linearity, hysteresis and repeatability. Moreover, the sensors' output characteristics were observed by considering the effect of positioning, area and flexibility of the loading medium used to transmit the applied forces. Five different cylindrical and elliptical instrumented handles were subsequently chosen to observe the input-output characteristics of the sensors under stationary and vibrating conditions. The measurements under static and dynamic conditions revealed good linearity and repeatability of the sensors, and affirmed their feasibility for accurate estimations of the hand grip and push forces. The sensors' outputs also showed strong dependence on the loading medium's area, position and flexibility as well as the length of the sensor suggesting the need for individual sensor calibration, which was noted as the primary limitation of the system.

The effectiveness of the measurement system was further explored through measurements of hand forces on a percussion tool handle and biodynamic responses of the human hand-arm system. The measurement system provided reasonably good estimations of the hand grip and push forces when applied to the percussion tool handle under both stationary as well as vibration conditions. The biodynamic impedance responses measured with six subjects showed trends similar to the reference response. However, a compensation function was necessary and subsequently proposed to account for the limited bandwidth of the sensors.

ACKNOWLEDGEMENTS

I wish to extend my sincerest gratitude to my supervisors Dr. Subhash Rakheja and Dr. Pierre Marcotte. Dr. Rakheja accepted me as a research assistant during my undergraduate studies and since then has continually challenged me with numerous tasks. His constructive criticisms and guidance have helped me develop a niche critical and analytical thought process enhancing my research competencies. Dr. Marcotte has further aided my research experience by generously granting me access to his laboratory at the Institut de recherche Robert-Sauvé en Santé et en sécurité du travail (IRSST) and introducing me to several research practices and methods I was previously unaware of. His input on several techniques and methods during the formulation of my methodology was highly invaluable.

I wish to thank Dr. Krishna Dewangan for his assistance in my experimentation and analysis over the past two years. I would also like to thank Dr. Surajudeen Adewusi for his involvement and assistance during the biodynamic aspect of my research. Their combined experience in the field of hand-arm vibration transmission was a great asset. I would also like to thank my fellow graduate friends and colleagues for their assistance with my experimentation and analysis.

Finally, I wish to thank my parents, brother and extended family for their continuous support. They were inspirational from the application process through the defence.

TABLE OF CONTENTS

LIST OF FIGURES

LIST OF TABLES

CHAPTER 1
INTRODUCTION

1.1. GENERAL

Occupational exposure to hand-transmitted vibration (HTV) arising from operating hand-held power tools has been associated to syndromes such as hand-arm vibration syndrome (HAVS) and Raynaud's syndromes. These syndromes may result in with an array of adverse health effects including vascular, neurological and musculoskeletal disorders [1-3]. Moreover, Raynaud's phenomenon is impaired blood circulation in the fingers and palm as a result of prolonged vibration and/or cold exposure, commonly known as vibration white-finger (VWF) disease. HTV exposure is prevalent in numerous industrial sectors such as forestry, mining, construction and manufacturing and can occur in low as well as high levels of vibration frequencies. [4] attributed several factors which influence the physiological risks associated with HTV including: characteristics of the HTV, duration of exposure as well as physical individualities between exposed subjects. [5] identifies a dose-response relationship based on the magnitude of HTV and daily as well as cumulative exposure duration, as well as the probability of exposed individuals developing HAVS. The HTV exposure is measured in terms of frequency-weighted acceleration of the vibrating tool handle using the method described in [5]. However, in addition to the HTV magnitude, frequency and/or exposure, the health effects are further influenced by variables such as the coupling forces including grip and push forces, grip type and grip-force distributions, dynamic torque, handle geometry, and other inter-individual factors. The HTV exposure assessment guidelines defined in [5] only address the contribution of the vibration magnitude and frequency, while neglecting the other contributing factors. Moreover, the standard has been widely challenged with regards to the frequency weighting and lack of consideration of the hand-handle coupling forces and the working posture. Moreover, a few recent studies have presented

contradictory findings with regard to the injury risks obtained from guidelines and the epidemiological studies [5-7].

The hand-handle interface coupling forces permit the flow of vibration energy from the tool into the hand and are widely considered as a combination of grip and push forces. The coupling forces thus directly affect the severity of vibration transmitted to the operator's hand and arm [4, 8]. The coupling forces associated with the operation of vibrating tools generally consist of two components: (a) the static hand forces applied to control and guide the tool in order to achieve the desired productivity level [9]; and (b) the dynamic force arising from the biodynamic response of the hand-arm system. It has been shown that the HTV and the hand-arm biodynamic responses increase with the grip force [10-12]. Furthermore, an increase in grip force tends to compress the soft tissues of the hand and fingers leading to impaired blood flow in the fingers and increased risk of Raynaud's syndrome [13]. A few studies have proposed additional weighting functions to account for the strong effects of hand-handle interface forces on the exposure assessment [14-16]. Although the necessity of coupling forces on the quantification of hand-arm vibration exposure has been widely recognized; the measurement of hand coupling forces on vibrating tools have resulted in limited success primarily due to the lack of definite relationships between the static coupling forces and the HTV in addition to a lack of reliable field-measurement systems. [17] investigated the feasibility of the capacitive sensors (NOVEL EMED system) to measure the hand-handle coupling forces. These sensors along with their data acquisition and processing system are extremely costly and pose challenges with regard to field applications.

This dissertation seeks to examine the feasibility of a low-cost measurement system for acquiring hand coupling forces during the operation of a vibrating handle. The feasibility of the measurement system is explored for applications on simulated cylindrical and elliptical

instrumented handles in addition to a power tool handle. It needs to be noted that the mechanical impedance (MI) responses of the hand-arm system have also shown strong dependence of the hand-handle coupling forces [18-20]. Furthermore, the biodynamic responses of the hand-arm system are obtained by applying an inertial correction to account for the contribution of the handle inertia, which can cause substantial errors [21, 22]. The proposed low-cost measurement system would not require an inertial correction due to its low mass; thus, providing more accurate measurements of the biodynamic responses. The feasibility of the resistive sensors are hence also explored for measurement of mechanical impedance of the hand-arm system under a broadband vibration excitation.

1.2. Literature Review

1.2.1. Significance of Hand Forces

A number of studies have shown important effects of coupling forces exerted at the hand-handle interface on the hand-arm biodynamic responses and vibration power absorption [10, 23-25]. [16] suggested the use of a hand force coupling factor to account for the effect of the coupling force on the vibration dosage value of the hand-arm system based on measured frequency weighted acceleration levels. The study showed insignificant differences between the acute effects of the hand grip and push forces and recommended the coupling force. The proposed correction factor ranged from 0.6 to 1.2 for coupling forces ranging from 20 to 200 N. The grip, push, contact and coupling forces in the context of the hand forces applied to a handle were further defined by [9]. The push force imposed by the hand is defined as the sum of axial components of all distributed elements denoted as $F_{c,i}$, which is caused by the distributed pressure p_i over the contact area S_i as shown in Figure 1.1, such that [9]:

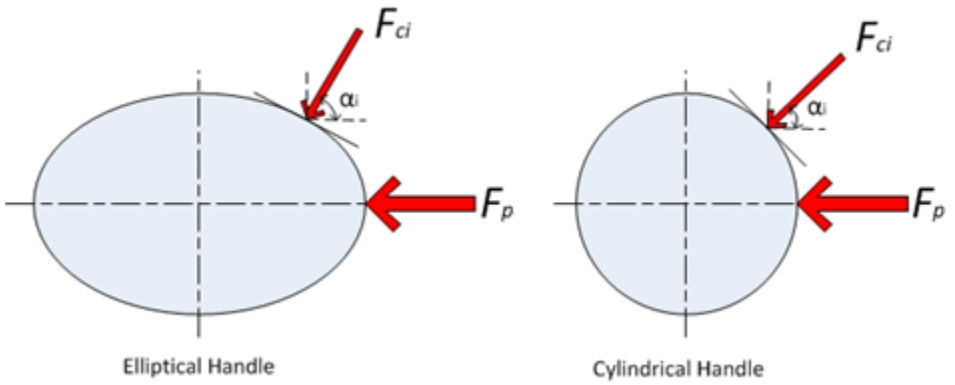

Figure 1.1: Representations of elemental contact forces and push force applied on elliptical and cylindrical handles.

$$F_p = \sum_i F_{c,i} \cos\alpha_i = \sum_i p_i S_i \cos\alpha_i \quad (1.1)$$

Where F_p is the push force, $F_{c,i,}$ is the contact elemental force, α_i is angle of the elemental force

The grip force, which is analogous to a 'squeeze' force, is compensated within the hand by the opposing gripping actions towards a dividing plane, as shown in Figure 1.2. The standard also defines the coupling force as the sum of hand grip and push forces [9]:

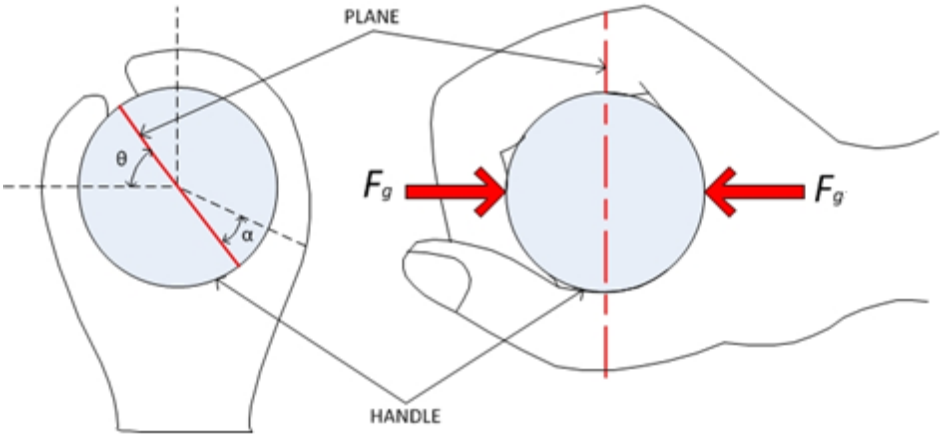

Figure 1.2: Representation of gripping force on a cylindrical handle.

$$F_{coup} = F_g + F_p \quad (1.2)$$

Where F_g is the grip force, F_{coup} is the coupling force

The studies reporting the effects of hand grip and push forces on the musculoskeletal loading, hand-transmitted vibration and biodynamic responses suggest that the quantification of hand forces is vital for understanding the human hand arm system responses to vibration [10, 11, 16, 23, 24]. The current frequency weighting defined in [5] has been challenged for lack of consideration of the hand-handle coupling forces [5, 25]. Due to the complexities associated with measurements of hand forces at the hand-handle interface; several studies have explored different measurement systems, some of which are briefly described in the following two sub-sections.

1.2.2. Instrumented Handles

Different designs of instrumented handles and force sensors have been developed for measuring the hand-handle forces under static as well as vibrating conditions. The initial designs of instrumented handles employed strain gauges for measuring hand grip force [13, 26-29]. These preliminary designs were used to study the effects of hand-handle coupling forces on HTV and biodynamic responses of the hand-arm system. The handles generally revealed resonances at frequencies below 1000 Hz and could not provide reliable measurements of biodynamic responses of the hand-arm system in the broad frequency ranges of typical vibrating tools [21, 22]. [26] proposed an instrumented handle comprising of six segments of cantilevers with strain gauges attached at the fixed end and [29] explored similar designs of 6, 8 and 10 segment instrumented handles. These studies concluded that a six segment instrumented handle provided more accurate measurements of coupling forces under various gripping tasks. A similar handle design was proposed by [28] for measurements of grip force and moment in hand-held tools, as shown in Fig. 1.3.

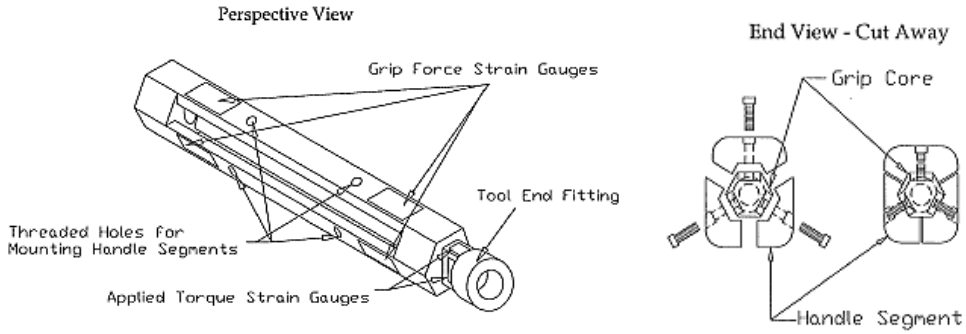

Figure 1.3: Preliminary instrumented handle design based on six strain gauges [28].

An alternate design for instrumented handles employing piezoelectric load cells was used to measure dynamic grip and push forces in studies assessing hand-arm biodynamic responses under the influence of vibration [11, 30-32]. The handles consisted of two load cells situated between a split handle design to measure hand grip force in conjunction with two additional load cells employed between the handle and the handle mount to measure the push force. These handles generally exhibit high stiffness and thus higher resonance frequencies above 1000 Hz. Figure 1.4 illustrates a schematic of the split instrumented handle design for measurements of static as well as dynamic hand coupling forces in addition to biodynamic responses of the hand-arm system and Figure 1.5 shows a pictorial representation. The two grip force sensors (Kistler 9212) are installed within the handle cavity and two additional load cells (Kistler 9317b) are located between the handle and its support for push force measurements. Figure 1.5a also shows a piezoelectric accelerometer placed inside the handle cavity to measure the reference acceleration. This handle design has also been recommended in [33] for evaluations of vibration transmissibility characteristics of anti-vibration gloves.

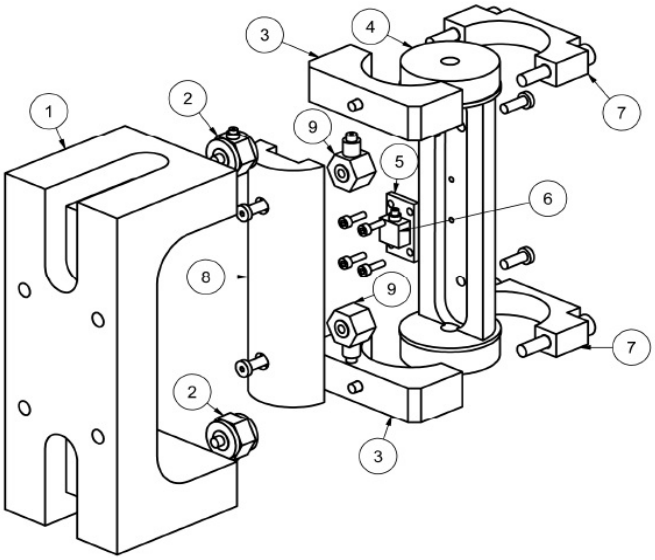

Parts List	
ITEM	DESCRIPTION
1	base
2	force sensor X 2
3	rear bracket X 2
4	handle 40mm
5	accelerometer base
6	accelerometer
7	front bracket X 2
8	front handle 40mm
9	small force sensor X 2

Figure 1.4: Exploded schematic representation of alternate instrumented handle design [34].

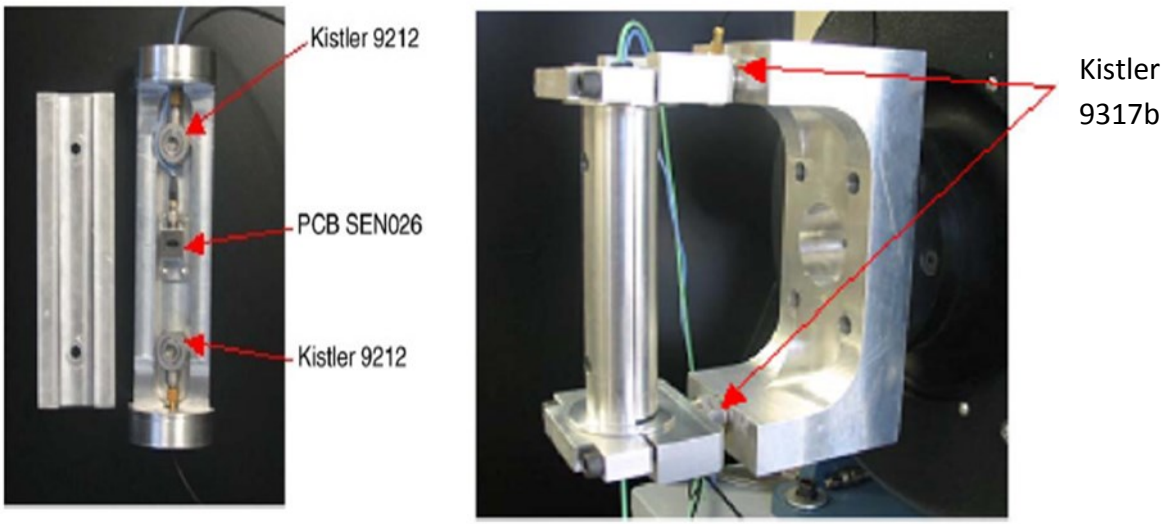

(a) (b)

Figure 1.5: Pictorial representation of an instrumented cylindrical handle (a) split view displaying grip forces sensors and (b) full mounted view showing push force sensors [11].

The aforementioned instrumented handles have been widely used in the laboratory for measurements of hand forces with stationary as well as vibrating handles. However, they are not versatile for field applications with hand-held power tools due to their implementation difficulties. Furthermore, it has been reported that split instrumented handle designs affect the rigidity of the handle in an undesirable manner. The dynamic responses of the handle may introduce significant

errors in the measured mechanical impedance particularly in the high frequency range [21, 22]. A number of studies have shown that instrumented handles employing either strain gauges or load cells are not always feasible for field usage with power tools [26, 28, 35, 36]. Therefore, a few studies have explored field-suitable measurement methods that could be easily applied to tool handles and are described in the subsequent sub-section.

1.2.3. Hand-handle interface measurement methods

The feasibility of thin-film pressure sensing systems for measurements of hand-handle coupling forces has been explored in several studies. These sensors exhibit adequate flexibility for applications to handles with varying cross-sections and curvatures. Semiconducting, capacitive and resistive thin film sensors have been used to measure hand-handle coupling forces under static conditions [37, 38]. The capacitive sensors consist of a dielectric material between elastomeric layers and their capacitance adequately varies with the applied normal load. Conversely, resistive sensors are designed with pressure sensitive resistors encased between two thin Mylar layers. The pressure sensing mats with matrix arrangements of capacitive or resistive sensors have been commercially developed for applications to power tool handles. [13] employed a 6x6 matrix of capacitive sensors on a cantilevered split handle to measure grip pressure distributions in static and dynamic conditions. Subsequently, [37, 38] used the capacitive sensing matrices for the acquisition of hand-handle contact and coupling forces only under static conditions. The studies employed instrumented handles with load cells to provide reference values to verify the results obtained from sensors. The studies also proposed empirical expressions relating hand grip, push, coupling and contact forces as a function of the handle size. It has been shown that the capacitive sensing matrix could provide accurate measurements of hand-handle grip, push and contact forces in a static laboratory setting under a controlled hand-arm posture. [39] used the capacitive sensing

matrix to map distributed hand-handle interface forces under different gripping and pulling tasks. [40] used a similar sensing matrix to determine hand grip force imparted on a hand-held olive harvester. [17] further explored a capacitive pressure sensing matrix, developed by Novel GmbH, to measure the grip and push forces on power tools. A capacitive pressure sensing hand matrix was developed to measure hand forces imposed on power tool handles [17, 41]. The system provided the hand-handle interface pressure distributions by wrapping the sensing matrix around the handle as well as placing several sensor segments over a gloved hand as shown in Figure 1.6.

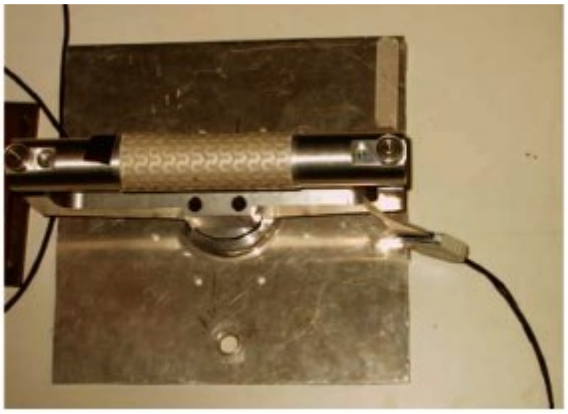

(a)

(b)

Figure 1.6: The NOVEL capacitive pressure sensing system: (a) a sensing matrix wrapped around a cylindrical handle; and (b) shown as sensing segments placed on an instrumented glove [17,18].

The study conducted a thorough static and dynamic analysis of the pressure sensing system for direct measurement of hand-handle interface pressure distribution and indirect measurements of grip and push forces considering different handle diameters.

Alternatively, few studies have explored low cost force sensing resistors (FSR) for hand-handle interface force measurements. The FSR were applied in different matrix arrangements for the acquisition of hand-handle force distributions similar to their capacitive counterparts. [42] evaluated three different thin and flexible sensors for grip force measurements imposed on a golf club. These included a resistive force sensing grid developed by Tekscan Inc. (USA) (denoted Tekscan 9811), an arrangement of small size force sensing resistors, also developed by Tekscan Inc., and flexible Quantum tunneling composite (QTC) sensors.

The study evaluated the relative performance of the sensors under controlled laboratory conditions in terms of static accuracy, hysteresis, repeatability, drift errors, dynamic accuracy, and shear loads and surface curvature effects. The study concluded superior performance of the resistive force sensing grid and FlexiForce sensors compared with the QTC sensor. The results further showed reduced measurement sensitivities of both the resistive sensors compared to the static sensitivity of the QTC sensor and stated the sensitivity of all the three sensors decreased with their usage. In a recent study, [43] applied resistive pressure sensors (Tekscan 3200) to study the influence of handle diameter on the hand forces. The findings of the study were similar to those reported in [17, 37, 38].

1.2.4. Measurements of hand-arm biodynamic responses

The biodynamic response characteristics of the hand-arm system to hand-transmitted vibration have been widely characterized to obtain mechanical-equivalent properties of the hand and arm, define alternate frequency-weighting correlations and develop a better understanding of

the vibration power absorption. The biodynamic responses have been described in terms of through-the-hand-arm and to-the-hand response functions according to [44]. The through-the-hand-arm response function describes the transmission of vibration to different segments of the hand-arm system and is expressed as the ratio of the vibration magnitude measured at a specific segment on the hand-arm system to that at the hand-handle interface [10]. The to-the-hand biodynamic response relates vibration in the vicinity of the hand to the force at the driving point, expressed in terms of the driving-point mechanical impedance (DPMI) or apparent mass (APMS) or absorbed power, explained as:

$$Z(j\omega) = \frac{F(j\omega)}{v(j\omega)} \qquad M(j\omega) = \frac{F(j\omega)}{a(j\omega)} \qquad P(\omega) = Re[Z(j\omega)]v^2 \tag{1.3}$$

Where Z and M are the complex DPMI and APMS frequency response functions, respectively, P is the absorbed power frequency, v is the velocity measured at the driving point, a is the acceleration measured at the driving point, F is the force measured at the driving-point along the axis of the motion, ω is the circular frequency of vibration, $j = \sqrt{-1}$ and Re denotes the real component of the DPMI.

The biodynamic responses of the hand-arm system have been widely characterized in the laboratory using instrumented handles under different experimental conditions such as: magnitude and frequency of handle vibration, hand-arm posture, hand-grip and push forces, and handle geometry and sizes [11, 21-25, 27, 30-32, 45, 46]. These have generally presented the response in terms of the DPMI as a frequency response function relating the dynamic force and the velocity at or close to the hand-handle interface:

$$Z(j\omega) = \frac{S_{Fv}(j\omega)}{S_{vv}(j\omega)} \tag{1.4}$$

Where S_{Fv} is the cross spectral density of the force F and the velocity v, S_{vv} is the auto spectral density of the velocity.

The DPMI characteristics describing the biodynamic response of the hand-arm system have been extensively investigated under a wide range of vibration excitations and test conditions. These have shown that the biodynamic responses of the hand-arm system strongly depend upon the hand forces. The DPMI magnitude increases with increasing hand grip force [25, 27, 32, 47, 48]. It has been suggested that the biodynamic response of the hand-arm is relatively less sensitive to variations in the push/pull forces which, is supported by only a limited number of studies [49,50]. The effect of the grip force alone has thus been emphasized by [49]. [51] investigated the influence of various physical factors on the DPMI measured at the palmar surface of the finger. The results showed that the transmission of vibration to the fingers is highly dependent on the magnitude of the contact force. The biodynamic measurements performed using instrumented handles may exhibit considerable errors partly attributed to handle dynamics and inertia effects [21, 22]. An inertial correction is invariably applied to account for the inertia of the instrumented handle by subtracting the DPMI of the handle alone from the DPMI of the combined handle and the hand-arm:

$$Z_{hand-arm}(j\omega) = Z_{coupled}(j\omega) - Z_{handle}(j\omega) \quad (1.5)$$

Where $Z_{hand\text{-}arm}$ is the DPMI of the hand-arm system, $Z_{coupled}$ is the directly measured DPMI of the coupled handle-hand-arm system, Z_{handle} is DPMI of the handle alone.

The magnitude of the DPMI of the handle could be substantially higher than that of the hand at higher frequencies particularly when the handle mass supported by the force sensors is more prevalent. It has been shown that the contributions due to handle inertia at higher frequencies cannot be entirely eliminated through mass cancellation [21]. A few studies have shown that the APMS of the hand-arm system tends to be very low at frequencies above 500 Hz and approaches about 25 g near 1000 Hz, which is significantly lower than the instrumented handle's APMS [22,

30]. The discrepancies among the reported impedance responses above 500 Hz were thus partly attributable to the inertial effect of the instrumented handles [21]. The magnitude of error due to inertial effect could be minimized by reducing the effective handle mass supported by the force sensors. However, reducing the mass tends to increase flexibility of the handle structure and thus lowers its resonant frequency. Thin-film pressure sensing matrices of negligible mass can be applied directly to the handle surface to measure the driving point force while preserving the handle's rigidity. In addition to the hand grip and push force measurements the FSR could also be used to measure the dynamic forces in order to obtain DPMI responses without any inertial correction. The accuracy of the dynamic measurements would, however, greatly depend upon the bandwidth and frequency response characteristics of the pressure sensing systems, which have yet to be explored.

1.3. Objectives of the Study

The overall objective of this study is to contribute towards developments in low cost devices for measurements of hand-handle coupling forces with hand-held power tools. The primary goal in order to achieve the objective is to explore the feasibility of a low cost resistive force sensor for measurements of hand-handle forces under static and dynamic conditions. The specific objectives of the study include:

1. Developing a two-channel signal conditioning circuit and measuring the validity of the FlexiForce sensors and the conditioning circuit through systematic static sensor calibration tests;

2. Identifying optimal locations of sensors through analysis of hand-handle interface pressure distributions;

3. Examining the validity of the sensors for capturing hand grip and push forces under static and dynamic test conditions;

4. Exploring the feasibility of the sensors for measurements of the biodynamic response of the human hand-arm system exposed to broadband random vibration along the forearm axis;

5. Exploring the feasibility of the measurement system for measuring the grip and push forces while grasping a percussion tool handle under static as well as vibrating conditions.

The study was conducted in four systematic phases. During the initial phase, the FlexiForce sensors were used to measure the static contact force through a force indenter by implementing a two-channel variable gain signal conditioning circuit. The calibrations of the sensors were performed under a wide range of forces where the sensor was placed on flat as well as curved surfaces. During the second phase two sensors were applied on the palm and finger sides of a cylindrical handle and a LabView program was developed to estimate from the sensors' output signals in terms of voltage versus the reference handle grip and push forces in Newtons. Previously reported hand-handle interface pressure distribution data was thoroughly reviewed to identify the optimal positions of the sensors on different handle sizes. The static calibrations of the sensors were verified on various cylindrical and elliptical handles of different sizes using a sample of eight subjects. The feasibility of the measurement system for determining the hand grip and push forces with vibrating handles was further evaluated under broadband random vibration applied to the handle. The feasibility of the sensors for measuring the biodynamic response of the hand-arm system was thus explored in the third phase. The applicability of the measurement system to real tools handles was examined in the final phase of the study using a chisel hammer operating in an energy dissipator. The validity of the sensors was examined with the hand grasping the static as well as vibrating tool handle under a wide range of hand coupling forces.

1.4. Organization of the Thesis

This dissertation is organized in a "Manuscript" format consisting of five chapters and an appendix. Chapter two presents the detailed methodology for measurements of hand-handle interface forces. Although some of the measurement methodologies have been briefly described in the manuscripts in Chapters 3 and 4, this chapter presents detailed methodologies. The chapter also explains the functionality and principles of the FlexiForce force resistive sensors as well as the methodology for static sensors calibration. An in-depth review of the reported hand-handle contact pressure distributions is presented to identify near optimal FlexiForce sensor positions on the handles. Experimental methods for characterizing the static and dynamic hand-handle forces on instrumented handles and the percussion tool as well as the biodynamic responses of the hand-arm system is also presented.

Chapter three briefly presents the sensor properties obtained from the static sensor calibrations, while Appendix A presents the properties in detail. The chapter also presents static and dynamic force measurement on instrumented handles as well as the tool handle force measurement results under stationary and vibrating conditions in the following article:

Kalra, M., Rakheja, S., Marcotte, P., Dewangan, K.N., Adewusi, S., "Measurement of coupling forces at the power tool hand-handle interface". Under review, Int. J. of Industrial Ergonomics (Submitted: November 2014)

This paper explored a low-cost measurement system to estimate hand-handle coupling forces imposed under static and dynamic conditions and its feasibility when applied to instrumented laboratory handles and eventually to a hand-held percussion tool handle. Initially, the characteristic properties of the inexpensive, thin-film, flexible and trimable FlexiForce (force resistive) sensors were explored as a viable option for measurements of the hand-handle interface

forces. Static calibration tests performed on a flat surface under applied loads from a force indenter showed very good linearity, hysteresis and repeatability; although, considerable differences were evident in the static sensitivity amongst different sensors. The calibration tests were also performed with sensors placed on a semi-circular curved surface to mimic an instrumented handle. The appropriate locations of the sensors on the instrumented handle surface were subsequently determined on the basis of the hand-handle geometry and reported contact force distributions. The study concluded that two sensor positions would be necessary to effectively measure hand-handle forces on the instrumented handles. The validity of the measurement system was investigated for measuring the hand grip and push forces with subjects grasping five different stationary instrumented handles (cylindrical: 32, 38 and 43 mm diameter; and elliptical: 32×38 and 38×44 mm) considering two different positions of the sensors on the handle. The validity of the measurement system was also investigated under vibration for the 38 and 43 mm diameter cylindrical handles while employing only one sensor position. The results showed good linearity and repeatability of the sensors for all subjects and handles under static conditions, while the sensors' outputs differed for each handle. In general the FlexiForce sensors accurately measured hand-handle interface forces with relatively low error under vibration. The feasibility of the measurement system was also examined for measurements of hand forces on a power chisel hammer handle. The evaluations were conducted with three subjects grasping the chisel handle under stationary as well as vibrating conditions and different combinations of hand grip, push and coupling forces. The measurements revealed very good correlations between the hand forces estimated from the FlexiForce sensors and the reference values for the stationary as well as the vibrating tool and it was concluded these sensors can indeed serve as an accurate measure of hand-handle interface forces.

Chapter four presents the biodynamic measurements conducted with the FlexiForce sensors in the following article:

Kalra, M., Rakheja, S., Marcotte, P., Dewangan, K.N., Adewusi, S., "Feasibility analysis of low-cost flexible resistive sensors for measurements of driving point mechanical impedance of the hand-arm system". Under review, Int. J. of Industrial Ergonomics (Submitted: October 2014)

The feasibility of the FlexiForce (force resistive) sensors for measurement of the hand-arm biodynamic response was explored in the aforementioned article. Two FlexiForce sensors were installed on a 38 mm diameter cylindrical instrumented handle symmetrically about the handle's centerline to measure the palm-handle and finger-handle interface dynamic forces. Four force sensors were installed inside the handle as well as on its mounting bracket in order to provide reference hand grip, push and driving point forces. An accelerometer was also installed inside the handle to measure its vibration. The measurements were performed with six subjects grasping the handle using nine different combinations of grip (10, 30 and 50 N) and push (25, 50 and 75 N) forces under two levels of broad-band random vibration (1.5 and 3.0 m/s^2 weighted rms acceleration) in the 4–1000 Hz frequency range. The data acquired from the instrumented handle was analyzed to determine the palm and finger impedance responses, which served as the reference values to evaluate the feasibility of the FlexiForce sensors' responses. The FlexiForce palm and finger impedance trends were similar amongst all subjects in comparison with the references results; yet, the magnitudes differed in both cases. Moreover, the FlexiForce and reference comparisons revealed very similar trends; albeit, the impedance magnitude responses obtained from the FlexiForce sensors were substantially lower over the entire frequency range versus the reference responses. A correction function was subsequently developed and applied to the FlexiForce measured data, which resulted in almost identical hand-arm impedance response trends

compared to the reference values. It was concluded that the low-cost FlexiForce sensors could be applied for measurements of biodynamic responses of the hand-arm system in real tool handles in the field.

Chapter five summarizes the major contributions and conclusions together with some recommendations for possible future works.

CHAPTER 2
MEASUREMENT METHOD OF THE HAND HANDLE INTERFACE

The primary objective of this dissertation research is to develop a low cost hand-handle interface force measurement system to estimate hand grip and push forces exerted on a tool handle. This chapter presents a description of the functionality of the FlexiForce sensors used for developing the measurement system together with detailed methods for assessing the measurement system. The design of the measurement system was developed using the FlexiForce (model 1230) resistive sensors, which were selected for their low cost, thin and flexible design for application to curved handle surfaces, rapid response time, higher acquisition sampling rate, simple signal conditioning and the ability to trim the sensor dimensions for different handle lengths. Unlike the pressure sensing systems, which comprise a large matrix of sensors, the selected sensor is applied as a single unit to measure the total force imposed on the entire contact surface and thereby it could provide measurements at a very high sampling rate. A series of experiments were designed to: (i) evaluate static properties of the FlexiForce sensors in terms of linearity, hysteresis and repeatability when applied to flat as well as curved surfaces; (ii) identify appropriate positions of the FlexiForce sensors on a handle for accurate measurements of the hand forces; and (iii) assess feasibility of the sensors for measuring hand forces on simulated laboratory handles as well as tool handles under stationary and vibration conditions; and (iv) measure the biodynamic response of the hand-arm system.

2.1. SENSOR DESCRIPTION AND SIGNAL CONDITIONING

A force sensing resistor (FSR) consists of two polymer layers. The outer layer contains a pair of intertwined conductive substrates forming the active sensing area. Since each substrate contains a checkered (or intertwined) pattern of conductive strips whereby one is not a mirror image of the

other; combining two opposing substrates creates an interwoven network of conductive strips. The second and inner layer is an adhesive layer coated with carbon-based FSR ink. The sensor measures 149×40×0.21 mm and is pictorially shown in Figure 2.1. In the absence of a force the resistance between the two layers may be as high as 10 MΩ as shown in Figure 2.2 and the sensors behave similarily to an open circuit. Based upon the general principle of FSR an applied force on the sensor causes the ink to contact the conductive strips and create a short circuit which dramatically decreases the resistance. However, the conductance of the sensors varies linearly with the applied force as shown in the figure.

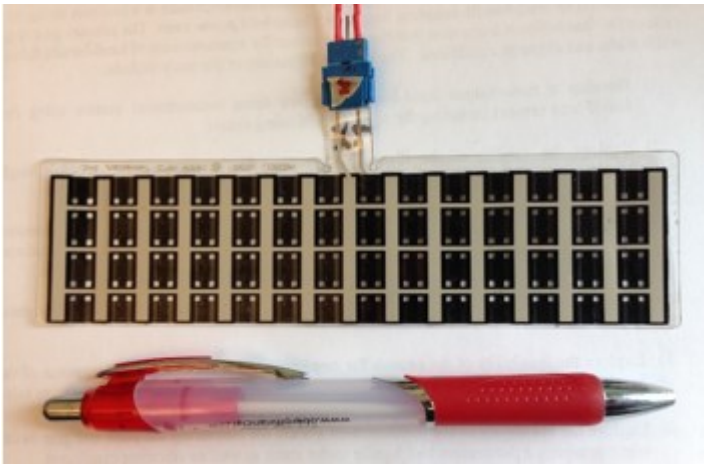

Figure 2.1: Tekscan Flexiforce (model 1230) resistive force sensor.

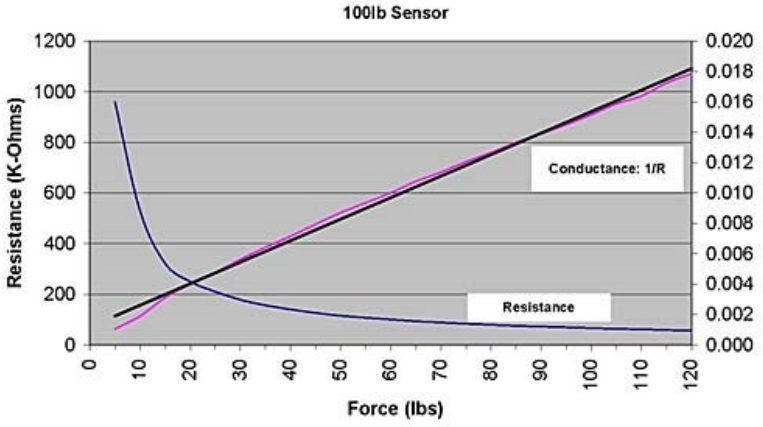

Figure 2.2: Variations in resistance & conductance of an FSR with an applied force [52].

The resistance decrease that occurs from an applied force can be quantified by the use of a two-channel signal conditioner in terms of the change in the circuit's voltage. A conditioning circuit (Figure 2.3) which consists of an inverted operational amplifier setup that compares the sensor resistance to a reference resistance and produces an analog voltage output was constructed based on a circuit recommended by the manufacturer. Preliminary force measurements using the circuit resulted in substantial output voltage drift as well as output saturation under relatively low force levels in the order of 50 N. The circuit was thus modified to increase the measurement range up to 200 N. Since the sensor voltage output is highly influenced by subtle force changes a zeroing circuit was implemented to control the voltage drift and potential bias caused by a preload. Finally, a variable gain circuit was implemented to ensure a digital voltage readout range corresponding to the measurement range of 0-200 N.

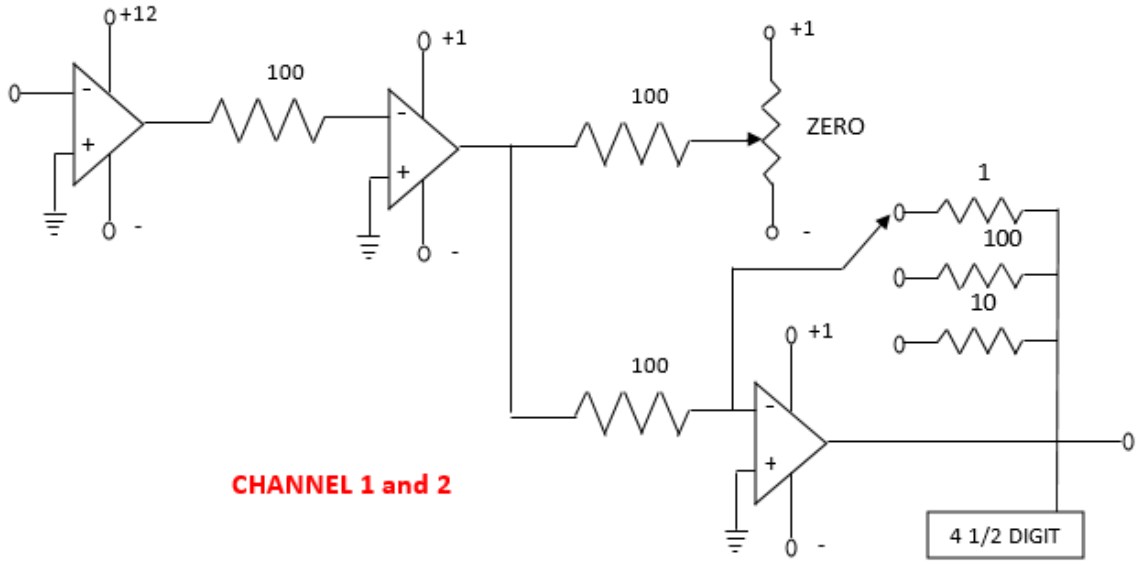

Figure 2.3: Dual channel conditioning circuit (only one channel shown).

The assembled dual-channel conditioner is pictorially shown in Figure 2.4. It is essential to note that the sensors will only yield an output when a force is applied at a location where conductive strips (from each substarte) intersect, also denoted as a 'sensel'. Since the strips form a weave pattern only a portion of the sensor contains intersecting conductive sensels. For a surface load this characteristic is (mostly) irrelevant since this load would span over several sensels and result in an output corresponding to the total load applied to all the sensels. The selected FlexiForce sensor (model 1230) comprised a total of 102 sensels.

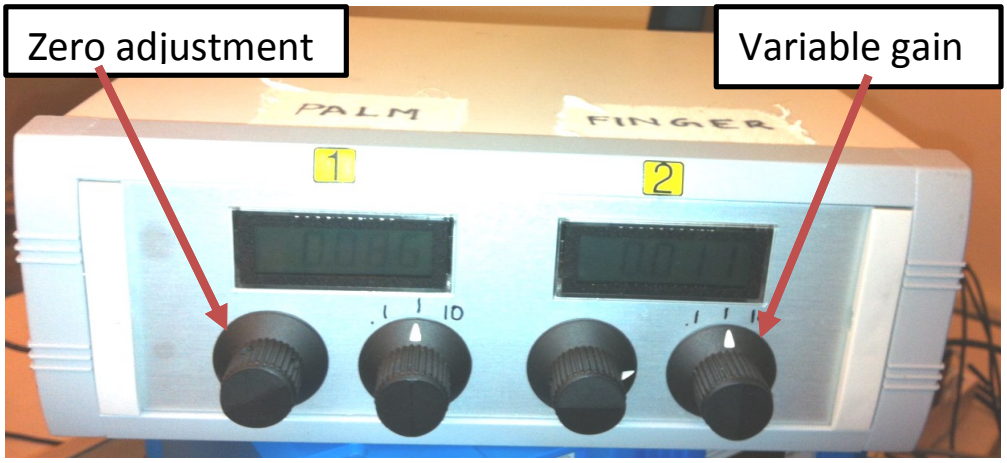

Figure 2.4: Dual channel conditioner with zero and variable gain adjustments.

2.2. Experimental Methods

A series of experiments were designed to:

(i) characterize the static properties of the FlexiForce sensors in terms of linearity, hysteresis and repeatability on flat as well as curved surfaces;

(ii) evaluate the effects of sensor length, load position, load elastomer stiffness and loading elastomer contact area;

(iii) identify appropriate positions of the sensors on the instrumented cylindrical and elliptical handles;

(iv) evaluate sensor feasibility on stationary and vibrating cylindrical and elliptical handles;

(v) assess the feasibility of the sensors for measurements of hand grip and push forces on an impact tool handle under stationary as well as operating conditions;

(vi) evaluate sensor feasibility for measurements of biodynamic response of the hand-arm system.

The detailed methodology used for each of the aforementioned tasks is presented in the following sub-sections.

2.2.1. Methodology for the sensor calibration on flat and curved Surfaces

Prior to implementing the sensors on a tool or curved handle a series of in depth static calibration tests were conducted to observe the relationship between applied force and the sensor output while placing the sensor on a flat and a curved surface. In order to ensure uniform force transmission the force was applied through an 8 mm thick relatively stiff elastomer for measurements on the flat surface. A Dillon Model GL 500 digital force indenter (range: 0-500 N; resolution: 0.2 N) with a digital display was used to apply the load on the sensor through the elastomer. A 12 mm thick aluminum strip was placed between the indenter and the elastomer to ensure uniform elastomer deflection. Figure 2.5 illustrates the measurement setup together with the loading elastomer. For calibration purposes the maximum applied force was established as 100 N and was incremented in intervals of 10 N.

The applied force along with the voltage output from the dual-channel conditioner allowed for the sensor sensitivity to be evaluated as:

$$S = \frac{V}{F} \tag{2.1}$$

Where V is the voltage, F is the force and S is the sensitivity.

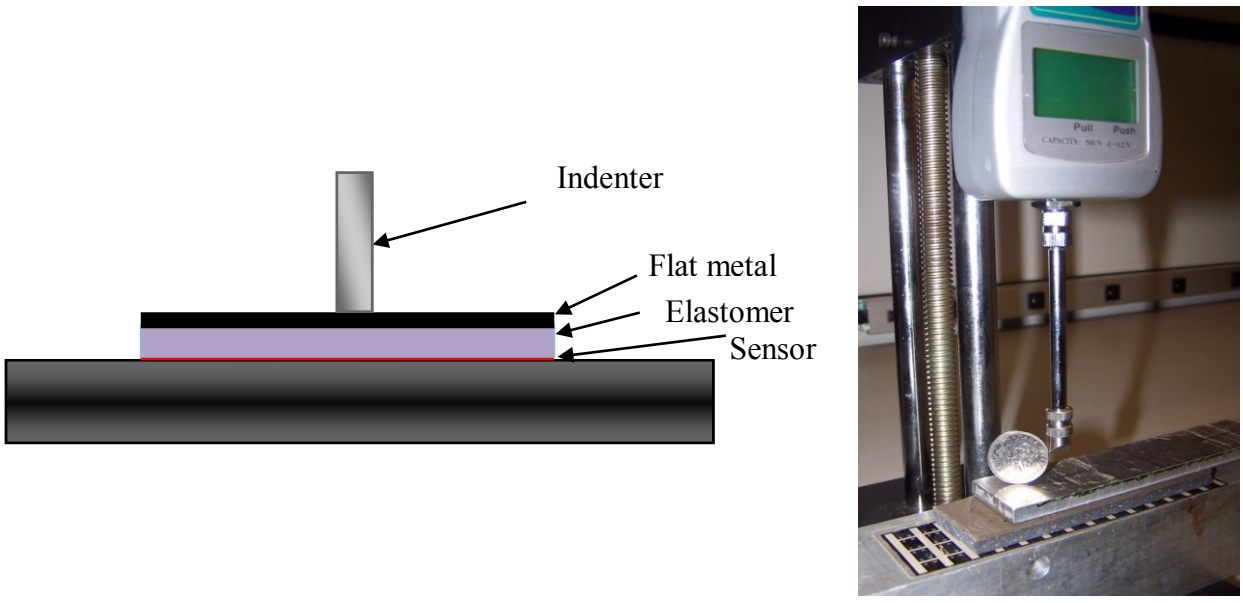

(a) (b)

Figure 2.5: (a) Schematic displaying the layers surrounding the sensor during calibration tests; and (b) Complete setup of calibration tests with force indenter.

The input-output properties of different sensors were subsequently evaluated when placed on a cylindrical surface to assess their feasibility for applications to tools handles. For this purpose, a curved loading cap was designed to apply uniform loading on the sensor positioned on a 38 mm diameter semi-cylindrical surface, as seen in Figure 2.6. The length of the loading cap was identical to the sensor's length. A 2 mm thick relatively soft elastomer was applied to the curved surface to ensure more uniform contact between the senor and the loading cap. A preload of 7 N was also applied to the cap prior to the measurements since the stiffness of the sensor resisted the weight of the cap. The stiffness of this elastomer was substantially lower than that of the loading pad used for experiments on the flat surface. The effect of elastomer stiffness was also evaluated through measurements on the flat surface. The measurements on the curved surface permitted the evaluation of the linearity and repeatability of the sensors under the effect of curvature. In order to distinguish between the elastomers used on the flat surface versus the curved surface the two

elastomers are denoted as ‘stiff’ and ‘soft’, respectively; although, no attempts were made to quantify their stiffnesses.

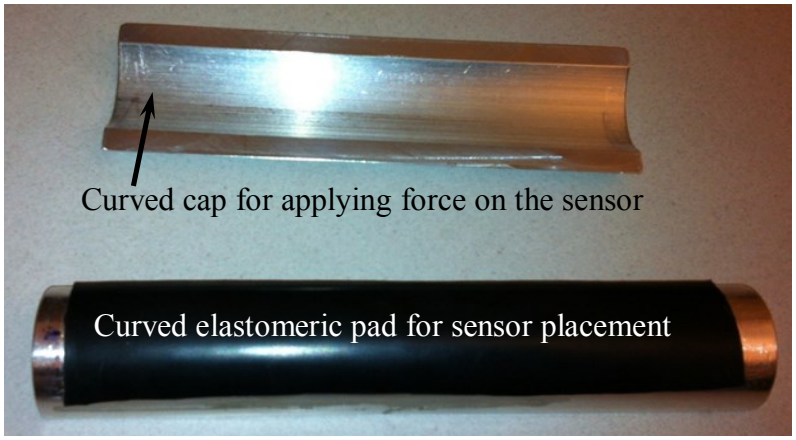

(a)

(b)

Figure 2.6: (a) Top view of curved handle along with soft elastomer and curved surface cap; and (b) side view of curved handle along with soft elastomer and curved surface cap.

Static calibrations were initially performed to evaluate the linearity, hysteresis and repeatability of the sensors’ outputs. The tests were also conducted to evaluate the effects of sensor length, loading position, elastomer contact area and the elastomer material stiffness on the output. The linearity of a number of sensors was evaluated in the 0-100 N range, while the hysteresis was evaluated in the 0-120 N range. The measurements were performed on full-length sensors subject to loading via the ‘stiff’ elastomer measuring 141.7×33.3 mm. The elastomer was positioned

symmetrically about the center of the sensor and the indenter applied force at the center of the metal plate placed on top of the elastomer as shown in Figure 2.5a. The experiments were also designed to study the effect of sensor length, contact area and load positions on the sensors' outputs. The sensor length exceeded the length of the standardized instrumented handle used for evaluating the biodynamic responses of the hand-arm system and the antivibration performance of gloves as described in [33]. It was therefore necessary to trim the sensors from the original length of 149 mm to 117 mm when conducting tests on the instrumented handles. The static calibration experiments were thus also performed with trimmed sensors to study the effect of sensor length. The trimmed sensor required trimmed elastomers measuring 115.6×32.7 mm and were denoted as 'medium' length elastomers, whereas the elastomers used on nominal full-length sensors were henceforth denoted as 'long'. A third elastomer was cut to measure 60.7×30 mm and denoted as 'short'. The effect of load contact area was evaluated by measuring the outputs with three elastomer pads placed symmetrically around the center of the sensor. Furthermore, preliminary measurements with the short elastomer revealed substantial effects of the elastomer's loading position on the sensor output. This was attributed to the number of sensels contained within the contact area. The effect of sensor output versus elastomer positioning was thus also examined by applying a load to the short elastomer as it was shifted to four different positions along the long-axis of the sensor.

2.2.2. Distribution of hand force on the handles

Preliminary measurements conducted with the FlexiForce sensors revealed substantial effects of the sensors positions on the output depending on their placement at different positions on the handle surface. This output variation was likely due to non-uniform distributions of the hand force on the handle surface. The reported hand-handle interface pressure distributions on

different sizes of cylindrical handles were thus thoroughly analyzed to identify adequate positions of the sensors to achieve reliable estimates of the hand grip and push forces. [37, 38] have reported distributed hand-handle interface force on the 30, 40 and 48 mm diameter cylindrical handles under different combinations of hand grip and push forces. The hand-handle interface force distributions were measured using a capacitive pressure sensing matrix (NOVEL GmbH) wrapped around the handle as shown in Figure 2.7. The sensing matrix comprised 16 x 11 (16 rows and 11 columns) pressure sensors encased within a 2 mm thick elastomeric mat. Each sensor covered an area of 0.766 cm^2 including the spacing between the adjacent sensors. The overlapping of active sensors encountered with smaller handles was eliminated by masking selected rows of sensors. A total of four and two rows of the sensing matrix were masked for the 30 and 40 mm handles, respectively, while no masking was needed for the 48 mm handle.

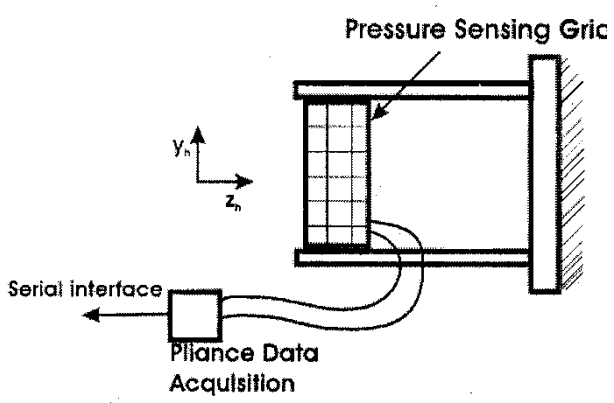

Figure 2.7: Capacitive pressure mat wrapped around the instrumented handle for measurements of hand-handle interface contact pressure [36].

A total of 10 male adult subjects had participated in the reported study. Each subject was advised to stand on a force platform and grasp the instrumented handle with his dominant right hand with a specified arm posture (elbow angle ≈ 90° and neutral wrist position). The platform height was adjusted to ensure nearly horizontal forearm and zero shoulder abduction. The experiment design consisted of three handles and five levels of grip force (F_g = 0, 15, 30, 50 and 75 N) combined with

four levels of push force (F_p = 0, 25, 50 and 75 N) to study the effect of force variation on the magnitudes and locations of the peak contact pressures.

The hand–handle contact pressure distribution data were analyzed using the Pliance system software, which also provided the peak pressures within specified contact areas. The hand surface was divided into five different contact zones, as shown in Figure 2.8, to study the localized peak pressures and contact forces developed within each zone. These zones were identified upon consideration of the hand/handle geometry and the range of hand sizes considered in the study. Zone 1 contains the tips of the second, third and fourth digits for the range of hand sizes considered, while zone 2 envelops the tip and middle phalange of the first digit and the middle phalanges of digits II, III and IV. Zone 3 consists of the proximal phalanges of the four digits and the adjacent upper extremity of the palm. Zone 4 encompasses the upper lateral side of the palm in the vicinity of the thenar region, while Zone 5 envelops the upper medial side of the palm.

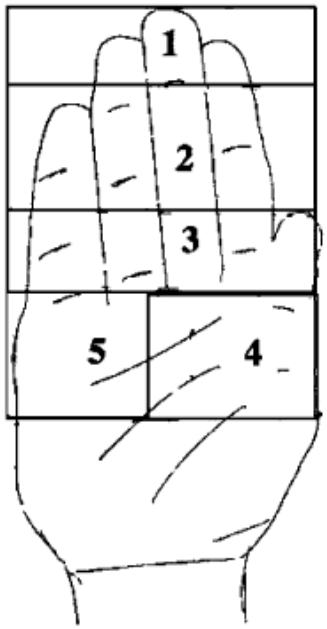

Figure 2.8: Illustration of five hand-handle contact zones defined for study of contact force distributions [37].

The contact force developed over the entire contact surface and within individual zones could be derived through integration of the local pressure over the effective contact area. The effective contact area was defined by the area enclosed by the active sensors with pressure values exceeding a threshold value of 0.143 N/cm^2. Since each sensor area is constant, assuming uniform pressure over the small sensor area, the contact force F_c (overall and within a zone) was estimated from:

$$F_c = \Delta A \sum_{i=1}^{n} p_i \tag{2.2}$$

Where ΔA = 0.766 cm^2 is the sensor area, p_i is the pressure measured by sensor i and n is the number of active sensors within a zone.

The subject's hand position with respect to the sensing matrix on each handle was marked during the first test and the subject was advised to use the same position in the subsequent tests. The data acquired for 10 subjects and two trials were analyzed to derive the means and standard deviations (SD) of the overall and local pressure peaks, and contact force corresponding to each test condition. The data attained for two trials revealed good repeatability in terms of the contact force. However, larger variations in the peak pressures were observed, which were attributed to variations in the hand's position in relation to a particular sensor location within the grid, the hysteresis effect of the pressure sensors and inconsistencies in the localized pressure imparted by the hand. Yet, the results showed consistent locations of the high pressure zone irrespective of the hand force combination. The mean peak pressures for all subjects and handles generally occurred in zone 4.

For the 48 mm handle the peak pressures invariably occurred in zone 4 irrespective of the hand force combination. The peak pressures obtained for the 40 mm handle also showed the same trend, except in the absence of the push force resulting in lower pressure from the lateral side of the palm (zone 4). Gripping the handle in this case resulted in pressure applied mostly from the

fingers, specifically from the fingertips. The location of the peak pressure shifted to zone 1 under grip conditions exceeding 30 N. Similar trends were also observed for the 30 mm diameter handle. The application of high grip force coupled with low push force such as grip/push combinations of 50/25 N and 75/25 N also caused the peak pressure to shift from zone 4 to zone 1. It was further reported that application of high grip and push forces could shift the peak pressure towards zone 3. Under these conditions the peak pressures were observed to occur over the surface adjoining zones 3 and 4.

Moreover, the results suggested that the peak pressure location is also dependent upon the handle size, particularly under low-magnitude push forces, which could be attributed to the effective contact area. On the 48 mm handle the subjects applied grip force using the entire hand surface which resulted in a relatively higher pressure in zone 4 even when the push force was absent. The subjects also maintained a more stable and controlled grip with the two smaller handles, leading to a higher concentration of the contact force as well as peak pressures near the fingertips. The 30 mm diameter handle displayed considerably higher mean peak pressures in zone 1 under zero push force.

The distribution of the contact force at the hand-handle interface was further analyzed for different handle sizes and combinations of grip/push forces in terms of the contact force ratio (CFR), defined as the ratio of the contact force developed within a zone to the total hand-handle contact force. Figure 2.9 illustrates a sample of the mean CFR for the five zones under different combinations of grip and push forces for the 30 mm handle with the zones are denoted as '*Zn*, *n*=1,2,3,4 and 5'.

The CFR results confirmed that zone 4 contributes the most to the total hand–handle interface force for the 48 mm handle irrespective of the grip and push force combination. The CFR

of zone 4 generally increased with an increase in the push force and decreased slightly with an increase in the hand grip force. The CFR values in zones 2 to 4 approached steady state values with an increase in the push force due to the saturation of the effective contact areas. Under the application of a push force alone the contribution of zone 3 to the total contact force was the highest following the contribution from zone 4, while the contribution of zone 1 is almost negligible. The steady-steady values of the CFR of zone 1 increased with increasing grip force. As grip force increased zones 2 and 3 resulted in comparable values of CFR, while the contribution due to zone 5 was almost negligible for all grip/push combinations considered in the study.

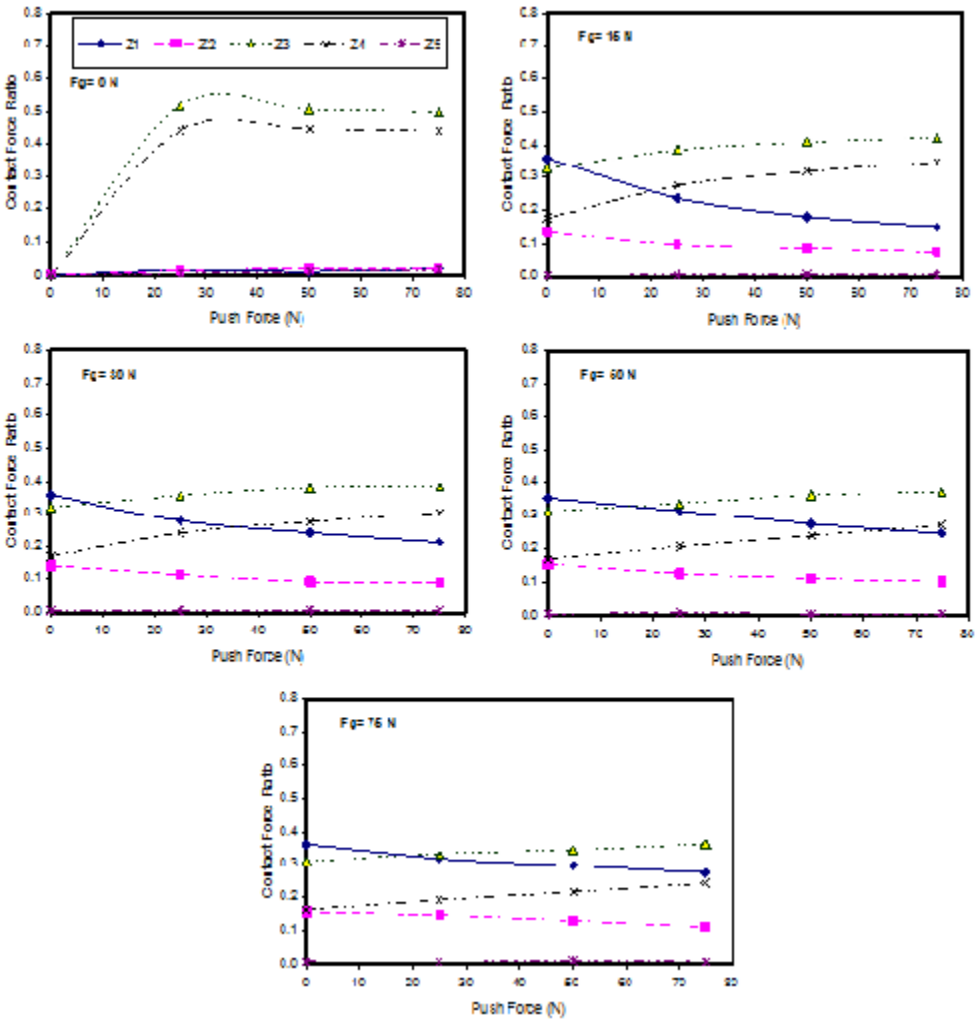

Figure 2.9: Contact force distribution at different zones for different grip/push forces (30 mm handle) [37].

Distributions of the contact forces for the 30 and 40 mm handles differed considerably from those for the 48 mm handle. For the 40 mm handle zone 4 revealed the highest CFR under either zero or light grip force ($0 \text{ N} \leq F_g \leq 50$) with push force bring greater than 25 N; while zone 1 showed the largest CFR under zero push force. The contribution of zone 3 was higher than that of zone 2. An increase in the push force caused an increase in the CFR of zones 3 and 4 with a decrease in those of zones 1 and 2. For the 30 mm handle zone 3 contributed the most to the total contact force specifically when the push force was above 15 N; whereas, zone 1 yielded higher CFR for zero push force suggesting more contact between the fingertips and the proximal phalanges. The CFR of zone 4 was considerably smaller than those presented for the 40 and 48 mm handles.

2.2.3. Identification of FlexiForce sensors positions on the handle

The measured hand-handle interface pressure and contact force distributions generally suggested higher contact force in zone 4 particularly for the 40 and 48 mm diameter handles for a push force of 25 N or greater. The peak contact force shifted towards the fingers side (zones 1 and 2) in the absence of a push force. Since the cylindrical handles used in [37, 38] were similar to those used in the current study these findings were applied to identify suitable positions of the FlexiForce sensors for capturing the palm- and finger-side forces in a reliable manner. Three cylindrical handles measuring 32, 38 and 43 mm in diameter were chosen for the current study. Furthermore, the current study also explored the effect of the FlexiForce sensors on two elliptical handles measuring 32×38 and 38×44 mm.

The locations of the individual zone profiles on the different cylindrical and elliptical handles were further mapped by considering the hand dimensions of four male subjects. The hand sizes of the selected subjects ranged from 9 to 10, as per [44]. With tracing paper taped on each handle each subject's hand profile was traced while he grasped the handle. The trace was divided

into four zones outlining zones 1 to 5 as shown in Figure 2.8 (with zones 4 and 5 considered as one overlapping zone). The length of each zone allowed for a visual representation of the area covered by each zone on all five handles. The mean CFR values reported by [37] for the cylindrical handles were subsequently mapped for each zone considering the 30 N grip and 50 N push condition. This force combination was chosen in accordance with the recommended values in [33]. The CFRs are indicated at the center of each zone, assuming uniform pressure over each individual zone, since the center of pressure data was not available. Due to the lack of reported data for elliptical handles, the geometry of the elliptical handles was used to estimate their respective zone maps. Since the elliptical handles were created by inserting a 6 mm spacer within the cylindrical handle cavity the elliptical hand contact zones were mapped by shifting the cylindrical zones by 6 mm. Figure 2.10 illustrates the profiles of the zones mapped around the handles' circumferences for a single subject as well as proportions of mean CFR (on cylindrical handles) and their locations over each zone.

From the illustration, it is evident that zones 4 and 5 are mostly located around the central axis of the handle, irrespective of the handle size. It is further seen that zone 2 also lies around the central axis of most of the handles, opposite to zones 4 and 5, with the exception of the smallest handle (32 mm diameter). In cylindrical handles, zone 3 also lies close to the central axis of the handles. Moreover, the majority of the contact force occurs within the zones 4 and 5, followed by zones 2 and 3, with a small exception in case of the smallest handle. From these results, it is deduced that a FlexiForce sensor covering the zones 4 and 5 and positioned around the handle's central axis could provide good estimates of the palm-side force. Another sensor covering zones 2 and 3 and positioned on the opposite side could provide good estimate of the finger-side force. It should be noted that the diameters of the handles considered in the reported study differed only

slightly from those employed in the current study. The effect of small variation was assumed negligible.

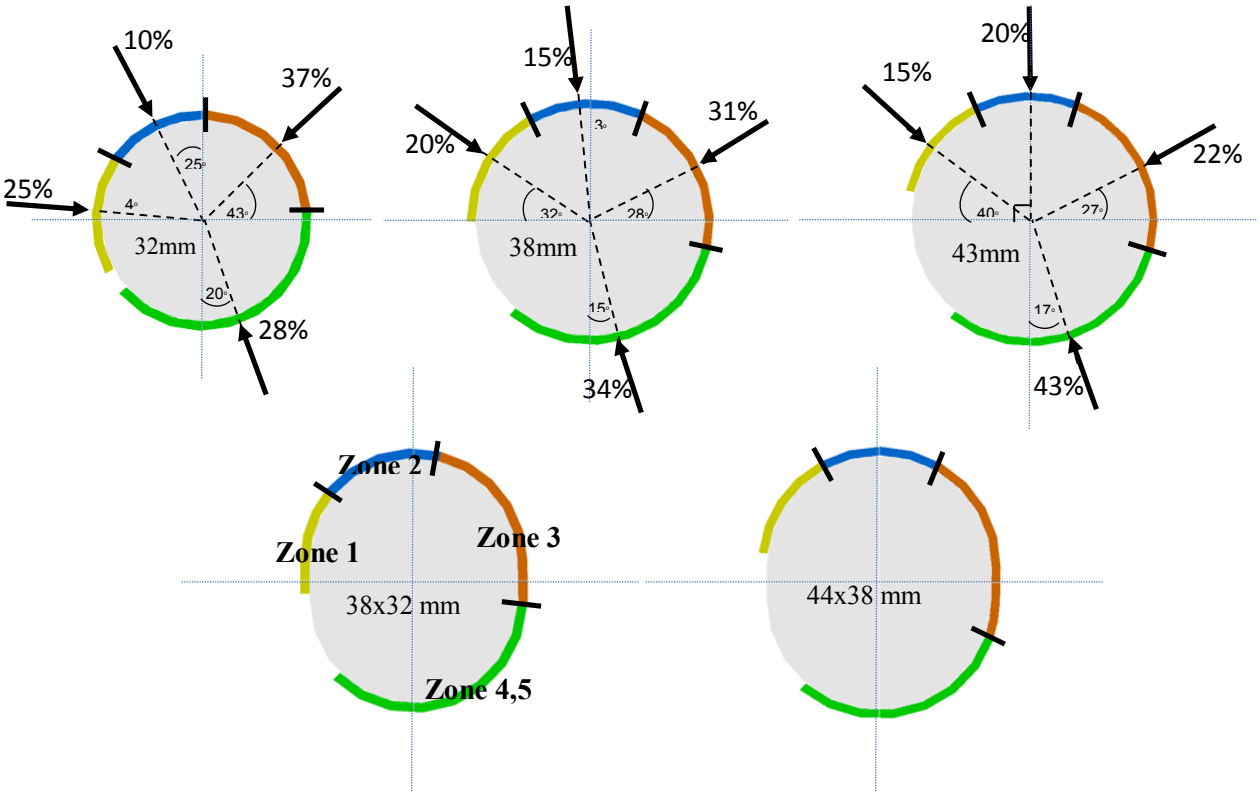

Figure 2.10: Locations of different contact zones on the cylindrical and elliptical handles and the distribution of mean contact force ratio (Hand size = 9).

Considering the FlexiForce sensor width of 40 mm each sensor would cover a span of ± 36°, ± 30°, and ± 27° about the vertical centerline for the 32, 38 and 43 mm handles, respectively, as shown in Figure 2.11. For the 38 mm diameter handle, which is widely recommended in the standardized test methods [33], it is observed that the center of pressure of the zones 4 and 5 lies about 15° from the central axis. Furthermore, zone 1 reveals a relatively higher CFR value. It was therefore deduced that the two sensors shifted by 5 mm counter-clockwise from the central axis may yield better estimates of the palm- and finger-side forces. Static and dynamic calibrations of the sensors were thus performed by locating two sensors symmetrically about the central axis of

the handles and by shifting them by 5 mm counter-clockwise from the central axis, denoted hereafter as ‘0 mm’ and ‘5 mm’, respectively.

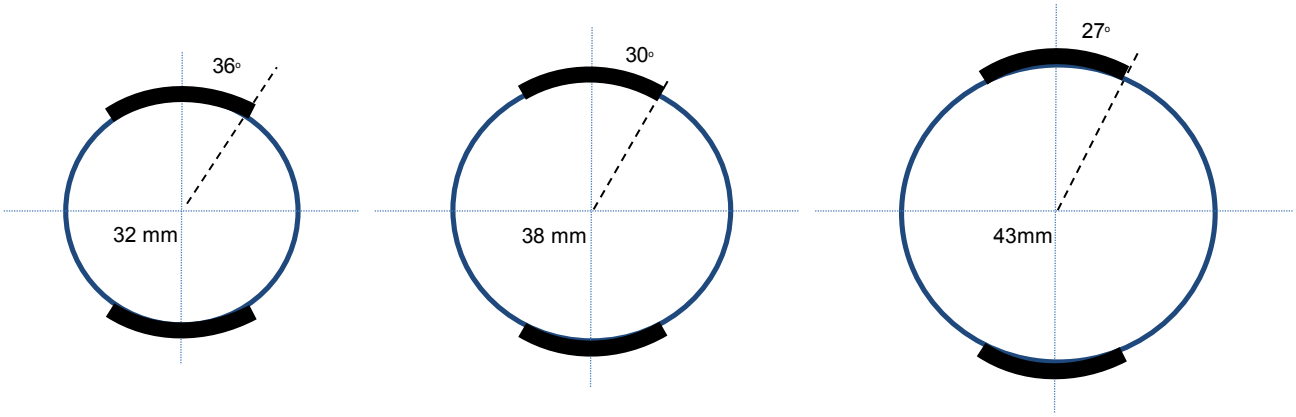

Figure 2.11: Sensor placement maps of ‘0 mm’ sensor locations for the cylindrical handles.

2.2.4. Applications of sensor to the instrumented handles under static and dynamic conditions

The feasibility of the sensors for measuring hand-handle grip and push forces were evaluated using three instrumented cylindrical handles (32, 38 and 43 mm in diameter) and two elliptical handles (38×32 and 44×38 mm). Two FlexiForce sensors were placed on each handle in order to measure the hand forces imparted on the handles by the subjects. The measurement of hand-handle forces, handle construction, handle mounting and hand-handle test methodology are presented below. The hand grip and push forces imparted on the handle were obtained from the palm and finger forces measured by the FlexiForce sensors. According to the international standard [9] the grip and push forces can be derived from the combination of axially applied palm and finger forces along the forearm axis. The palm force displaces the handle in the positive push direction; thus, the palm force is identical to the push force in the absence of finger force. Moreover, a push force is synonymous to a ‘displacement’ force. Applying only a finger force will pull the handle towards the subject and hence is indicated by an opposite sign compared to a pure palm motion.

The resultant of a palm and finger force combination is the push force and is defined as the difference between palm and finger forces as shown in Figure 2.12:

$$F_p = F_{palm} - F_{finger} \tag{2.3}$$

Where F_p is the push force, F_{palm} is the palm force and F_{finger} is the finger force.

The hand grip force is synonymous to the 'squeezing' force and a pure gripping action does not displace the handle's position. The handle experiences a push or pull only when the palm and finger forces are unequal. The grip force is defined as the scalar sum of the palm and finger forces minus the push force [53]:

$$F_g = \frac{1}{2}\left(F_{palm} + F_{finger} - \left|F_{palm} - F_{finger}\right|\right) \tag{2.4}$$

Where F_g is the grip force.

The term '$F_{palm} - F_{finger}$' in the above equation is the hand push force as seen in (2.3). The absolute value of the push force is used since the overall push force under a pulling action is negative. Finally, it is important to note that the grip force under a pushing action equals the finger force. The measurements were performed using standardized instrumented handles. Two FlexiForce sensors were applied to each handle (displayed as the shaded regions) to measure the axial components of the palm and finger forces as shown in Figure 2.12.

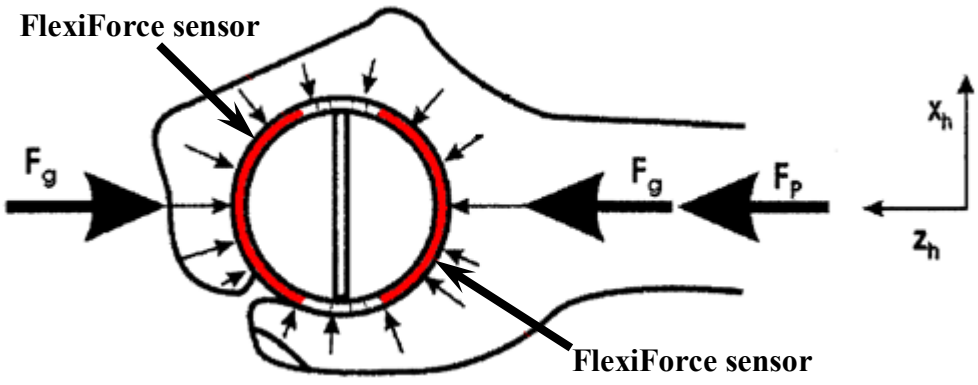

Figure 2.12: Application of FlexiForce sensors used to estimate palm and finger axial force components.

The validity of the sensors placed symmetrically about the z_h axis (shown in Figure 2.12) and with the sensors offset by 5 mm in the counter-clockwise direction was evaluated for the five handles. The three cylindrical handles were fabricated based on the designs recommended in the international standard ISO-10819 [33]. Each handle was designed as a split handle to accommodate force measurement sensors and an accelerometer to measure handle vibration. Figure 1.4 depicts the exploded view of an instrumented cylindrical handle. The handle cap is removable to allow for two reference grip force measurement sensors (Kistler model 9212) and a tri-axial accelerometer (PCB 356A01) to be fitted within the handle cavity. Two additional force sensors (Kistler model 9317b) are installed on the electrodynamic shaker mounting block to measure the reference push force also shown in Figure 1.4. Two FlexiForce sensors are placed on the exterior surface of the handle to measure the palm and finger forces. Figure 2.13a further shows the reference grip force sensors and accelerometer placement in the handle cavity, while Figure 2.13b shows the reference push force sensors mounted on the handle bracket as well as the FlexiForce sensors placed on the handle for the 0 mm. The overall measurement setup is shown in Figure 2.13c.

2.2.5. Measurement of static and dynamic hand-handle forces

Nine adult male subjects were recruited for the first two of the four test phases involving the FlexiForce sensors. Eight subjects were chosen for the static tests on the sensors, while seven subjects participated in the dynamic measurements. Each subject's hand was measured according to the guidelines established in [44]. Table 2.1 displays these measurements along with the nine subjects' height and weight values.

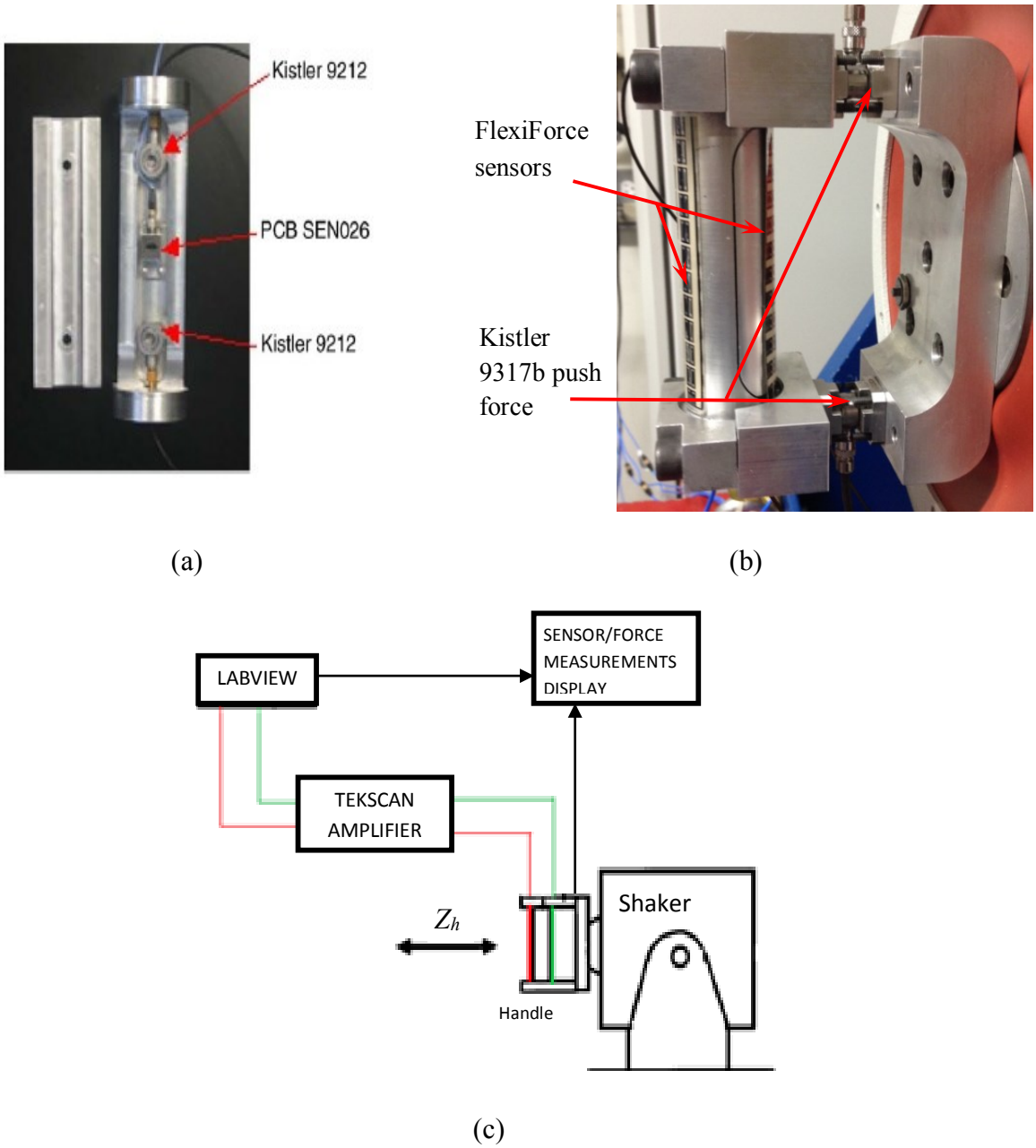

Figure 2.13: (a) Split handle design with grip force sensors and an accelerometer; (b) Assembled split handle design showing FlexiForce sensors and push force sensors applied on the bracket mount; and (c) Experimental setup for calibrations of FlexiForce sensors under static and dynamic conditions.

Subject#	Height (cm)	Weight (kg)	Hand Length (cm)	Width at metacarpal (cm)	Width at thumb (cm)	Length of Distal phalange (cm)	Length of middle phalange (cm)	Length of proximal phalange (cm)	Palm length (cm)	Hand thickness at thumb (cm)	Hand size
1	182.0	95	19.0	8.6	9.9	1.6	2.5	2.5	11.8	4.2	**9**
2	164.5	75	18.2	8.2	10.0	2.3	2.4	2.4	10.2	4.9	**8-9**
3	178.0	65	18.5	8.4	10.1	2.7	2.4	2.5	10.8	3.1	**9**
4	176.5	91	20.5	9.5	10.9	2.9	3	3.1	12.0	5.1	**10**
5	164.0	62	20.0	8.0	9.6	2.9	2.6	3.1	11.2	4.6	**10**
6	175.3	77	18.2	7.7	9.6	2.3	2.1	2.9	11.0	3.8	**8-9**
7	173.2	70	17.0	8.5	9.9	2.5	2.7	2.5	10.1	4.0	**8-9**
8	188.0	74	19.7	8.6	10.4	2.7	2.5	2.9	11.7	4.2	**10**
9	180.0	77	21.2	8.7	10.4	3.1	2.7	3.1	12.8	4.5	**10-11**
Mean	175.7	76.2	19.1	8.5	10.1	2.6	2.5	2.8	11.3	4.3	
SD[1]	7.78	10.9	1.32	0.50	0.42	0.45	0.25	0.30	0.88	0.60	

[1]SD – standard deviation

Table 2.1: Hand dimensions, standing height and mass of nine subjects.

The static calibrations were performed using twelve different combinations of push (25, 50, 75 N) and grip forces (10, 30, 50 N) considering both sensor positions for all five instrumented handles. The dynamic calibration were conducted on the 38 and 43 mm cylindrical handles with the 0 mm sensors position. Two levels of broadband random vibration signals with 1.5 and 3.0 m/s^2 frequency weighted RMS acceleration with a nearly flat acceleration power spectral density (PSD) in the range of 4-1000 Hz were used during the dynamic phase. For both tests, each the subject was asked to grasp the handle while maintaining a 90^o angle at the elbow joint and ensuring the forearm is collinear with the axis of motion as recommended in [33]. Table 2.2 lists the randomized force combinations used for both static and dynamic tests as well as all other test conditions.

Randomized hand forces		
Push (N)	Grip (N)	Static calibrations
0	0	**Cylindrical handles:** 32 mm, 38 mm, 43 mm
75	30	**Elliptical handles:** 32 x 38 mm, 38 x 44 mm
50	50	**Sensor Positions**: 0 mm and 5 mm
75	10	**Number of subjects:** 8
25	30	**Posture**: Standing upright with 90^{o} elbow angle
0	30	
25	50	Dynamic calibrations
0	50	**Excitation:** Broadband random vibration in 4 - 1000 Hz frequency range; 1.5 and 3.0 m/s^2 weighted RMS acceleration
75	50	
50	10	**Cylindrical handles:** 38 mm, 43 mm
50	30	**Sensor Position**: 0 mm
25	10	**Number of subjects:** 7
0	10	**Posture**: Standing upright with 90^{o} elbow angle

Table 2.2: Test protocol summary for static and dynamic calibrations of the FlexiForce sensors applied to instrumented handles.

Each subject was allowed several practice trials to become accustomed to the grasping method and the force levels. It was established from the static sensor calibrations that several sensors would be required due to their gradual degradation with usage. Hence, the sensors were replaced during the testing whenever their output no longer produced linear or consistent results due to degradation. Since the sensors used during the dynamic phase differed from the set used during the static phase a static measurement was repeated prior to each dynamic measurement.

2.2.6. Measurement of hand forces on a percussion tool

The estimation of hand-handle forces under the influence of an impact tool using the FlexiForce sensors was performed on a chipping hammer (model 11313 EVS, BOSCH) handle. The tool comprised a variable speed electric drive capable of delivering 1300 to 2600 blows per minute (BPM) under no load condition. The operator would normally grasp the tool using its two handles. The measurements were conducted with sensors placed on the primary handle, located on the main tool housing with the motor drive, where the operator imparted the grip and push forces. The secondary handle was located near the chuck, which was used for necessary tool guidance.

The tool was positioned in an energy dissipater in the laboratory, where the chisel bit was replaced by an anvil, as recommended in [50]. Considering an upright posture of a standing operator, it was decided to place the sensors on the top and bottom surfaces of the primary handle for measurements of the palm and finger forces, as shown in Fig. 2.14. Masking tape was used to secure the sensors to the handle surface. The measured palm and finger forces were subsequently applied to determine the hand grip and push forces using Eqs. (2.3) and (2.4), which were also displayed to the experimenter and the subject, when necessary.

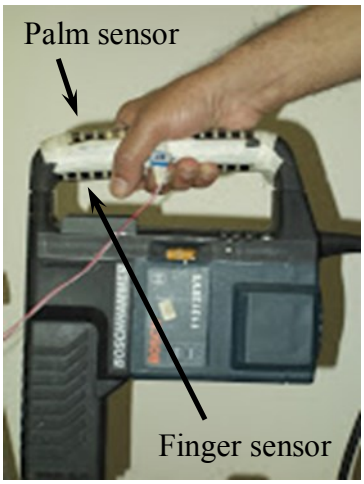

Figure 2.14: Palm- and finger-side FlexiForce sensors installed on the chipping hammer handle.

The measurements with the chipping hammer were conducted in three sequential stages using three subjects. The first stage involved the determination of static sensitivities of the palm and finger sensors. In the second stage, the validity of the sensors was examined for different combinations of grip and push forces imparted by each subject on the stationary tool handle. In the final stage, the measurements were repeated with each subject operating the tool. The tool speed was selected by the subject arbitrarily, while each measurement was repeated three times.

Unlike the simulated instrumented handle, the experiments with the tool handle posed difficult challenges in establishing the reference values of the palm and finger forces. The subject

stood on a force plate in an upright posture and the subject controlled the push force by monitoring the force plate signal. During the first stage of experiments, the palm side sensor was initially calibrated by applying four different palm forces (25, 50, 75 and 100 N). The subject was advised to hold the handle in a power grip manner and apply the desired push force, while ensuring nearly zero grip or finger force. This permitted the sensor evaluations under a more representative hand position for the tool operation. In this case, the finger FlexiForce sensor output was also displayed to the subject. All three subjects were able to achieve this condition with peak finger side force below 2 N. The data was subsequently used to determine the palm sensor sensitivity. For calibration of the finger side sensor, the subject applied a known palm force by monitoring the displayed outputs from both the palm sensor and the force plate, which were nearly identical. The subject was then advised to gradually increase the finger force to fully compensate the push force output of the force plate, while retaining steady output from the palm sensor. This approach provided reference values of the grip or finger force for the calibration of the finger-side sensor, which was conducted for four different levels of the finger force (25, 50, 75 and 100 N).

In the second stage of experiments, the validity of the calibrated FlexiForce sensors was examined while the subject grasped the handle under five different combinations of grip and push forces (F_g/F_p = 0/30, 30/30, 30/50, 30/75 and 50/75 N). The outputs of the force plate and the finger-side FlexiForce sensor were displayed for the subject to apply the controlled forces. The output of the palm sensor, however, was hidden from the subject. The validity of the FlexiForce measurements was evaluated through correlations between: (i) the push force estimated from the difference of the palm and finger sensors' outputs and the reference values obtained from the force plate; and (ii) the palm force and the coupling force (sum of the force plate and finger sensor

outputs). The order of grip and push forces was randomized and each measurement was repeated three times.

The methodology used in second stage was also employed in the final stage of the experiment, where the subject operated the tool. Neither the tool speed nor the handle vibration was monitored in this stage, since the goal was to examine validity of the FlexiForce sensors with the vibrating tool. All three stages of measurements were conducted in a sequential manner using a fresh set of FlexiForce sensors for each subject.

2.2.7. Measurement of biodynamic response of the hand-arm system

Measurements of biodynamic responses of the human hand-arm system were conducted using two different methods. The first method employed an instrumented 38 mm diameter cylindrical handle for acquiring dynamic palm and finger forces at the handle interface, which has been widely used in studies reporting DPMI of the hand-arm system [30, 51]. The handle's base fixture was installed on an electrodynamic shaker, as shown in Fig. 2.13c. The measured grip and push forces were processed through a low-pass filter and displayed to the subjects to allow maintenance of the hand forces in the desired ranges. A miniature accelerometer was also installed inside the handle to measure the handle vibration along the forearm axis (z_h-axis). This accelerometer also served as the feedback sensor for control and synthesis of the handle vibration via a vibration controller. In the second method, the dynamic palm and finger forces were measured using two FlexiForce sensors installed at the 0 mm position to obtain the DPMI response of the hand-arm system. One of the sensors was oriented to predominantly capture the dynamic force at the palm-handle interface, while the other sensor captured the finger side force.

The experiments were conducted simultaneously with both the measurement systems. Six adult male subjects participated in the study. The hand dimensions of each subject were measured

to obtain the hand size in accordance with EN-420 [44]. The hand size of the participants ranged from 8 to 10. The experiments were performed using nine different combinations of hand forces involved three different grip forces (10, 30 and 50 N) and three different push forces (25, 50 and 75 N). The measurements were conducted under two levels of broadband random vibration in the 4–1000 Hz range (frequency weighted rms acceleration = 1.5 and 3 m/s^2). A static calibration of the FlexiForce sensors was conducted for each subject prior to the dynamic measurements.

The signals from the handle accelerometer, instrumented handle force sensors and the FlexiForce sensors were acquired in a multi-channel data acquisition and analysis system (Brüel & Kjær Pulse system) to compute the DPMI of the hand-arm system. The hand-handle impedance computed from the instrumented handle was inertia corrected to account for contributions of the handle inertia, as described in [21]. The resulting DPMI response served as a reference for evaluating the feasibility of the FlexiForce sensors. The palm and finger FlexiForce sensors signals were analyzed in a similar manner to compute the palm- and finger-side DPMI responses. Each measurement was repeated twice. The data were acquired for a duration of 20 s during each measurement.

The mechanical impedance of the hand-arm system corresponding to each force combination and vibration level was measured in two stages involving the mechanical impedance at the palm (Z_{palm}) and the fingers (Z_{finger}). The handle was initially oriented to align the grip force measuring cap with the palm. The FlexiForce sensor was installed on the measuring cap of the instrumented handle to capture the palm force. The signals from the grip force sensors integrated within the instrumented handle, the FlexiForce sensor and the accelerometer were analyzed to derive the DPMI at the palm. The handle was subsequently rotated by 180 degrees to align the finger-side contact with the measuring cap, which provided the measurement of the finger side

force and the impedance. The total impedance of the hand-arm system Z could be obtained through summation of the palm and finger impedance [51]:

$$Z(j\omega) = Z_{palm}(j\omega) + Z_{finger}(j\omega) \tag{2.5}$$

Where ω is the excitation frequency in rad/s and $j = \sqrt{-1}$. In the above analysis, the palm force is the taken as sum of the grip and push forces measured by the instrumented handle [53].

2.3. Data Acquisition and Analysis

The two voltage outputs from the Tekscan FlexiForce sensors via the signal conditioner as well as the two grip and push force signals from the Kistler sensors via their respective charge amplifiers were routed to a data acquisition module (National Instruments NI-9172 DAQ). This device was paired with National Instruments LabVIEW data acquisition software for signal monitoring and storage. Figure 2.15 shows a sample LabVIEW screen with the four displayed outputs (Kistler push force in N, Kistler grip force in N, Tekscan palm voltage in mV and Tekscan finger voltage in mV). The signals were refreshed at a rate of four sample/s while the LabVIEW screen was projected on a monitor placed near the eye level approximately 1 m from the subject. The subjects were asked to grasp the handle and maintain the desired grip and push forces by monitoring the display. The reference force signals and the FlexiForce sensors signals were recorded for 5 s and three trials were taken for each measurement.

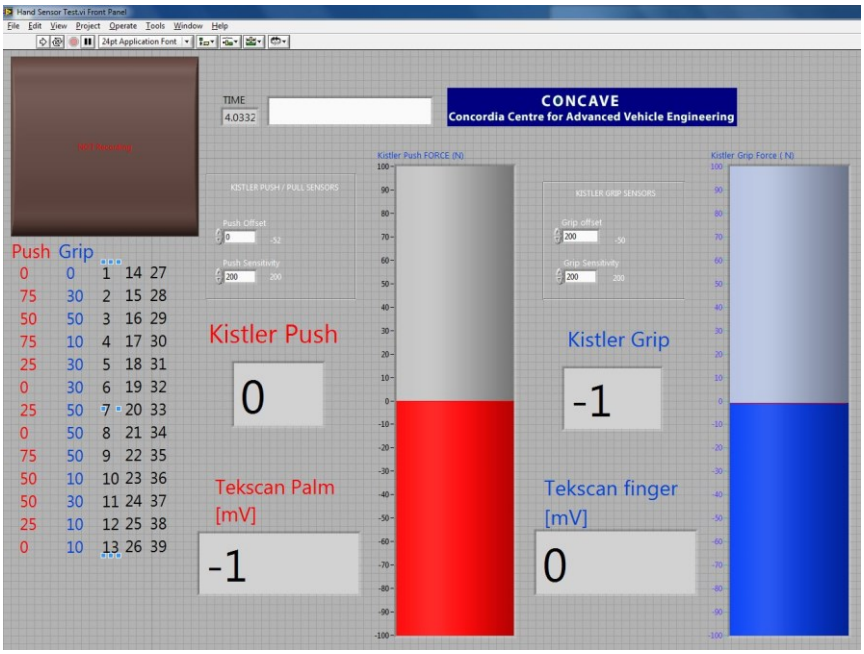

Figure 2.15: On screen display of the four acquired force signals.

The Kister palm force was calculated based on Eq. (2.6) derived from Eq. (2.3). The Kistler finger force was taken as equal to the Kistler grip force.

$$F_{kis,palm} = F_{kis,g} + F_{kis,p} \tag{2.6}$$

Where $F_{kis,palm}$ is the Kistler palm force, $F_{kis,g}$ is the measured Kistler or reference grip force and $F_{kis,p}$ is the measured Kistler or reference push force.

The mean static sensitivity of the FlexiForce sensors amongst the three trials was calculated using Eqs. (2.7a) and (2.7b), while the FlexiForce palm and finger forces were calculated using Eqs. (2.8a) and (2.8b).

$$S_{palm} = \frac{F_{kis,palm}}{V_{palm}} \tag{2.7a}$$

$$S_{fin} = \frac{F_{kis,fin}}{V_{fin}} \tag{2.7b}$$

$$F_{tek,push} = S_{palm}V_{palm} - S_{fin}V_{fin} \tag{2.8a}$$

$$F_{tek,grip} = \frac{1}{2}\left(S_{palm}V_{palm} + S_{fin}V_{fin} - \left|S_{palm}V_{palm} - S_{fin}V_{fin}\right|\right) \tag{2.8b}$$

Where $F_{kis,fin}$ is the equal to the reference grip force, V_{palm} is the measured Tekscan palm voltage, V_{fin} is the measured Tekscan finger voltage, $F_{tek,push}$ is the Tekscan push force and $F_{tek,grip}$ is the Tekscan grip force.

The resulting Tekscan FlexiForce grip and push force values obtained from the FlexiForce signals were compared with the measured reference values with the expectation that the comparison would result in a unity ratio between the two.

2.4. SUMMARY

Detailed experimental methods presented in this chapter were used to characterize the properties of the sensors and assess their feasibility for the measurement of hand-handle interface forces and the hand-arm system biodynamic response. The results of the measurements are presented in the manuscripts in Chapters 3 and 4. The detailed properties of the sensors could not be presented in its entirety in Chapter 3 and are presented in Appendix A.

CHAPTER 3
MEASUREMENT OF COUPLING FORCES AT THE POWER TOOL HAND-HANDLE INTERFACE

3.1. INTRODUCTION

Occupational exposure to hand-transmitted vibration (HTV) arising from operating hand-held power tools has been associated with an array of adverse health effects, including vascular, neurological and musculoskeletal disorders, collectively termed as hand-arm vibration syndrome (HAVS) and Raynaud's syndrome of occupational origin [1-3]. The magnitude and frequency of HTV are strongly influenced by the coupling forces, grip type, handle geometry and other inter-individual factors. The HTV exposure is measured in terms of frequency-weighted acceleration of the vibrating tool handle using the method described in [5]. However, the guidelines do not account for the effects of coupling forces exerted at the hand-handle interface, although many studies have shown the importance of these forces in the transmission of vibration to the hand-arm system [10]. The hand-handle interface coupling force, often considered as a combination of the grip and push forces, permits the flow of vibration energy from the tool into the hand [9, 30]. The coupling force thus directly affects the severity of vibration transmitted to the operator's hand and arm [4, 8]. Furthermore, an increase in grip force tends to compress the soft tissues of the hand and fingers, which may lead to reduced blood flow in the fingers and thus a greater risk of developing Raynaud's syndrome [13].

A few recent studies have presented contradictory findings on the basis of the injury risks obtained from the ISO 5349-1 guidelines and epidemiological studies [6, 7]. [16] suggested the use of a hand force coupling factor to account for the effect of the coupling force on the vibration dosage of the hand-arm system. The study showed insignificant differences between the acute effects of the grip and push forces, and thus recommended the sum of the two to derive the

coupling force. A few studies have proposed additional weighting functions to account for strong effects of hand-handle interface forces on the exposure assessment [14-16].

Although the importance of considering the coupling forces on the quantification of the hand-arm vibration dosage has been widely recognized, the measurements of hand forces on vibrating tools have met only limited success. This is primarily attributed to the lack of definite relations between the static coupling forces and the HTV, and the lack of reliable measurement systems, particularly for field applications. Different designs of instrumented handles have been developed for measuring the hand forces with static as well as vibrating handles. [26] proposed an instrumented handle comprising 6 segments of cantilevers with strain gauges attached at the fixed end. [29] explored the designs of 6, 8 and 10 segment instrumented handles similar to the design presented by [26]. These studies concluded that a six segment instrumented handle provided more accurate measurements of coupling forces under various gripping tasks. A similar handle design was proposed for measurements of grip force and moments developed within the hand-handle interface [28]. The instrumented handles employing piezoelectric load cells have been designed for measurements of the static and dynamic hand grip and push forces for studies on hand-arm biodynamic responses to vibration and for the assessment of anti-vibration gloves [11, 30-33].

While the aforementioned instrumented handles have been widely used in the laboratory for measurement of hand forces with static as well as vibrating handles, their implementations to real tools in the field would involve considerable complexities. Furthermore, it has been reported that split instrumented handle designs affect the rigidity of the handle in an adverse manner. A number of studies have shown that instrumented handles employing either strain gauges or load cells are not always feasible for field usage with hand-held power tools since these require special fixtures [26, 28, 35, 36]. Moreover, [54] demonstrated the distribution of contact forces over a

hand surface's during wheelchair propulsion. It was concluded that an increase in contact surface area resulted in lower contact forces.

[55] used a hydro-electric force meter along with an ALP pressure transducer and electronic manometer to measure coupling forces during logging operations. Calibrations results yielded highly favourable force measurement results (0–1.29% error) with forces in the range of 55–300 N; however, error exceeded 25% for smaller forces within the 0–55 N range. Since the current study employs a variety of low level forces alternate methods of measurement were explored.

In recent years, a few studies have explored the feasibility of thin film pressure sensing systems for the measurement of hand-handle coupling forces. These semiconducting, capacitive and resistive sensors exhibit adequate flexibility for applications to handles with different cross-sections and curved surfaces. The capacitive sensors consist of dielectric material separated by elastomeric layers and thus provide adequate flexibility and capacitance variations with the applied normal load. Resistive sensors, on the other hand, are designed with pressure-sensitive resistors encased between two thin polymer layers. [13] employed a 6×6 matrix of capacitive sensors on a cantilevered split handle for the measurement of grip pressure distribution under static as well as dynamic conditions. Subsequently, [37, 38] used the capacitive sensing matrices for the acquisition of hand-handle contact and coupling forces under static conditions alone. The studies employed instrumented handles with load cells for the verification of the capacitive sensing matrix, and proposed empirical expressions relating grip, push, coupling and contact forces as a function of the handle size. These studies have shown that the capacitive sensing matrix could provide accurate measurements of hand-handle grip, push and contact forces in a static laboratory setting under a controlled hand-arm posture. [40] used the similar sensing matrix for the determination of hand

grip force imparted on a hand-held olive harvester. [39] used the capacitive sensing matrix to map distributed hand-handle interface forces under different gripping and pulling tasks.

[17] further explored a capacitive pressure sensing matrix, developed by Novel GmbH, to measure the grip and push forces on power tools as a part of the comprehensive VIBTOOL project, sponsored by the European Union. Although the VIBTOOL project clearly demonstrated the reliability of the capacitive pressure sensing matrix for measurement of the hand-handle interface pressure distributions and coupling forces, the measurement system is not considered to be well-suited for field applications due to its very high cost. The capacitive sensors are also known to be relatively fragile and may incur damage and/or failure during field applications. Moreover, the validity of such sensors in capturing the dynamic hand-handle forces in frequency ranges of power tools has not yet been demonstrated.

Alternatively, a few studies have explored low cost force sensing resistors (FSR) for the measurement of hand-handle interface forces. Similar to the capacitive measurement system the FSR have also been applied in different matrix arrangements for the acquisition of interface force distributions. [42] evaluated three different thin and flexible sensors for measurements of grip force imposed on a golf club. These included a resistive force sensing grid (model 9811, Tekscan), an arrangement of small-size FlexiForce sensors, developed by Tekscan Inc. (USA), and flexible Quantum tunneling composite (QTC) sensors developed by Peratech, Holdco Limited, UK. The study evaluated relative performance of the sensors under controlled laboratory conditions in terms of static accuracy, hysteresis, repeatability, drift errors, dynamic accuracy, shear loads and surface curvature effects. The study concluded better performance of the resistive force sensing grid and Flexiforce sensors compared to the QTC sensor, although all the sensors revealed high drift errors. The results of the study further showed reduced measurement sensitivities of both the resistive

sensors compared to the static sensitivity of the QTC sensor. Furthermore, the sensitivity of all the three sensors decreased with their usage. In a recent study, [43] applied resistive pressure sensors (Tekscan 3200) to study the influence of handle diameter on the hand forces. The findings of the study were similar to those reported in [17, 37, 38].

The resistive pressure sensing systems, owing to their substantially lower cost and flexibility, offer attractive potential for measurements of hand-handle coupling forces in the field during typical work conditions. Such sensing matrices have been commercially developed with high-speed scanning hardware and software, which could permit acquisition of the coupling forces in both static as well as dynamic environments [47]. The primary advantage of such sensors is their very low cost compared to the capacitive sensors. The effectiveness of such sensors in providing reliable measurements of hand-handle interface forces under different static and dynamic conditions, however, has not yet been thoroughly explored.

This study describes the development and assessments of a measurement system using low-cost flexible resistive sensors (FlexiForce) for acquiring hand-handle interface forces in static as well as dynamic conditions. The properties of the FlexiForce sensors were systematically evaluated and optimal locations of two sensors on the handle surface were determined for accurate measurements of the hand forces. The validity of the proposed measurement system under static as well as dynamic conditions was demonstrated through measurements obtained with standardized instrumented handles. The feasibility of the proposed measurement system was further evaluated with a vibrating tool handle under different combinations of grip, push and coupling forces.

3.2. Materials and methods

Experiments were designed to: (i) evaluate static properties of the FlexiForce sensors in terms of linearity, hysteresis and repeatability when applied to flat as well as curved surfaces; (ii) identify appropriate positions of the FlexiForce sensors on a handle for accurate measurements of hand forces; and (iii) assess feasibility of the sensors for measuring hand forces on laboratory as well as tool handles under stationary and vibration conditions.

3.2.1. Development of force measurement system

A low cost hand-handle interface force measurement system was developed for the measurement of hand grip and push forces imparted on tool handles. Resistive FlexiForce sensors (model 1230, Tekscan Inc., USA) were selected for this study due to their many distinct advantages. The thin (0.208 mm) and flexible sensors could be applied to the curved handle surfaces. Each sensor measured 149×40 mm and could be trimmed to a desired length to adapt to different sizes of tools handles. Each sensor comprised a matrix of 102 closely-spaced sensing cells or sensels. The effective contact area would thus not only rely on the total number of sensels covered by the applied load but also the load position on the sensor. The resistive sensors provided rapid response and required minimal signal conditioning. Unlike the pressure sensing systems, which comprise a large matrix of sensors, the selected sensor is applied as a single unit to measure the total force imposed on the entire contact surface, and thereby could provide measurements at a very high sampling rate.

A dual-channel signal conditioner was developed for simultaneous acquisition of data from two sensors located on a handle. The conditioning circuit was initially developed using the design recommendation by Tekscan, which revealed substantial drift in the output, as reported by [42]. Moreover, saturation of the output was also observed even under a low level force. The

conditioning circuit with a variable gain circuit was subsequently developed to obtain measurements in the 0–200 N range. A zeroing circuit was also integrated to offset a possible bias due to preload on the sensor and to control the drift.

3.2.2. Characteristics of FlexiForce sensors

The static calibrations of 12 different FlexiForce sensors coupled with the dual-channel signal conditioner were initially performed on a flat surface to examine linearity, hysteresis and repeatability properties of the measurement system. The loading on each sensor was applied using a force indenter (Dillon GL 500 force gauge, USA) with a digital force display with a resolution of 0.2 N. The force was applied through an 8 mm thick elastomeric pad to ensure more uniform contact with the sensor. The elastomer was permitted to relax for nearly 1 minute after each load change until a steady force value was attained. Measurements were conducted by gradually increasing the force applied to the sensor from 0–120 N in increments of about 10 N. The applied force was gradually decreased to 0 N in order to evaluate hysteresis of the sensors. Measurements were repeated for three loading and unloading cycles to examine the repeatability.

The effect of sensor length and the loading pad size on the sensor output was also evaluated through measurements on a flat surface. A number of 149 mm long standard sensors were trimmed to 117 mm length so as to apply them onto a standardized instrumented handle [33]. The measurements were initially performed on a nominal sensor. The same sensor was subsequently trimmed and its output was compared with that of the nominal to assess the effect of sensor length. The trimmed sensor, however, was loaded using a relatively shorter pad (115.6×32.7 mm). The effect of size and location of the loading elastomer pad on the sensors' output and linearity was also examined through repeated measurements. For this purpose, three different rectangular shaped elastomeric pads (141.7×33.3, 115.6×32.7 and 60.7×30.0 mm, denoted 'long', 'medium' and

'short', respectively) were placed around the center of a nominal-length sensor, and the sensor outputs were measured under static loads up to 100 N. A smaller pad (60.7×30.0 mm) was further used to study the effect of position of the loading pad on the sensor surface by placing the pad at four different positions along the sensor's long-axis. [42] suggested that the output of a FlexiForce sensor decreases with its usage. The experiment was designed to measure the outputs of two different sensors over a period of about three weeks to evaluate the deterioration of the sensor output with usage.

The input-output properties of the sensors were subsequently evaluated when placed on a cylindrical surface to assess their feasibility for applications to tools handles. For this purpose, a curved loading cap was designed to apply uniform loading on the sensor positioned on the curved surface, as seen in Fig. 3.1. A 2 mm thick elastomer was applied to the curved surface to ensure more uniform contact between the senor and the loading cap. A preload of 7 N was also applied to the cap prior to the measurements. The stiffness of this elastomer was substantially lower than that of the loading pad used for experiments on the flat surface.

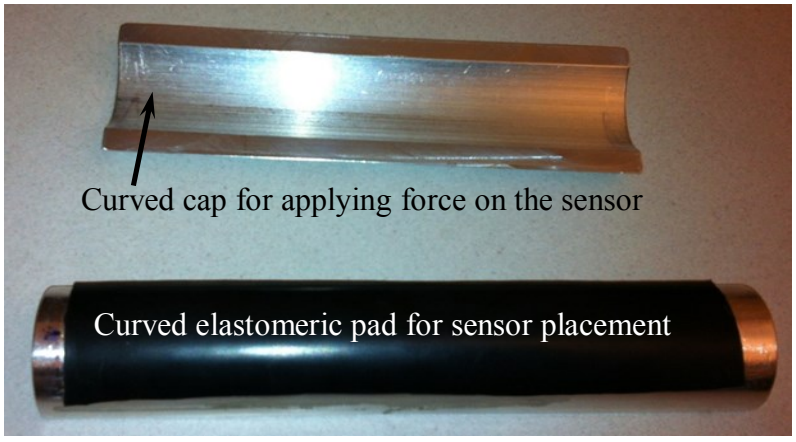

Figure 3.1: Cylindrical surface with a soft loading pad and custom designed cylindrical cap.

3.2.3. Identification of FlexiForce sensors positions on handles

The international standard ISO 15230 [9] defines the push force as the sum of axial components (along the forearm axis) of the hand-handle contact force, as shown in Fig. 3.2(a). The grip force is the resultant compensated axial force within the hand due to opposing gripping actions of the palm and the fingers. While the push force may be directly related to the net force imparted on the handle, the grip force is expressed by the compensating axial force on the finger side. The relationships between the palm and finger forces, and the grip and push forces can thus be expressed as [53]:

$$F_g = \frac{1}{2}\left(F_{palm} + F_{finger} - \left|F_{palm} - F_{finger}\right|\right) \quad (3.1)$$

$$F_p = F_{palm} - F_{finger} \quad (3.2)$$

where F_g and F_p are the grip and push forces, respectively, while F_{palm} and F_{finger} denote the axial components of the palm and finger contact forces, respectively.

The above relations suggest that the determination of hand grip and push forces require the measurements of axial force components on the palm and finger sides of the hand. The FlexiForce sensors applied around the palm and finger contact regions, as shown in Fig. 3.2(a), could provide good estimates of these force components.

The preliminary measurements conducted with the FlexiForce sensors, however, revealed substantial effects of the sensors positions around the handle and the handle size. The hand-handle interface pressure distributions, reported for different handle sizes, were thus analyzed to identify appropriate positions of the sensors to achieve reliable estimates of the hand grip and push forces. [37] reported distribution of the static contact force over five different zones of the hand, shown in Fig. 3.2(b), grasping cylindrical handles of three different sizes (30, 40 and 48 mm diameter). The study showed high contact pressure peaks and contact force in zone 4 (the upper lateral side

of the palm), particularly for the 40 and 48 mm diameter handles, and push force of 25 N or greater. The peak contact force, however, shifted towards the fingers-side (zones 1 and 2) in the absence of a push force. These findings were applied to identify suitable positions of the FlexiForce sensors for capturing the palm and fingers forces in a reliable manner for the handles considered in this study.

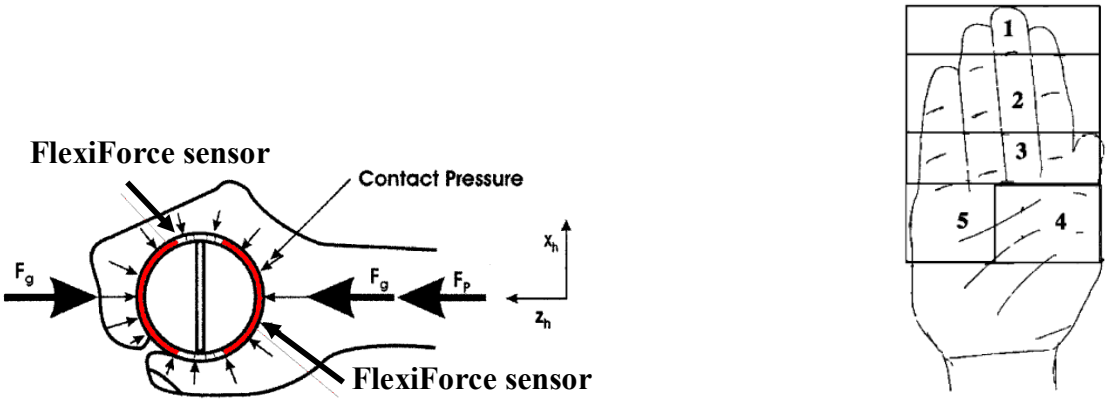

Figure 3.2: (a) Layout of two FlexiForce sensors on a cylindrical handle to obtain the axial components of the palm and finger contact forces; and (b) Illustration of five hand-handle contact zones defined for study of contact force distributions [37].

The hand-handle contact force and geometry were further studied by locating the dominant contact zones on different cylindrical and elliptical handles considering the hand dimensions of four subjects. The hand sizes of the selected subjects ranged from 9 to 10, as per [44]. The subjects' right hands were traced on a paper, which was then divided into five zones as seen in Fig. 3.2(b). The distributed contact force data reported for the three cylindrical handles by Aldien et al. were subsequently used to reflect the contact force ratios (CFR) corresponding to different zones [37]. The results were used to identify most suitable positions of the palm- and finger-side sensors on the handles. It should be noted that the diameters of the handles considered in the reported study differed from those employed in the current study.

3.2.4. FlexiForce sensors applied to instrumented handles

The experiments were conducted with the instrumented handles that have been widely used for characterization of hand-arm biodynamic responses and for assessment of antivibration gloves [11, 32, 33]. The linearity and repeatability of the FlexiForce sensors were evaluated when applied to different stationary instrumented handles. These included three cylindrical (diameter: 32, 38 and 43 mm) and two elliptical (32×38 and 38×44 mm) handles. Each handle employed force sensors to measure the hand grip and push forces, as described in [33], which served as the reference values. An accelerometer (model 356A01, PCB) was also mounted within the handle to measure handle vibration for characterizing the sensors' outputs under vibration.

Two FlexiForce sensors were positioned on each instrumented handle to measure the axial components of the palm- and finger-forces, as seen in Fig. 3.3(a), which was mounted on an electro-dynamic vibration exciter, as shown in Fig. 3.3(b). The signals from the handle's grip and push force sensors, and the FlexiForce sensors were acquired through a multi-channel data acquisition system (model cDAQ-9172, National Instrument). The grip and push forces obtained from the instrumented handle were displayed on a computer monitor that was installed about 1 m away from the subject grasping the handle. The force displays were refreshed at a rate of 4 samples/s. The grip and push forces estimated from the FlexiForce signals, using Eqs. (3.1) and (3.2), were compared with the respective reference values to evaluate their feasibility. Figure 3(b) schematically shows the measurement and the data acquisition setup.

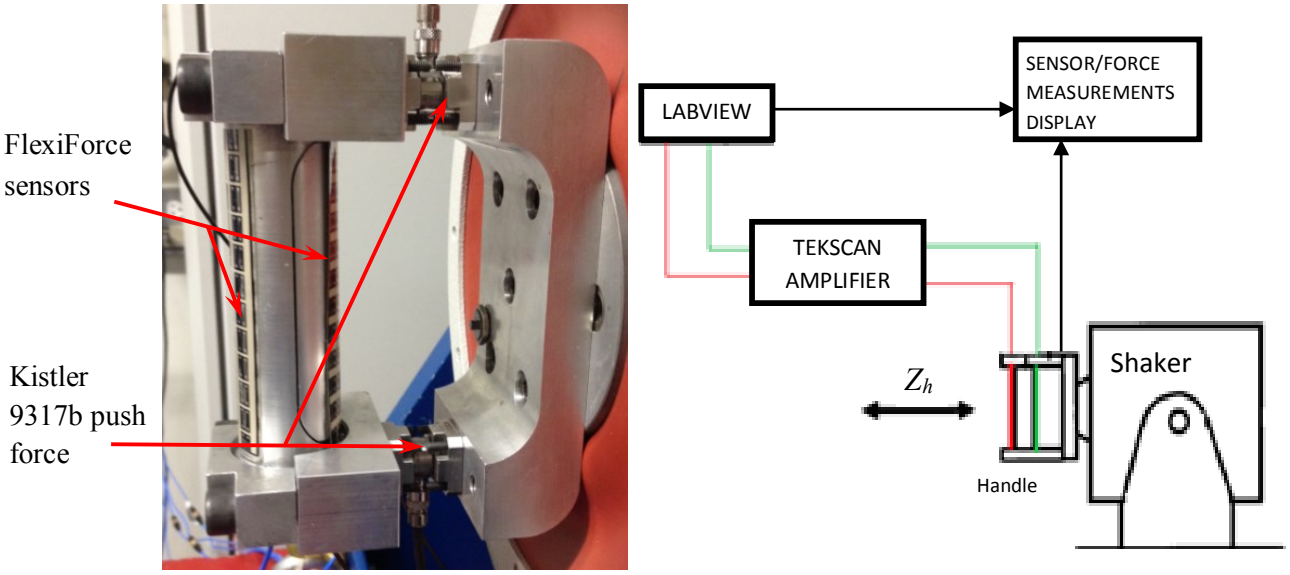

(a) (b)

Figure 3.3: (a) Instrumented handle with FlexiForce sensors supported on two push force sensors; and (b) Experimental setup for calibrations of FlexiForce sensors under static and dynamic conditions.

The static evaluations of the sensors were performed for all the five handles, considering two different positions of the FlexiForce sensors: (i) symmetrically about the handle central axis along the forearm, denoted as '0 mm'; and (ii) sensors shifted 5 mm counter clockwise from the handle centerline, denoted as '5 mm'. The two positions were selected to capture the dominant contact force between the palm and the sensor, and the fingers and the sensor. The outputs of the sensors positioned symmetrically (0 mm) were also obtained under vibration for two cylindrical vibrating handles (38 and 43 mm diameter). For this purpose, the vibration exciter was operated to generate two different levels of broadband random handle vibration (1.5 and 3.0 m/s^2 frequency weighted rms acceleration) with nearly flat acceleration power spectral density (PSD) in the 4 to 1000 Hz frequency range.

The static and dynamic calibrations of the sensors were performed considering combinations of 4 levels of the push force (0, 25, 50 and 75 N) and 3 levels of the grip force (10, 30 and 50 N). A total of 8 and 7 adult male subjects participated in the static and dynamic

experiments, respectively, from a pool of 9 total subjects. The protocols for all the experiments had been approved by the Research Ethics Committee of Concordia University prior to the study. Table 1 summarizes the dimensions of the subjects' right hand together with the hand size in accordance with [44].

The output sensitivity of the palm-side FlexiForce sensor, $S_{palm,}$ was obtained from the reference palm force $F_{r,palm}$ and the sensor output V_{palm}, such that:

$$S_{palm} = \frac{V_{palm}}{F_{r,palm}} \tag{3.3}$$

The reference palm force in the above relation was obtained from the grip and push forces measured by the instrumented handle, such that:

$$F_{r,palm} = F_{r,g} + F_{r,p} \tag{3.4}$$

where $F_{r,g}$ and $F_{r,p}$ are the reference grip and push forces, respectively, obtained from the instrumented handle. Similarly the sensitivity of the finger-side FlexiForce sensor, S_{finger}, was computed from the reference finger force $F_{r,finger}$ and the sensor output V_{finger};

$$S_{finger} = \frac{V_{finger}}{F_{r,finger}} \tag{3.5}$$

The reference finger force in the above equation is identical to the reference grip force $F_{r,g}$.

Prior to the experiments, each subject was briefly trained with regard to the gripping and pushing the handle while monitoring the hand grip and push forces, and the standing posture. Subjects were permitted a number of practice runs prior to the measurements. Each subject was advised to grip and push the handle with his right hand, while standing upright with 90^o elbow angle, and forearm aligned along the handle axis (z_h). The subject was asked to maintain a selected grip and push force combination for about 6 s by monitoring the reference force signals, while the order of forces was randomized. Each measurement was repeated three times. The signals from

the reference force and FlexiForce sensors were recorded for 5 s, after the subject demonstrated near stable forces within 10% of the desired forces. The static and dynamic measurements were conducted in a sequential manner to evaluate feasibility of the measurement system in the presence of handle vibration. The measured palm and finger force data were subsequently used to determine the grip and push forces using Eqs. (3.1) to (3.5). The data also provided the static sensitivity of the FlexiForce sensors together with their correlations with the reference signals.

3.2.5. Evaluations of FlexiForce sensors applied to a tool handle

An experiment was designed to evaluate the applicability of the sensors for measuring hand forces when coupled with a chipping hammer (model 11313 EVS, BOSCH) handle. The tool comprised a variable speed electric drive capable of delivering 1300 to 2600 blows per minute (BPM) under no load condition. The operator would normally grasp the tool using its two handles. The measurements were conducted with sensors placed on the primary handle, located on the main tool housing with the motor drive, where the operator imparts the grip and push forces. The secondary handle is located near the chuck, which is used for necessary tool guidance. The tool was positioned in an energy dissipater in the laboratory, where the chisel bit was replaced by an anvil, as recommended in ISO 8662-2 [50]. Considering an upright posture of a standing operator, it was decided to place the sensors on the top and bottom surfaces of the primary handle for measurements of the palm and finger forces (Fig. 3.4). Masking tape was used to fix the sensors to the handle surface. The measured palm and finger forces were subsequently applied to determine the hand grip and push forces using Eqs. (3.1) and (3.2), which were also displayed on-line to the experimenter and the subject, when needed.

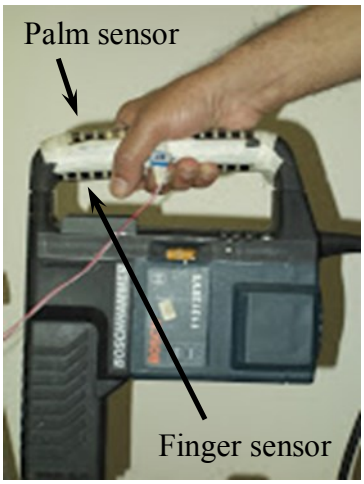

Figure 3.4: Palm- and finger-side FlexiForce sensors installed on the chipping hammer handle.

The measurements with the chipping hammer were conducted in three sequential stages using three subjects. The first stage involved the determination of static sensitivities of the palm and finger sensors. In the second stage, the validity of the sensors was examined for different combinations of grip and feed forces imparted by each subject on the stationary tool handle. In the final stage, the measurements were repeated with each subject operating the tool. The tool speed was selected by the subject arbitrarily, while each measurement was repeated three times.

Unlike the simulated instrumented handle, the experiments with the tool handle posed difficult challenges in establishing the reference values of the palm and finger forces. The subject stood on a force plate in an upright posture, and the subject controlled the push force by monitoring the force plate signal. During the first stage of experiments, the palm side sensor was initially calibrated by applying 4 different palm forces (25, 50, 75 and 100 N). The subject was advised to hold the handle in a power grip manner and apply the desired push force, while ensuring nearly zero grip or finger force. This permitted the sensor evaluations under a more representative hand position for the tool operation. In this case, the finger FlexiForce sensor output was also displayed to the subject. All 3 subjects were able to achieve this condition with peak finger side force below

2 N. The data was subsequently used to determine the palm sensor sensitivity. For calibration of the finger side sensor, the subject applied a known palm force by monitoring the displayed outputs from both the palm sensor and the force plate, which were nearly identical. The subject was then advised to gradually increase the finger force to fully compensate the push force output of the force plate, while retaining steady output from the palm sensor. This approach provided reference values of the grip or finger force for the calibration of the finger-side sensor, which was conducted for 4 different levels of the finger force (25, 50, 75 and 100 N).

In the second stage of experiments, the validity of the calibrated FlexiForce sensors was examined while the subject grasped the handle under 5 different combinations of grip and push forces (F_g/F_p = 0/30, 30/30, 30/50, 30/75 and 50/75 N). The outputs of the force plate and the finger-side FlexiForce sensor were displayed for the subject to apply the controlled forces. The output of the palm sensor, however, was hidden from the subject. The validity of the FlexiForce measurements was evaluated through correlations between: (i) the push force estimated from the difference of the palm and finger sensors' outputs and the reference values obtained from the force plate; and (ii) the palm force and the coupling force (sum of the force plate and finger sensor outputs). The order of grip and push forces was randomized and each measurement was repeated three times.

The methodology used in second stage was also employed in the final stage of the experiment, where the subject operated the tool. Neither the tool speed nor the handle vibration was monitored in this stage, since the goal was to examine validity of the FlexiForce sensors with the vibrating tool. All three stages of measurements were conducted in a sequential manner using a fresh set of FlexiForce sensors for each subject.

3.3. Results and discussion

3.3.1. Properties of the FlexiForce sensors

The measurements obtained with sensors placed on a flat surface generally revealed linear sensors' outputs with the applied load, although a few sensors revealed rapid output saturation. As an example, Fig. 3.5a illustrates the input-output characteristics of two different sensors acquired during gradual loading and unloading. The vast majority of the sensors, however, revealed linearity well below 3% and very low hysteresis (below 3.5%), while the static sensitivity of the sensors differed. Through further discussions with the manufacturer, it was recognized that these sensors were designed only for qualitative tactile sensing and would likely show poor repeatability of objective measurements across a sample of sensors. It was thus concluded that these sensors would be feasible for static force measurements provided that each sensor is calibrated individually.

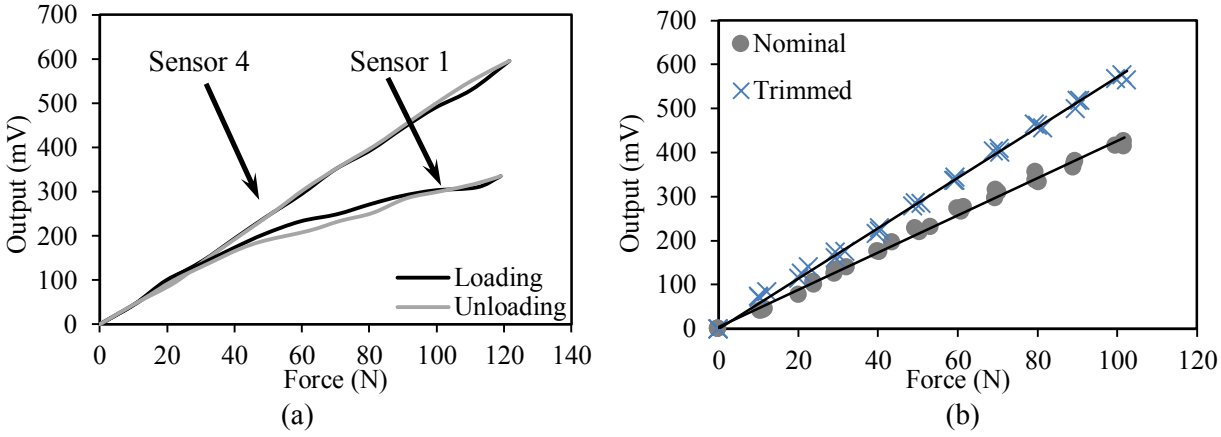

Figure 3.5: (a) Input-output properties of two sensors subject to gradual loading and unloading; and (b) Input-output characteristics of nominal length (149 mm) and trimmed length (117 mm) sensors during three trials.

Figure 3.5b illustrates the differences between the measured input-output properties of the nominal (149 mm long) and trimmed (117 mm long) sensors, obtained during three trials. The results are presented for the same sensor, which show reasonably good linearity (r^2>0.99) and good

repeatability of measurements during the three trials. The trimmed sensor, however, showed higher sensitivity compared to the nominal sensor, which was attributed to reduced contact area and thereby higher contact pressure under the same load. The mean sensitivity of the nominal sensor was obtained as 4.28 mV/N (SD = 0.06 mV/N), while that of the trimmed sensor increased to 5.71 mV/N (SD = 0.07 mV/N). The results suggest that output of the FlexiForce sensor depends on both the applied force and the effective contact area. Trimming of the sensor, however, does not affect the linearity.

The input-output properties of two sensors applied on the 38 mm diameter curved surface are compared in Fig. 3.6a. The figure shows measurements obtained during the three trials, which show nearly linear input-output properties and good repeatability, as observed in measurements on the flat surface. The sensors' outputs, however, differ from those obtained from the flat surface, which is partly attributable to differences in the effective contact area for the two surfaces, and in-part to differences in the elastomers used in two experiments as shown in Fig. 3.6b from the input-output results of sensor #4 when placed on the flat and curved surface.

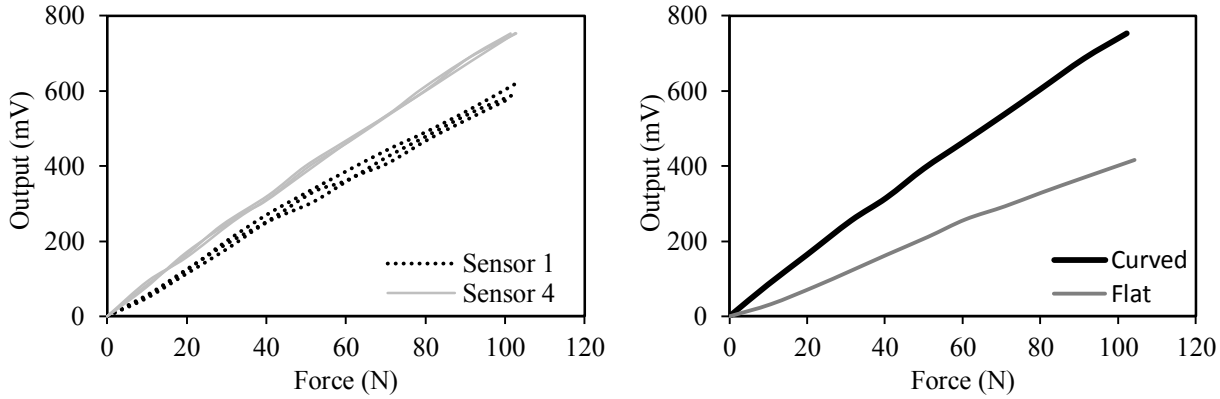

Figure 3.6: (a) Static input-output characteristics of two sensors subject to loading on the curved surface and (b) Sensor #4 input-output characteristics subject to leading on the flat vs. curved surface.

The input-output characteristics of the sensors were observed to depend upon the loading elastomer size, position, and stiffness. The repeated measurements were conducted with a relatively soft pad that was used for the curved surface in order to evaluate the effect of the loading

pad stiffness. The results shown in Fig. 3.7(a) suggest substantial effect of the pad stiffness on the sensor output. The substantially lower sensor output with the 'soft' pad was partly attributed to large deformations of the soft elastomer, which could cause non-uniform pressure distribution on the contact surface apart from longer relaxation time. The results suggest that the sensors' outputs would vary with different hand sizes and skin stiffnesses, when applied to power tools handles. A calibration of the sensors would thus be required for each individual subject.

The effective contact area and pressure between the loading elastomer and the sensor affect the sensor output in an opposing manner. The effective contact area relied not only on the total number of sensels covered by each loading pad but also its position on the sensor. Figure 3.7(b) presents the mean input-output properties of a sensor subject to loading via three elastomeric pads of different lengths (long: 141.7×33.3 mm; medium: 115.6×32.7 mm; short: 60.7×30.0 mm). The results suggest notable effect of the loading pad length. The short and long pads exhibit comparable sensor output only up to 60 N force, while the long pad yields lower output compared to the short pad under higher forces. This is most likely due to higher concentrated contact pressure imposed by the short pad on the sensor. The medium pad, however, resulted in considerably lower sensor output in the entire force range.

Figure 3.7(c) illustrates the effect of loading pad position on the mean sensor output. The figure presents the results obtained from the short loading pad positioned at four distinct locations along the long axis of a nominal sensor, as seen in Fig. 3.7(d). The 'position 1' refers to the pad located near the sensor edge (x=0 mm), while 'position 2' refers to the pad located symmetrically about the sensor center (x=44 mm). The 'position 3' and 'position 4' correspond to the pad located 60 mm and 85 mm, respectively, from the sensor edge. In each case, the pad covered a total of 42 sensels. The results clearly show substantial effect of position of the load on the sensor output. The

output sensitivities of the sensor were obtained as 3.68, 4.22, 2.45 and 1.93 mV/N, respectively, for the four loading positions considered. The results suggest strongly unpredictable relation between the sensor output and the loading pad position.

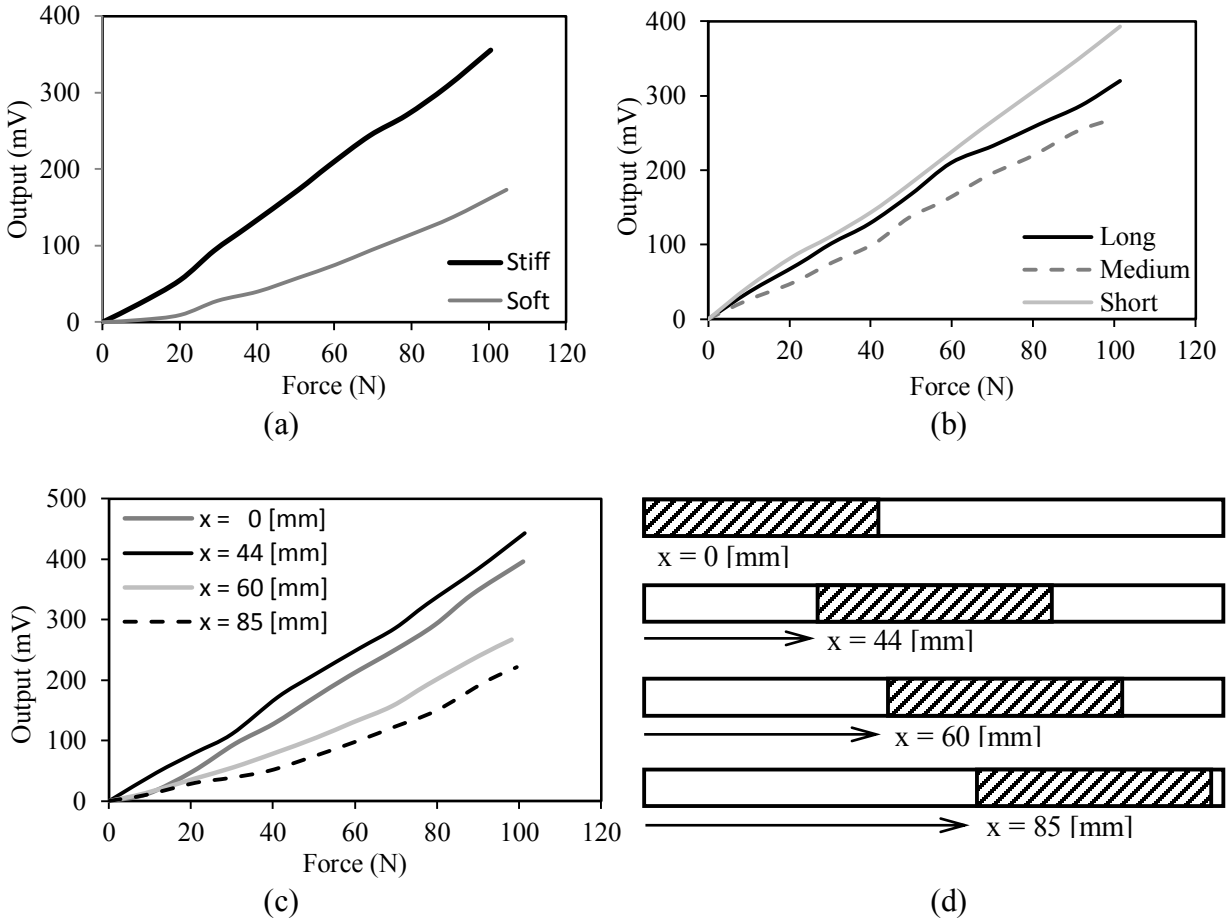

Figure 3.7: (a) Influence of elastomeric pad flexibility on the sensor output, (b) Effect of length of the loading pad on the sensor output, (c) Effect of elastomer load position on the sensor output and (d) visual representation of four load positions.

3.3.2. Identifications of FlexiForce sensors positions on the handle

The locations of the individual zone profiles, defined in Fig. 3.2(b), on the different cylindrical and elliptical handles were further mapped by considering the hand dimensions of four male subjects with hand sizes ranging from 9–10. Each subject's hand profile was traced while

grasping each handle. The trace was divided into four zones outlining zones 1–5 (with zones 4 and 5 considered as one overlapping zone). Figure 3.8(a) illustrates the mapping of the five hand-handle contact zones around the circumference of different cylindrical and elliptical handles. The figure also shows the proportions of mean CFR over each zone corresponding to 30 N grip and 50 N push forces, as reported by [37] for the cylindrical handles. The CFRs are indicated at the center of each zone, assuming uniform pressure over each individual zone. The proportions of mean CFR for the elliptical handles, however, were not available. From the illustration, it is evident that zones 4 and 5 are mostly located around the central axis of the handle on the palm-side, irrespective of the handle size. It is further seen that zone 2 also lies around the central axis on most of the handles, opposite to zones 4 and 5, with the exception of the smallest handle (32 mm diameter). In cylindrical handles, zone 3 also lies close to the central axis of the handles. Moreover, the majority of the contact force occurs within the zones 2 and 3, followed by zones 4 and 5.

From these results, it is deduced that a FlexiForce sensor covering zones 4 and 5 and positioned around the handle central axis could provide good estimate of the palm force. Another sensor covering zones 2 and 3, and positioned on the opposite side could provide good estimate of the finger force. Considering the FlexiForce sensor width of 40 mm, each sensor will cover a span of $\pm 36^{o}$, $\pm 30^{o}$, and $\pm 27^{o}$ about the vertical centerline for the 32, 38 and 43 mm handles, respectively, as shown in Fig. 3.8(b). For the 38 mm diameter handle, which is widely recommended in the standardized test methods [33], it is observed that the center of pressure of the zones 4 and 5 lies about 15^{o} from the central axis. Furthermore, the zone 1 reveals a relatively higher CFR value. It was thus deduced that the two sensors shifted 5 mm counter-clockwise from the central axis may yield better estimates of the palm and finger forces. Calibrations of the sensors

were thus performed by placing two sensors symmetrically about the central axis of the handles, and shifting them by 5 mm, denoted hereafter as ‘0 mm’ and ‘5 mm’, respectively.

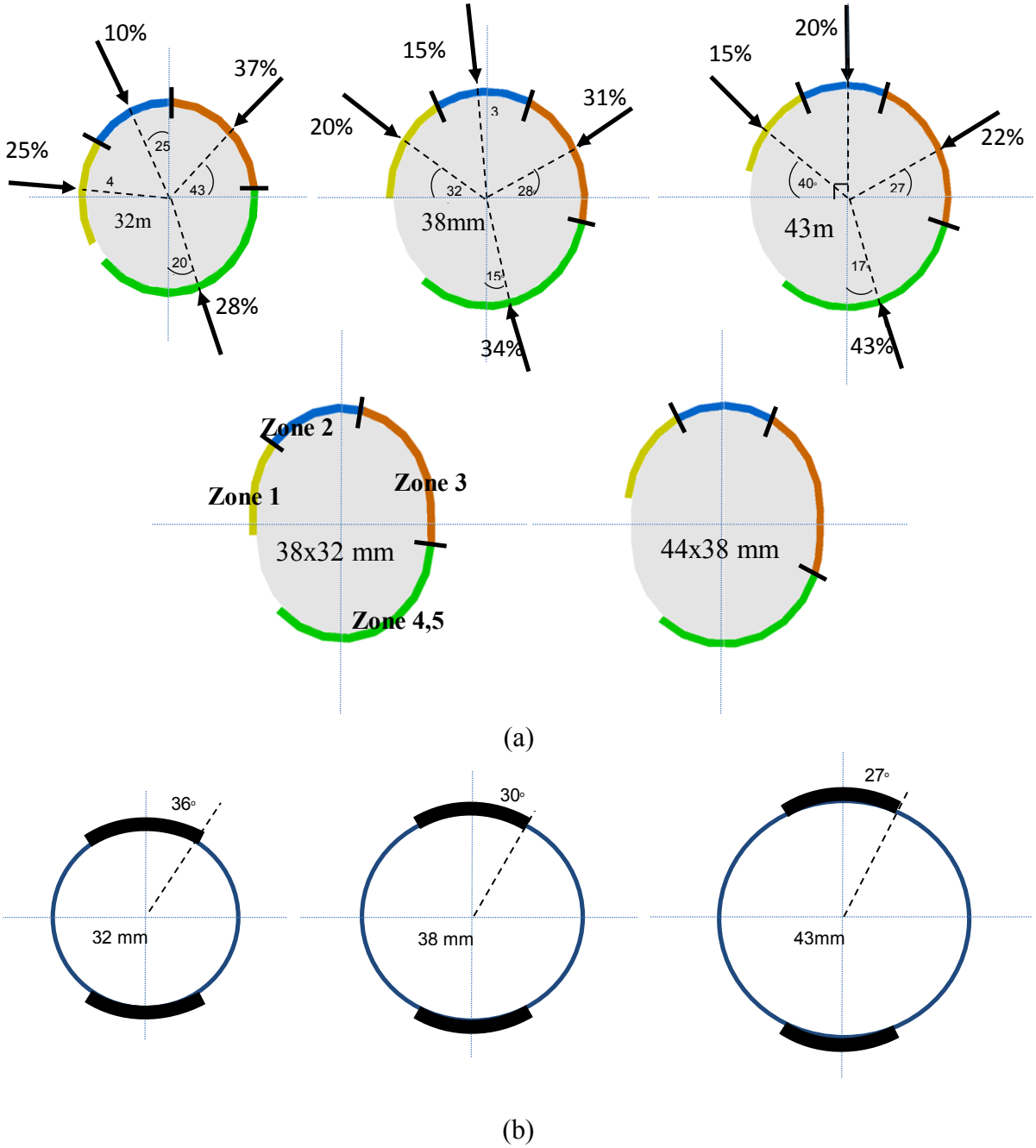

Figure 3.8: (a) Locations of different contact zones on the cylindrical and elliptical handles and the distribution of mean contact force ratio (Hand size = 9) and (b) Sensor placement maps of 0 mm sensor locations.

3.3.3. Properties of sensors applied to stationary handles

The feasibility of the sensors applied to different handles was investigated in terms of linearity and repeatability with eight subjects, and 12 grip and push force combinations (push: 0, 25, 50, 75 N and grip: 10, 30, 50 N). The measurements obtained from three trials in each case were analyzed to assess inter- as well as intra-subject variabilities in the sensors' sensitivities. The measurements were obtained with two positions of the sensors on the handle: 0 mm and 5 mm. The measurements obtained through three trials showed reasonably good linearity of measurements with all the subjects. As an example, Fig. 3.9 illustrates the linearity and repeatability of the measurements with one of the subjects (subject #5) for the palm and finger sensors located symmetrically about the central axis of the 38 mm instrumented handle. The mean sensitivity of the palm sensor was 4.37 mV/N (SD=0.06), while that of the finger sensor was 4.82 mV/N (SD=0.36). The r^2 values of the palm and finger force measurements were above 0.98 and 0.94, respectively. The relatively higher variation in the measured finger force was attributed to larger variability in the fingers position between the trials. Identical trends were also observed in the responses with other subjects and different handles considered in the study.

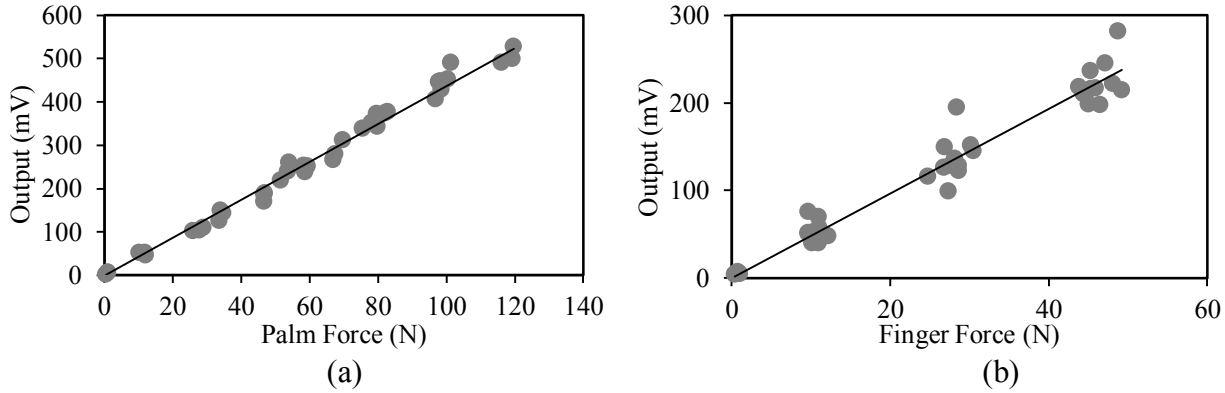

Figure 3.9: Static input-output characteristics of the palm- and finger-side FlexiForce sensors obtained during three trails with subject#5: (a) palm sensor (r^2>0.98); and (b) finger sensor (r^2>0.94).

The data obtained with eight subjects and an identical set of sensors applied to a particular handle revealed considerable variations in the sensitivity of the palm and finger-side sensors across the subjects (p<0.01). Tables 3.1 and 3.2, as examples, illustrate variations in the sensitivities of the palm and finger sensors for the 38 mm cylindrical and 38×44 mm elliptical handles, respectively. The tables also present the palm and finger lengths of the subjects. Similar variations were also observed in the sensors' outputs when the sensors were shifted 5 mm counter-clockwise from the central axis (results not presented in the tables). The static sensitivities of the shifted sensors, however, differed from those of the centrally-located sensors. One-way analysis of variation (ANOVA) was performed to identify the statistical significance of the differences in static sensitivities of the measurements with two sensors positions. The results showed that sensitivity of the palm and finger sensors placed at the two positions were significantly different (p<0.01) for all the cylindrical and elliptical handles, and the subjects.

Subject#	Palm length (cm)	Palm sensor sensitivity (mV/N)			Finger length (cm)	Finger sensor sensitivity (mV/N)		
		Mean	SD	CoV (%)		Mean	SD	CoV (%)
1	11.8	4.5	0.26	5.8	7.2	4.6	0.13	2.8
2	10.2	4.2	0.09	2.1	8.0	4.0	0.31	7.8
3	10.8	4.1	0.07	1.8	7.7	4.7	0.08	1.7
4	12.0	4.1	0.03	0.8	8.5	4.8	0.18	3.8
5	11.2	4.4	0.06	1.3	8.8	4.8	0.36	7.5
6	11.0	4.5	0.16	3.5	7.2	5.0	0.11	2.2
7	10.1	4.6	0.09	1.9	7.2	5.2	0.31	6.0
8	11.7	4.3	0.16	3.7	8.0	4.7	0.14	3.0
Overall		4.3	0.19	4.4		4.7	0.35	7.4

SD: standard deviation; CoV: coefficient of variation

Table 3.1: Inter- and intra-subject variabilities in the static sensitivities of the palm and finger FlexiForce sensors (38 mm cylindrical handle).

Subject#	Palm length (cm)	Palm sensor sensitivity (mV/N)			Finger length (cm)	Finger sensor sensitivity (mV/N)		
		Mean	SD	CoV (%)		Mean	SD	CoV (%)
1	11.8	1.1	0.07	6.1	7.2	1.9	0.23	11.8
2	10.2	1.8	0.14	7.5	8.0	2.3	0.08	3.6
3	10.8	2.3	0.26	11.7	7.7	2.7	0.13	5.0
4	12.0	1.7	0.07	4.1	8.5	2.5	0.08	3.3
5	11.2	2.1	0.15	7.1	8.8	2.7	0.12	4.6
6	11.0	1.8	0.08	4.6	7.2	2.7	0.08	2.9
7	10.1	2.0	0.13	6.2	7.2	2.2	0.04	2.0
8	11.7	1.8	0.02	0.9	8.0	1.5	0.02	1.5
Overall		1.8	0.34	18.6		2.3	0.45	19.2

SD: standard deviation; CoV: coefficient of variation

Table 3.2: Inter- and intra-subject variabilities in the static sensitivities of the palm and finger FlexiForce sensors (38×44 mm elliptical handle).

It should be noted that a different set of FlexiForce sensors were employed for measurements with different handles. The results obtained with the two handles thus differed considerably. The measurements obtained with the handles exhibit considerable variations in the static sensitivities of the FlexiForce sensors across the subjects, which are attributable to differences in the hand sizes of the subjects resulting in variations in the hand position on the sensors. A correlation between the hand dimensions and the sensors' outputs, however, could not be established. The coefficients of variations (CoV) of the measurements obtained during the three trials for the cylindrical and elliptical handles ranged from 0.8 to 7.8% and 0.9 to 11.8%, respectively. The CoV values, however, exceeded 10% for only two subjects grasping the elliptical handle. Similar variations were also observed for other handles with sensors located about the central axis and shifted 5 mm from the central axis. The mean results further confirmed the need for calibration of individual sensors for each subject and handle.

Figure 3.10 compares the mean static sensitivities of the palm and finger force sensors applied to the 38 mm cylindrical and 38×44 elliptical handles mm in 0 mm and 5 mm positions. It

should be noted that the two handles employed different sets of sensors. The CoV of the measurements with the 5 mm sensor position is evidently greater than that with the 0 mm position. This is likely due to differences in the finger contact areas (and lengths) across the subjects. The elliptical handle shows relatively higher CoV for both sensor positions. This is most likely caused by relatively lower effective contact areas of the hand and sensors since a greater proportion of the hand surface along the major axis does not contact the sensors. Moreover, Medola et al. [54] studied the distribution of contact forces over a hand surface's during wheelchair propulsion. It was concluded that an increase in contact surface area resulted in lower contact forces. In both the handles, the palm sensor sensitivity decreases when the sensor is shifted by 5 mm, while the shifting of the finger sensor resulted in slightly higher sensitivity for the cylindrical handle but lower for the elliptical handle. The mean sensitivities of the measurements performed with all the handles together with the SD and CoV of the means are summarized in Table 3.3. The results are presented for both positions of the FlexiForce sensors, 0 mm and 5 mm. The results clearly show greater variability of the measurements with both the elliptical handles compared to the cylindrical handles. The CoV of the mean sensitivities attained with cylindrical handles with centrally positioned sensors (0 mm) ranged from 4.4 to 8.2% for the palm sensors, and 7.3 to 11.4% for the finger sensors. The corresponding values for the sensors shifted by 5 mm were 8.2 to 9.4% and 11.0 to 15.9% for the palm and finger sensors, respectively. The CoV of the mean sensitivities obtained with the elliptical handles ranged from 10.9 to 20.0% for both the sensors positions. From the results, it is deduced that the sensors located symmetrically about the central axis could yield relatively lower inter-subject variability of the measurements and relatively higher static sensitivity of the sensors.

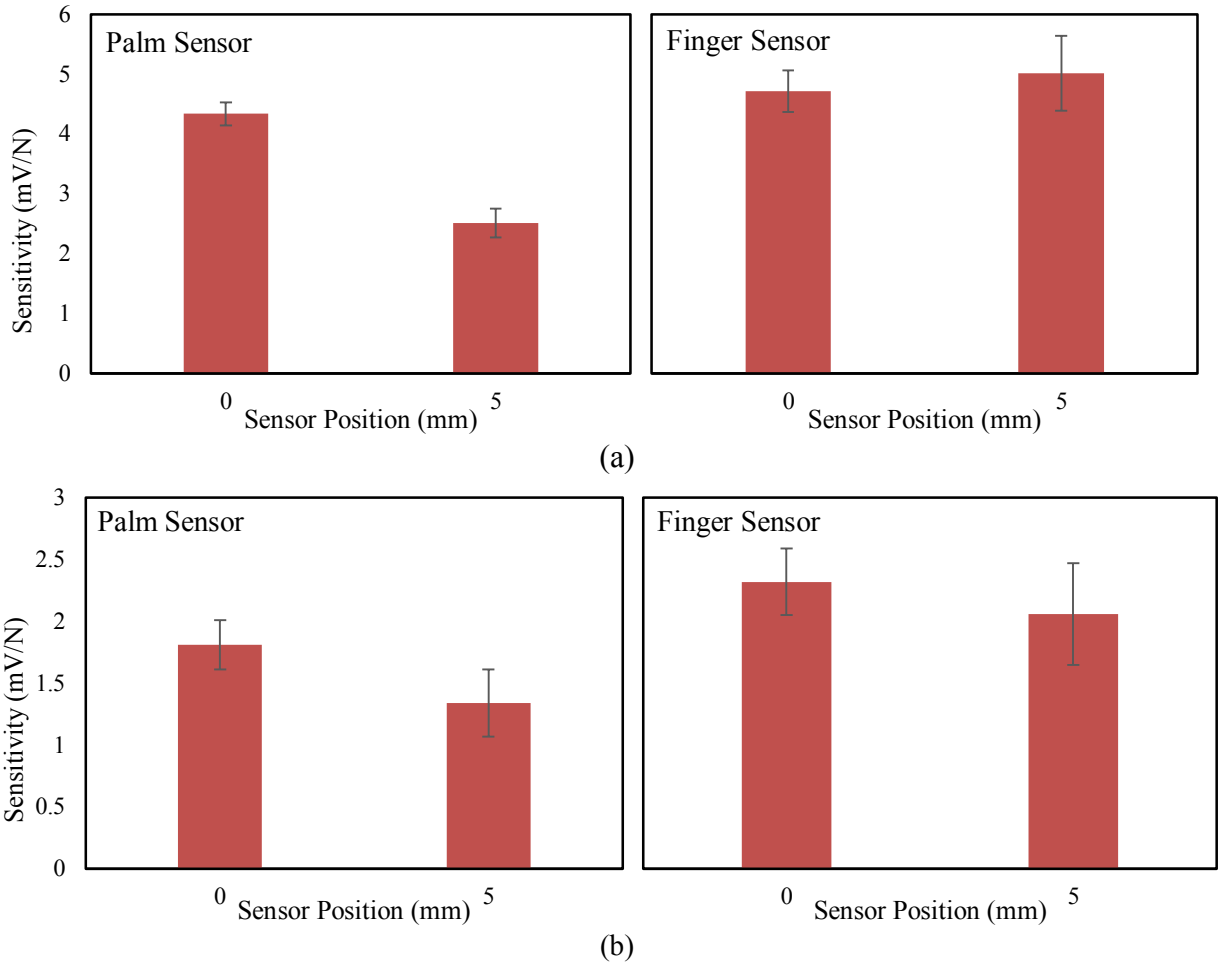

Figure 3.10: Mean static sensitivities and inter-subject variations of measurements for two sensors positions: (a) 38 mm cylindrical handle; (b) 38×44 mm elliptical handle.

Handle size (mm)	Palm							Finger						
	Sensor #	0 mm Mean	0 mm SD	0 mm COV (%)	5 mm Mean	5 mm SD	5 mm COV (%)	Sensor #	0 mm Mean	0 mm SD	0 mm COV (%)	5 mm Mean	5 mm SD	5 mm COV (%)
32	4	4.7	0.33	7.1	4.2	0.34	8.2	11	5.1	0.50	10.0	4.3	0.48	11.0
38	12	4.3	0.19	4.4	2.5	0.24	9.4	10	4.7	0.35	7.3	5.0	0.63	12.6
43	4	2.2	0.18	8.2	1.7	0.15	9.2	11	2.3	0.26	11.4	2.3	0.36	15.9
32×38	16	2.6	0.38	14.9	2.8	0.54	19.7	17	2.8	0.36	12.6	3.0	0.46	15.3
38×44	13	1.8	0.20	10.9	1.3	0.27	19.7	18	2.3	0.45	19.2	2.1	0.41	20.0

SD: standard deviation; CoV: coefficient of variation

Table 3.3: Mean static sensitivities (mV/N) of the palm and finger FlexiForce sensors applied to different handles at two different positions (0 and 5 mm).

It needs to be emphasized that above measurements were attained with the same set of sensors applied to individual handles, as shown by the sensor identifiers in Table 3.3. The sensor

calibrations, however, were repeated for each subject. The measurements with a given handle were performed during a single session of 4 hours, so as to reduce the sensor degradation effect. Subsequent tests with a single set of sensors (#4 and #11) revealed substantial decrease in the sensor outputs with usage, in the order of 50%.

A pairwise comparisons of the measured data showed that the static sensitivity of the palm sensors were significantly different ($p<0.01$) for the two sensor positions. However, the sensitivity for the finger sensor were significantly different only for the 32 mm cylindrical and 38×44 mm elliptical handles ($p<0.01$). Owing to the complex contributions of various factors, the data acquired for the 38 mm cylindrical handle, which showed the least inter-subject variability (Table 3.3), was further analyzed to identify the most appropriate position of the palm and finger sensors. The results in Fig. 3.10 and Table 3.3 clearly show substantially higher sensitivity of the palm sensor for most of the handles, when it is positioned symmetrically around the central position, compared to that shifted by 5 mm. The mean sensitivity of the palm sensor decreased nearly 42%, when it was shifted by 5 mm from the central position of the 38 mm handle. The finger sensor sensitivity, however, increased only slightly (6.3%) when shifted 5 mm from the central position. The data obtained for the 38×44 mm elliptical handle, however, showed an opposite trend in the finger sensor sensitivity, which was nearly 11% lower for the 5 mm position compared to the central position, as seen in Fig. 3.10(b). It is seen that the zones 2 and 3 of the hand lie either close to or towards the right-side of the center line (Fig. 3.2). The shifting of the finger sensor in the anticlockwise direction thus adversely affected the measurements for the elliptical handle. From the results, it is deduced that sensors located symmetrically about the center line of the handle would generally yield relatively higher sensors' outputs and repeatability.

3.3.4. Properties of sensors applied to vibrating handles

The input-output characteristics of the sensors, acquired with seven subjects grasping vibrating handles with twelve different combinations of grip and push forces (grip: 0, 25, 50, 75 N and push: 10, 30, 50 N) were analyzed to assess the feasibility of the sensors under vibration. The data were acquired only for the 38 mm and 43 mm cylindrical handles with centrally located palm and finger sensors (0 mm). Measurements with each subject were performed under two levels of vibration (1.5 and 3 m/s^2 frequency-weighted rms acceleration). The measurements with the stationary handle were also repeated prior to the dynamic measurements to determine the sensors' static sensitivities. The results in general showed negligible effects of vibration on the sensors' input-output characteristics.

As an example, Fig. 3.11 illustrates correlations of the mean palm and finger forces obtained from the FlexiForce sensors with the corresponding reference values from the 38 mm instrumented handle under 3 m/s^2 vibration excitation (subject #5). The results shown for three trials illustrate good repeatability and linearity of the measurements with the vibrating handles (r^2>0.97 for both sensors). A similar degree of repeatability and linearity was also observed in measurements with all the subjects.

The FlexiForce force output under vibrating condition was computed by considering the sensitivity in the absence of vibration and the sensor output in the presence of vibration. The measured force data were analyzed in terms of the mean force ratio (MFR), the ratio of the measured and reference forces, given by:

$$MFR = \frac{F_{si}}{F_{ri}} \tag{3.1}$$

where F_{si} is FlexiForce sensor force measured at location i (i = palm/finger) and F_{ri} is the reference force at the same location, obtained from Eqs. (2.3) and (2.4).

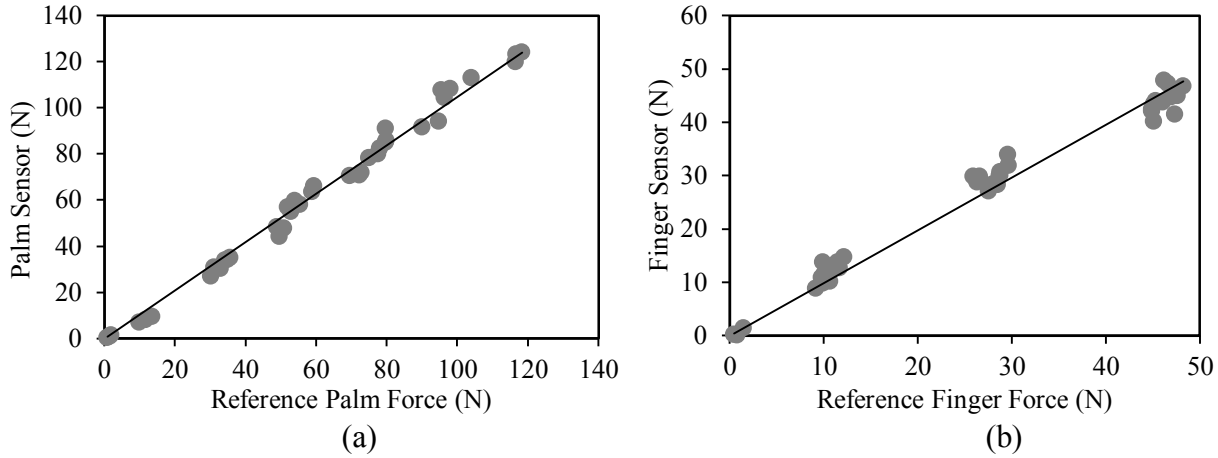

Figure 3.11: Input-output properties of FlexiForce sensors under handle vibration in the 4–1000 Hz frequency range: (a) palm sensor - r^2>0.98; and (b) finger sensor - r >0.96 (38 mm, subject#5).

Table 3.4 summarizes the MFR evaluated for the palm and finger forces obtained with seven subjects grasping the 38 and 43 mm handles subject under 3 m/s^2 vibration excitation. The MFR values for the palm force range from 0.94 to 1.07 in most cases, with the exception of subjects #3 and #4 grasping the 38 mm handle, and subjects #3, #4 and #5 with the 43 mm handle, where the error ranged from 12 to 22%. For the finger force, the MFR ranged from 0.94 to 1.08 for most subjects, with subject # 9 being the only exception. The observed errors in the MFR values could be partly attributed to differences in the hand sizes and the hands positions on the handles among the subjects. It is also essential to note that identical sensors were used by all the subjects under each vibration condition. The results of one way ANOVA revealed significantly different sensitivities of the palm and finger sensors between the subjects (p<0.01) for both the handles and vibration magnitudes. The mean sensitivities and inter-subject variabilities of the palm and finger sensors obtained with the seven subjects and two levels of vibration are further compared in Fig. 3.12 for the 38 and 43 mm handles. The figures also illustrate static sensitivity of the sensors measured prior to application of vibration. Although variability in mean sensitivities of the sensors exists across the subjects, the measurements suggest very small effects of handle vibration.

Analyses of the data revealed peak inter-subject variability in the palm and finger sensitivities of 9.6% and 17.4%, respectively, for the 38 mm handle. The corresponding variabilities for the 43 mm handle were 15.2% and 13.6%.

Subject #	Palm length (cm)	Palm sensor MFR		Finger length (cm)	Finger sensor MFR	
		38 mm handle	43 mm handle		38 mm handle	43 mm handle
1	11.8	0.99	0.94	7.2	0.95	1.08
2	10.2	1.04	1.07	8.0	1.08	1.06
3	10.8	1.21	1.12	7.7	0.98	0.96
4	12.0	1.16	1.22	8.5	0.99	1.06
5	11.2	1.05	1.15	8.8	0.99	1.05
6	11.0	0.96	1.01	7.2	1.00	1.04
9	12.8	1.02	1.04	8.4	0.85	0.94

Table 3.4: Mean force ratios (MFR) of the palm and finger sensors (38 mm and 43 mm cylindrical handle; 3 m/s^2 frequency-weighted rms acceleration excitation).

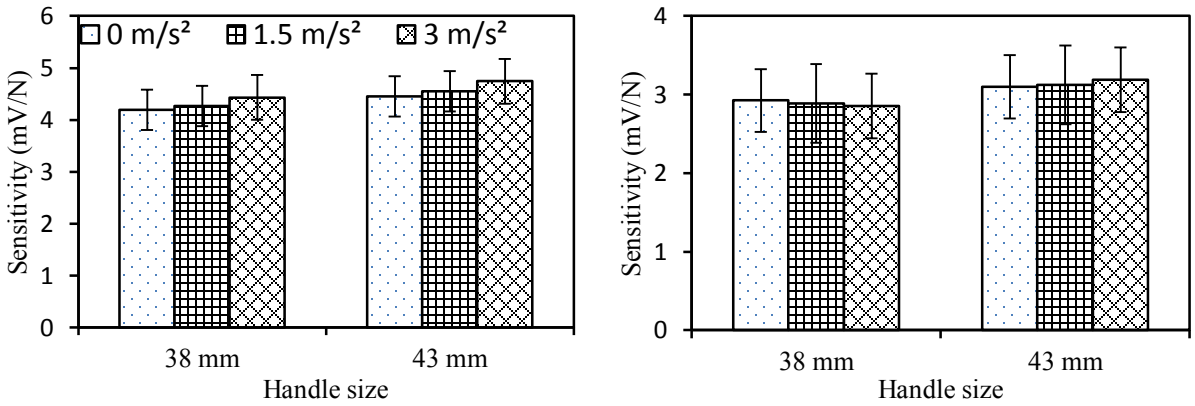

Figure 3.12: Influence of vibration magnitude on the overall mean sensitivities of the FlexiForce sensors: (a) palm sensor; and (b) finger sensor.

The results in general show slightly higher palm sensor sensitivities in the presence of vibration for both the handles compared to the respective static sensitivities, however the sensitivity is not significantly different (p>0.5). This may be due to higher contact pressures on the sensors, since the subjects tend to grasp the handle more firmly in the presence of vibration.

The finger sensor sensitivity, however, decreased with vibration for the 38 mm handle. This may be caused by larger variations in the finger handle contact pressure due to vibration and possible intermittent loss of finger handle contact. The measurements with the 43 mm handle showed slight increase in finger sensor sensitivity with vibration, which may be partly caused by the sensor mostly enveloping the contact zones 2 and 3, as seen in Fig. 3.2. From the results, it is evident that the sensors could be used for measurements of palm and finger forces in vibrating tool handles, since their outputs in the presence of handle vibration are similar to those attained under static conditions (within 6%).

3.3.5. Feasibility of the FlexiForce sensors applied to the tool handle

Figure 3.13(a) illustrates the static calibrations of three palm sensors used for the three subjects grasping the tool handle with pre-defined push forces. In this case, the force plate signal served as the reference value. The input-output characteristics of the three finger sensors used for the subjects are shown in Fig. 3.13(b). The reference finger force in this case was obtained from the calibrated palm force sensor, when the subjects fully negated the plate force by applying a finger force of the same magnitude, as described in section 2.2.6. The results show good linearity of all the palm and finger sensors with r^2 values above 0.86.

The sensitivities of three sets of sensors used with three subjects, however, differed, as expected. The sensitivities of the palm sensor ranged from 2.99 to 5.58 mV/N, while those of the finger sensors varied from 3.36 to 4.44 mV/N across the subjects. From the results it is concluded that the FlexiForce sensors applied to the handle yield good repeatability of measurements and linear outputs with the applied force.

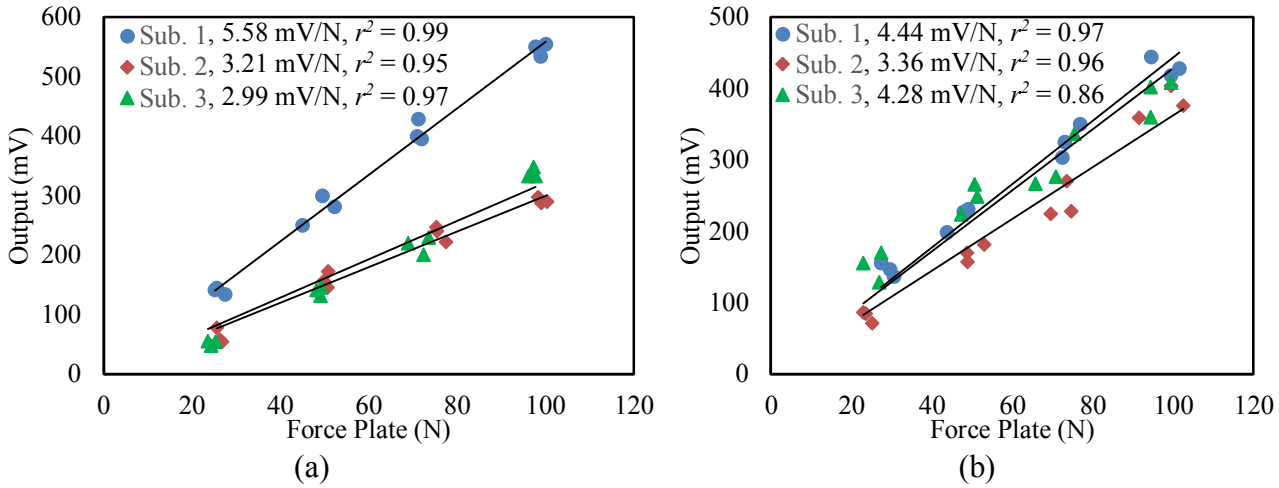

Figure 3.13: Input-output responses of three palm and finger sensors used with three subjects under three trials: (a) palm sensor; (b) finger sensor.

The validity of the sensors was subsequently evaluated with subjects grasping the stationary tool handle with different combinations of grip and push forces. The variations in the push force estimated from the measured palm and finger forces are compared with the force plate signal in Fig. 3.14(a). The results are presented for five hand forces combinations measured three times for a total of fifteen measurements. The results show very good repeatability of measurements and reasonably good correlation between the push forces obtained from the two measurement systems with r^2 values ranging from 0.88 to 0.92 for the three subjects. The ratio of the push force obtained from the FlexiForce sensors to the force plate signal ranged from a low of 0.93 for subject #3 to 1.02 for subject #2. The palm sensor measurements are also correlated with the hand-handle coupling force in Fig. 3.14(b) to further examine the validity of the measurement system, particularly the finger sensor. The coupling force is obtained from the summation of the force plate and finger sensor outputs. The results suggest better correlations of the palm sensor data with the coupling force with r^2 values ranging from 0.95 to 0.97 for the three subjects. The ratio of the palm force obtained from the FlexiForce measurement system to coupling force ranged from a low of 0.96 to 1.06. The results demonstrate the validity of the proposed measurement

system in obtaining reasonably good estimates of the hand grip, push and coupling forces, while grasping the handle of a stationary tool in a power grip manner.

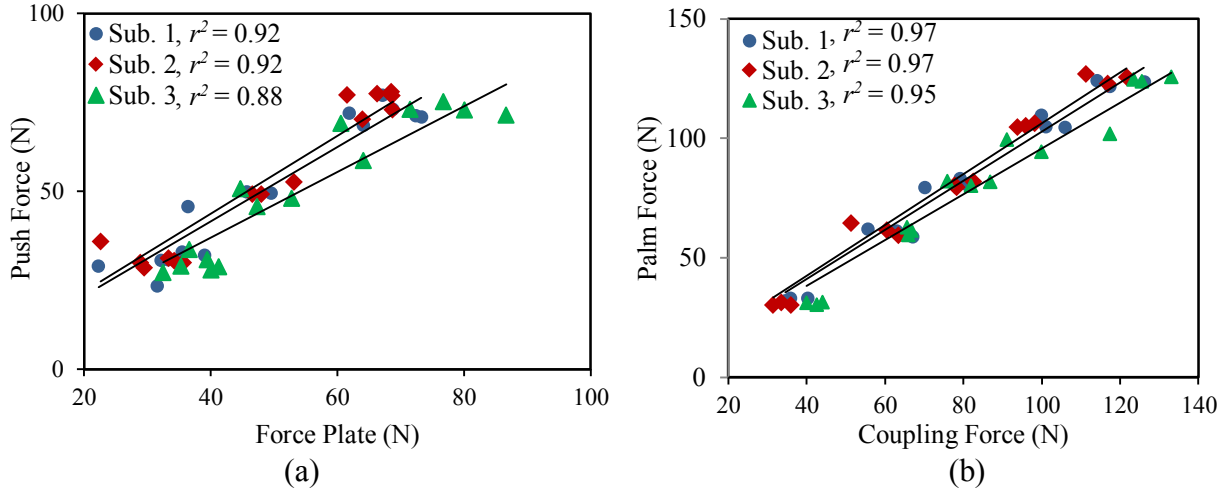

Figure 3.14: Correlations of the push force obtained from the FlexiForce sensors with those of the force plate and coupling forces for each subject grasping the stationary tool handle with 5 different grip and push forces: (a) plate force; (b) coupling force.

Figure 3.15(a) illustrates the correlations of the push force estimated from the FlexiForce sensors with those obtained from the force plate when subjects operating the power tool. The tool speed and thus the level of vibration in each case was neither monitored nor controlled. The r^2 values range from 0.82 to 0.95 for the three subjects. The ratio of the push force obtained from the FlexiForce measurement system to the force plate signal ranged from 0.94 to 1.08 for the three subjects. Figure 3.15(b) also illustrates very good correlations between the palm sensor measurements with the hand-handle coupling force. The r^2 values range from 0.93 to 0.98 for the three subjects, while the ratio of the measured palm force to the coupling force ranged from 0.96 to 1.05. Comparisons of the measurements obtained with the stationary and vibrating tool handle suggest that the FlexiForce measurement system yields equally accurate estimations of the push and coupling forces with the vibrating tool.

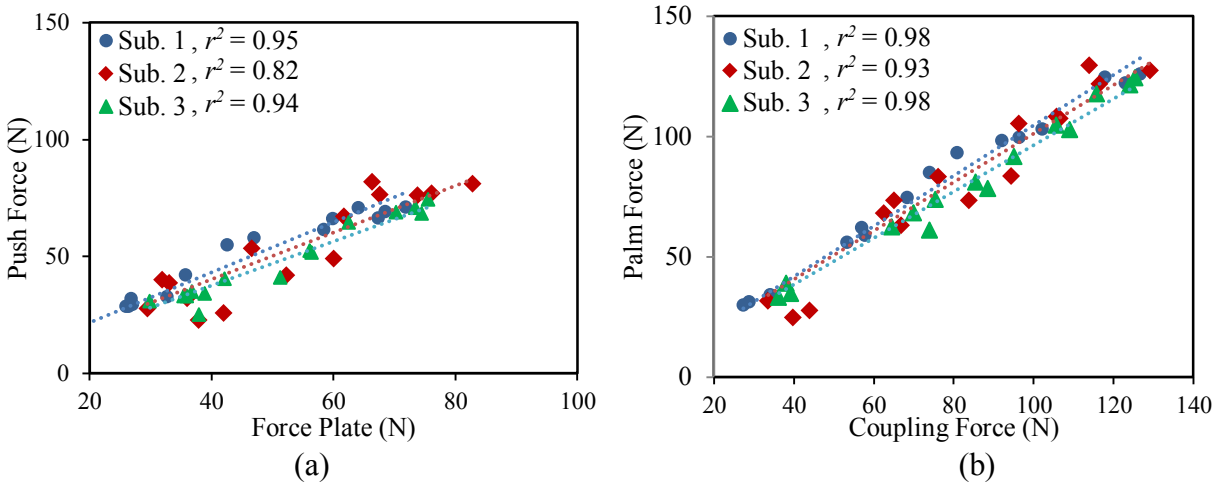

Figure 3.15: Correlations of the push force estimated from the FlexiForce sensors with those of the force plate and coupling forces for each subject grasping the vibrating tool handle with 5 different grip and push forces: (a) plate force; (b) coupling force.

3.4. Conclusions

It is concluded that two FlexiForce sensors applied symmetrically on the opposite sides around the central axis of the handle could provide accurate measurements of the palm and finger forces, and good estimates of the hand grip and push forces. The flexible FlexiForce sensors could be conveniently trimmed to desired length for applications to tool handles of different lengths, cross-sections and geometry. The sensors were able to provide good estimates of the hand forces imparted on the tool handle under static as well as dynamic conditions. The magnitude of handle vibration had a negligible effect on the output sensitivities of the sensors. The sensors, owing to their very low cost, could be discarded following measurements for a given tool and operating conditions. The primary limitations of the proposed system however lie with the lack of repeatability of the outputs of different sensors, and the need to calibrate for each subject and handle. Considering the very good repeatability and applicability of the sensors in addition to their low cost, a reliable hand-handle interface force measurement system could be developed with the availability of the sensors with consistent properties.

CHAPTER 4
FEASIBILITY ANALYSIS OF LOW-COST FLEXIBLE RESISTIVE SENSORS FOR MEASUREMENTS OF DRIVING POINT MECHANICAL IMPEDANCE OF THE HAND-ARM SYSTEM

4.1. INTRODUCTION

The biodynamics of the hand–arm system is one of the most important factors for understanding the mechanisms of vibration-induced disorders and for developing frequency-weighting factors for assessing risk due to vibration exposure. The biodynamic response of the hand-arm system exposed to vibration is also required for the design and assessments of vibration isolation methods, and for developing hand–arm simulators for testing and analysis of powered hand tools [11, 51]. The biodynamic responses of the hand-arm system have been widely characterized in the laboratory using instrumented handles under different experimental conditions [11, 21-23, 30, 48, 49]. These studies have generally presented the response in terms of driving point mechanical impedance (DPMI), which has shown a strong dependence on the level of hand forces.

Reported impedance responses have also shown wide differences among them, particularly at higher frequencies. The observed differences have been attributed to variations in intrinsic and extrinsic variables, test conditions, and the methodologies employed in the various studies. A few studies have shown that dynamic characteristics of the instrumented handle could contribute to considerable errors in the biodynamic response particularly those associated with the handle inertia forces [21, 22]. [21] showed that the contributions due to handle inertia at higher frequencies (above 500 Hz) cannot be entirely eliminated through mass cancellation. [22] observed uneven vibration distribution along the instrumented handle (above 500 Hz) that may cause measurement errors and changes in the coupling force at the hand handle interface. These studies suggested the use of a handle with very small effective mass and high stiffness, which forms a complex design

This chapter is a manuscript under review in Int J Industrial Ergonomics (Oct 2014)

challenge considering the high frequencies of tool handle vibration. The split designs of instrumented handles, which have been employed in the hand-arm impedance studies yield considerably lower stiffness and thus resonant frequencies compared to a handle without the split [21]. The standardized method for assessing the vibration performance of anti-vibration gloves also recommends the use of a split instrumented handle in order to measure the hand grip and push forces [33]. Furthermore, the characterization of hand-arm biodynamics with real tools in the field using such instrumented handle designs poses substantial challenges since it would involve major modifications of the tool.

Alternatively, thin-film flexible pressure sensing matrices with very light mass could be applied directly to the handle surface for measurements of static and dynamic hand-handle interface forces, while preserving the handle rigidity. Such sensors could be used to measure dynamic force so as to obtain the hand-arm DPMI response without any inertial correction and thus eliminate the errors attributed to effective handle inertia. Moreover, these sensors could be applied to the tool handles to enable measurement of biodynamic response under realistic field conditions in addition to the hand grip and push forces. The matrices of such sensors have been widely employed for measurements of grip strength, and mapping of static contact pressures on automotive seats, wheelchairs and hospital beds [37, 56-58]. The feasibility of such sensors in a dynamic vibration environment has been explored in a recent study involving measurement of apparent mass response of the seated body to low frequency whole-body vibration [59]. It was suggested that the accuracy of the dynamic measurements would greatly depend upon the bandwidth and frequency response characteristics of the pressure sensing systems. The feasibility of such sensors for measurement of dynamic contact forces has not yet been explored under high frequency vibration such as that encountered in power tools.

In the present study, the applicability of the thin film and flexible resistive (FlexiForce) sensors were explored for the measurement of biodynamic response of the hand-arm system exposed to vibration in the 4 to 1000 Hz frequency range. The DPMI response obtained from the Flexiforce sensors were compared with the reference response obtained from the widely-used instrumented handle. The responses of the two measurement systems were compared for nine different combinations of hand grip and push forces. The limitations of the measurement systems are discussed in view of the bandwidth and frequency response. An inverse frequency response function is subsequently proposed and applied to obtain reasonably accurate measurements of the hand-arm system DPMI responses.

4.2. Experimental setup and methods

A low-cost hand-handle interface force measurement system was developed, which could be used for the measurement of static as well as dynamic palm and finger forces imparted on the tool handles. Resistive FlexiForce sensors (model 1230, Tekscan Inc., USA) were used for this study primarily due to their substantially lower cost compared to the capacitive sensors that have been used in a few reported studies on characterization of hand-handle interface forces [37, 38]. The 0.208 mm thick FlexiForce sensor comprised a pressure-sensitive resistive grid encased between two thin and flexible polymer layers. The selected sensor measured 149×40 mm, and it could be trimmed to a desired length and width to adapt to a particular tool handle size. The mass of each sensor was negligible. Unlike the sensing matrices used in pressure mapping studies, the selected sensor is applied as a single unit to measure the total force imposed on the entire sensor surface, and thereby could provide acquisition at very high sampling rates.

A two-channel signal conditioner was developed for acquiring the FlexiForce sensor signals in terms of voltage, which was proportional to the change in sensor resistance and thereby

the applied force. The conditioner also employed a variable gain circuit to ensure adequate level of the voltage output in the desired force range (0 to 200 N). The linearity of the sensors and the conditioning circuit was thoroughly evaluated under a broad range of static palm and finger forces [60].

Measurements of biodynamic response of the human hand-arm system were conducted using two different methods. The first method employed an instrumented 38 mm diameter cylindrical handle for acquiring dynamic palm and finger forces at the handle interface, which has been widely used in studies reporting DPMI of the hand-arm system [30, 51]. Two force sensors (Kistler 9212) were integrated in the split handle design to measure the grip force, while two additional force sensors (Kistler 9317b) were installed between the handle support and its base fixture for measurement of the push and total dynamic force. The handle's base fixture was installed on an electrodynamic shaker, as shown in Fig. 4.1(a). The measured grip and push forces were processed through a low-pass filter and displayed to the subjects at a rate of 4 samples per second to allow the subjects to maintain the hand forces in the desired ranges. A miniature accelerometer (PCB 356A01) was also installed inside the handle to measure the handle vibration along the forearm axis (z_h-axis). This accelerometer also served as the feedback sensor for control and synthesis of the handle vibration via a vibration controller, as shown in Fig. 4.1(a).

In the second method, the dynamic palm and finger forces were measured using the proposed FlexiForce sensors to obtain the DPMI response of the hand-arm system. For this purpose, two FlexiForce sensors were installed on the same instrumented handle symmetrically about the center line of the handle along the forearm of the subjects, as seen in Fig. 4.1(b). One of the sensors was oriented to predominantly capture the dynamic force at the palm-handle interface, while the other sensor captured the finger side force. The positions of the two sensors were selected

on the basis of the hand-handle interface force distribution reported by [37]. This study showed the interface force is predominantly distributed around the handle center line along the forearm axis for the 40 and 45 mm diameter handles.

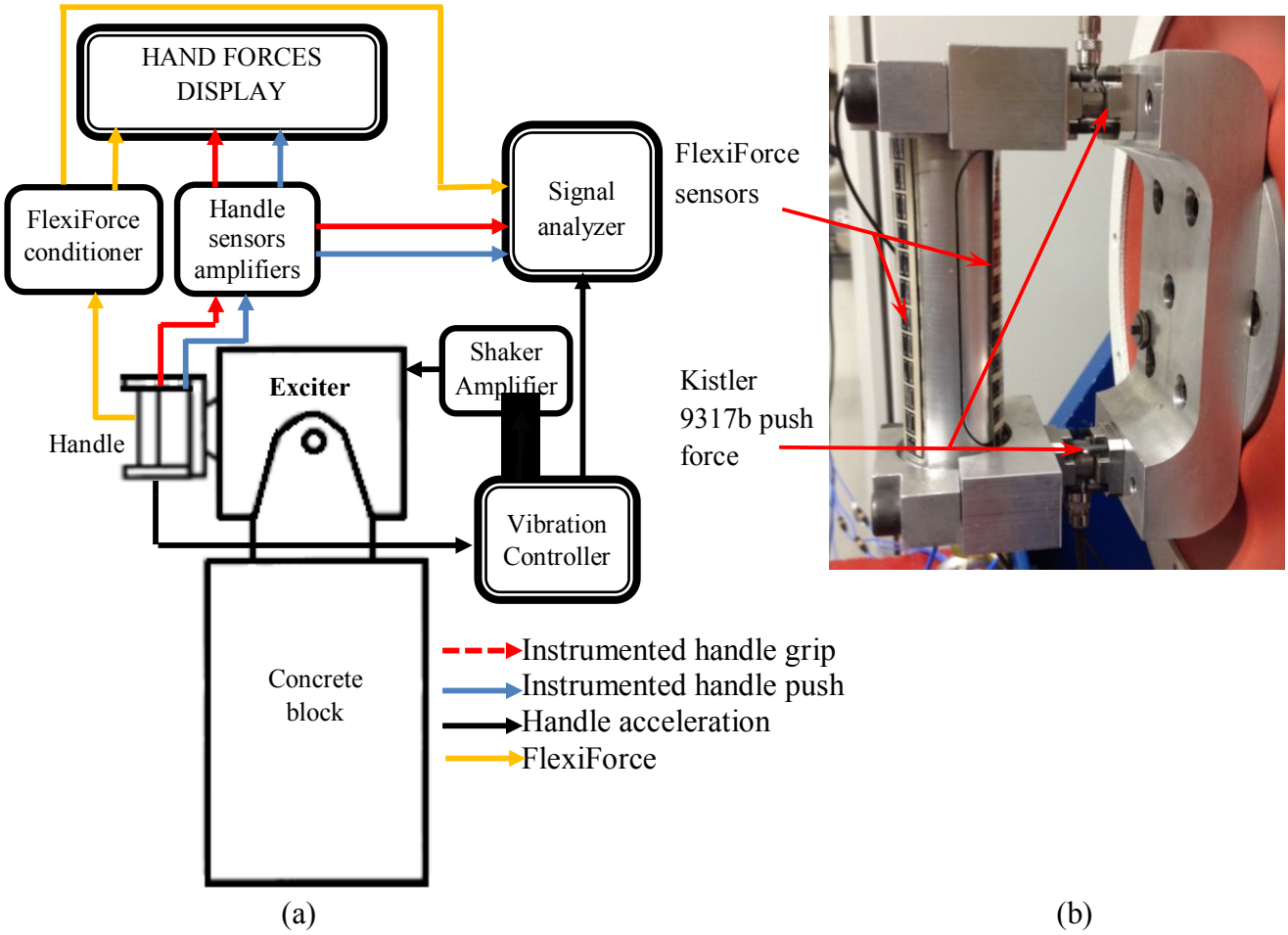

Figure 4.1: (a) Experimental setup for hand-arm impedance measurement using both the FlexiForce sensor and the instrumented handle; and (b) Placement of the FlexiForce sensors on the handle.

The experiments were conducted simultaneously with both the measurement systems. Six adult male subjects participated in the study. The hand dimensions of each subject were measured to obtain the hand size in accordance with [44]. The hand size of the participants ranged from 8 to 10. Each subject was advised to grasp the handle and maintain the desired grip and push forces,

while standing upright with the forearm horizontally aligned with the vibration axis and elbow flexed at an angle of 90º, as recommended in [33]. An adjustable standing platform was provided for each subject to achieve the desired hand-arm posture. The subject controlled the hand grip and push forces through monitoring of the forces measured by the instrumented handle, which were displayed on a monitor screen located in front of the subject. The experiments were performed using nine different combinations of hand forces involved three different grip forces (10, 30 and 50 N) and three different push forces (25, 50 and 75 N). The measurements were conducted under two levels of broadband random vibration in the 4–1000 Hz range (frequency weighted rms acceleration = 1.5 and 3 m/s^2). It has been shown that the FlexiForce sensors may deteriorate over usage [60]. A static calibration of the FlexiForce sensors was thus conducted for each subject prior to the dynamic measurements.

The signals from the handle accelerometer, instrumented handle force sensors, and the FlexiForce sensors were acquired in a multi-channel data acquisition and analysis system (Brüel & Kjær Pulse system) to compute the DPMI of the hand-arm system. The impedance computed from the instrumented handle was inertia corrected to account for contributions of the handle inertia, as described in [21]. The resulting DPMI response served as a reference for evaluating the feasibility of the FlexiForce sensors. The palm and finger FlexiForce sensors signals were analyzed in a similar manner to compute the palm- and fingers-side DPMI responses. Each measurement was repeated twice. The data were acquired for a duration of 20 s during each measurement.

The mechanical impedance of the hand-arm system corresponding to each force combination and vibration level was measured in two stages involving the mechanical impedance at the palm (Z_{palm}) and the fingers (Z_{finger}). The handle was initially oriented so as align the grip force measuring cap with the palm of the hand. The FlexiForce sensor was installed on the

measuring cap of the instrumented handle so as to capture the palm force. The signals from the grip force sensors integrated within the instrumented handle, the FlexiForce sensor and the accelerometer were analyzed to derive the DPMI at the palm. The handle was subsequently rotated by 180 degrees to align the finger-side contact with the measuring cap, which provided the measurement of the finger side force and the impedance. The total impedance of the hand-arm system Z could be obtained through summation of the palm and finger impedance [51]:

$$Z(j\omega) = Z_{palm}(j\omega) + Z_{finger}(j\omega) \quad (1)$$

Where ω is the excitation frequency in rad/s and $j = \sqrt{-1}$. In the above analysis, the palm force is the taken as sum of the grip and push forces measured by the instrumented handle [53].

4.3. Results and discussion

4.3.1. Inter-subject variability

Figure 4.2 presents the mean palm-impedance magnitude and phase responses of the six subjects obtained from the instrumented handle and the FlexiForce sensor under the same experimental conditions. The results, as an example, are shown for 30 N grip and 50 N push force combination (palm force = 80 N; finger force = 30 N), and 1.5 m/s^2 excitation. The figures also show the mean palm impedance responses for all the subjects. The results obtained from the two measurement systems exhibit comparable trends, while the DPMI magnitudes differ substantially. The measured data also shows considerable variations in the responses attained with six subjects. The responses measured with subject#2, in particular, showed large differences around the primary resonance peak. The impedance response of this subject, obtained from the instrumented handle exhibits a nearly flat magnitude in the 26–78 Hz frequency range, while the data for the other subjects show a resonance peak in this frequency range.

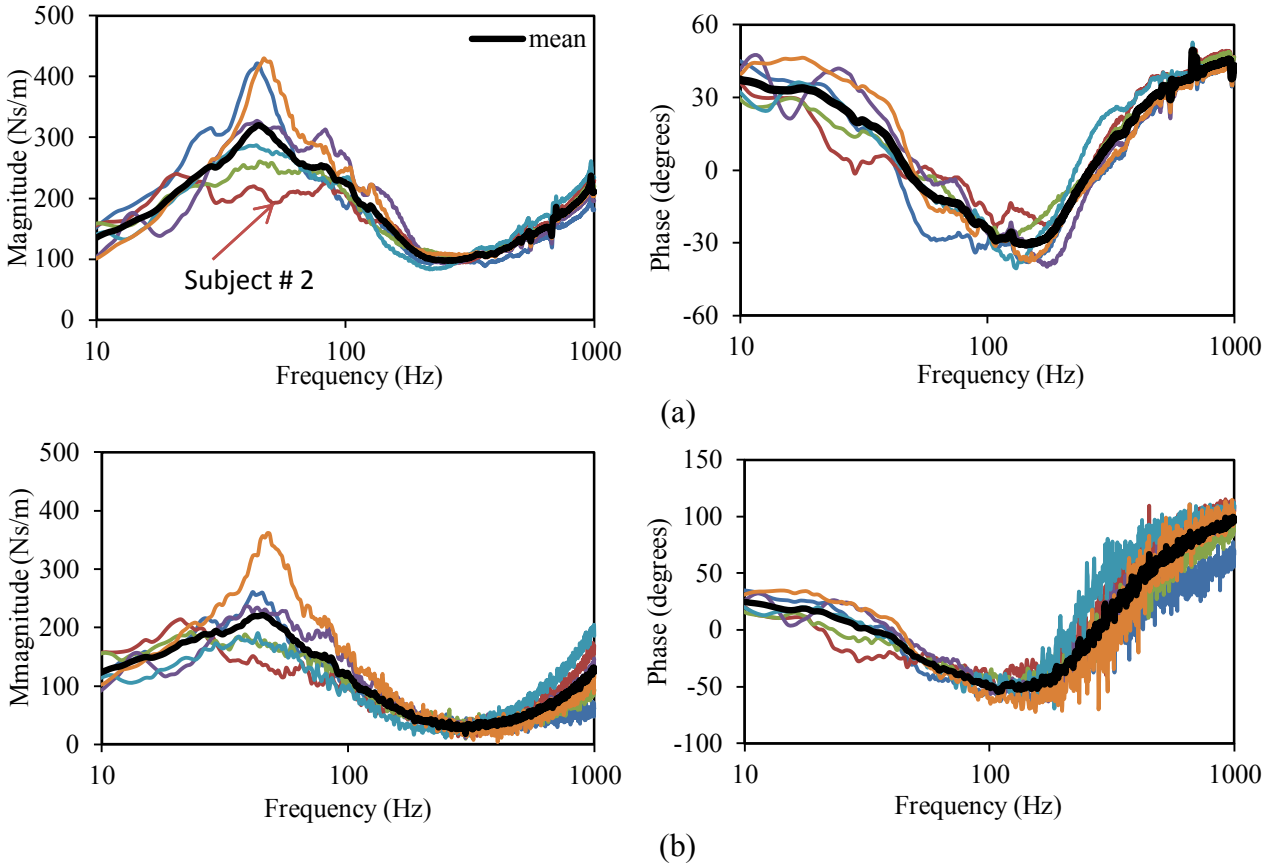

Figure 4.2: Comparisons of palm impedance magnitude and phase responses of 6 subjects together with the overall mean responses obtained from the instrumented handle and FlexiForce sensor: (a) instrumented handle; and (b) FlexiForce sensor (30 N grip, 50 N push and 1.5 m/s^2 excitation).

Figure 4.3 presents the impedance magnitude and phase responses of the subjects measured at the finger-handle interface using the instrumented handle and the FlexiForce sensor. The results are presented for 1.5 m/s^2 excitation, with 30 N grip and 50 N push forces. Large variability was observed in the finger impedance phase responses measured by both the measurement systems. The variability in the FlexiForce measurements was particularly very large which was partly attributed to considerably lower magnitudes of the finger force compared to the palm force, particularly at low frequencies and thereby low level FlexiForce signals. The phase response measurements obtained with FlexiForce sensors are thus not presented since these could not be considered representative. Large variability in the phase response measured using the instrumented

handle is also observed in Fig. 4.3(a), with deviations as high as 80 degrees near 10 Hz. The data obtained with the two measurement systems show comparable trends, while substantial differences in the finger impedance magnitude are also evident. The results show finger impedance magnitude increases with an increase in excitation frequency, while the phase response decreases with increase in the frequency.

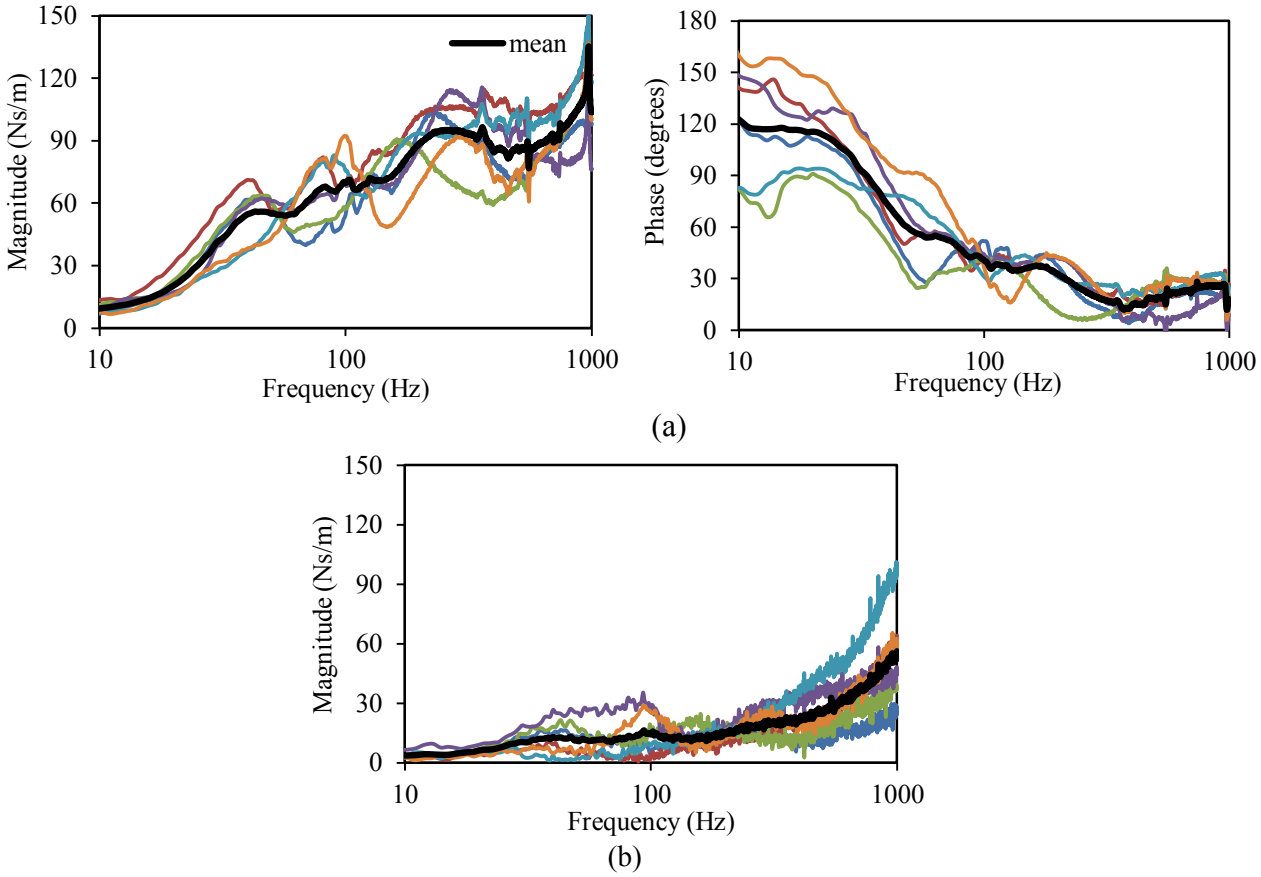

Figure 4.3: Comparisons of finger impedance responses of 6 subjects together with the overall mean responses obtained from the instrumented handle and FlexiForce sensor: (a) instrumented handle; and (b) FlexiForce sensor (30 N grip, 50 N push and 1.5 m/s^2 excitation).

4.3.2. Comparisons of measured response with the reported data

The palm and finger impedance responses of the hand-arm exposed to handle vibration have been reported in a single study [51]. The study reported palm and finger impedance responses under a constant velocity (14 mm/s) sinusoidal vibration at 10 discrete frequencies (16, 25, 40, 63,

100, 160, 250, 400, 630 and 1000 Hz). The frequency weighted acceleration due to this excitation was 1.4 m/s^2 rms, which is comparable with the lower magnitude excitation used in this study. The hand-arm posture used in the reported study was similar to the present study, whereas it employed a 50 N grip and 50 N push force combination. The validity of the measurements was examined through comparisons of the mean palm and finger impedance responses measured using the FlexiForce sensor and the instrumented handle with the reported responses. The mean palm and finger impedance responses corresponding to two grip/push force combinations (30/50 N and 50/50 N) measured using the FlexiForce sensor and the instrumented handle are compared with the reported responses in Fig. 4.4.

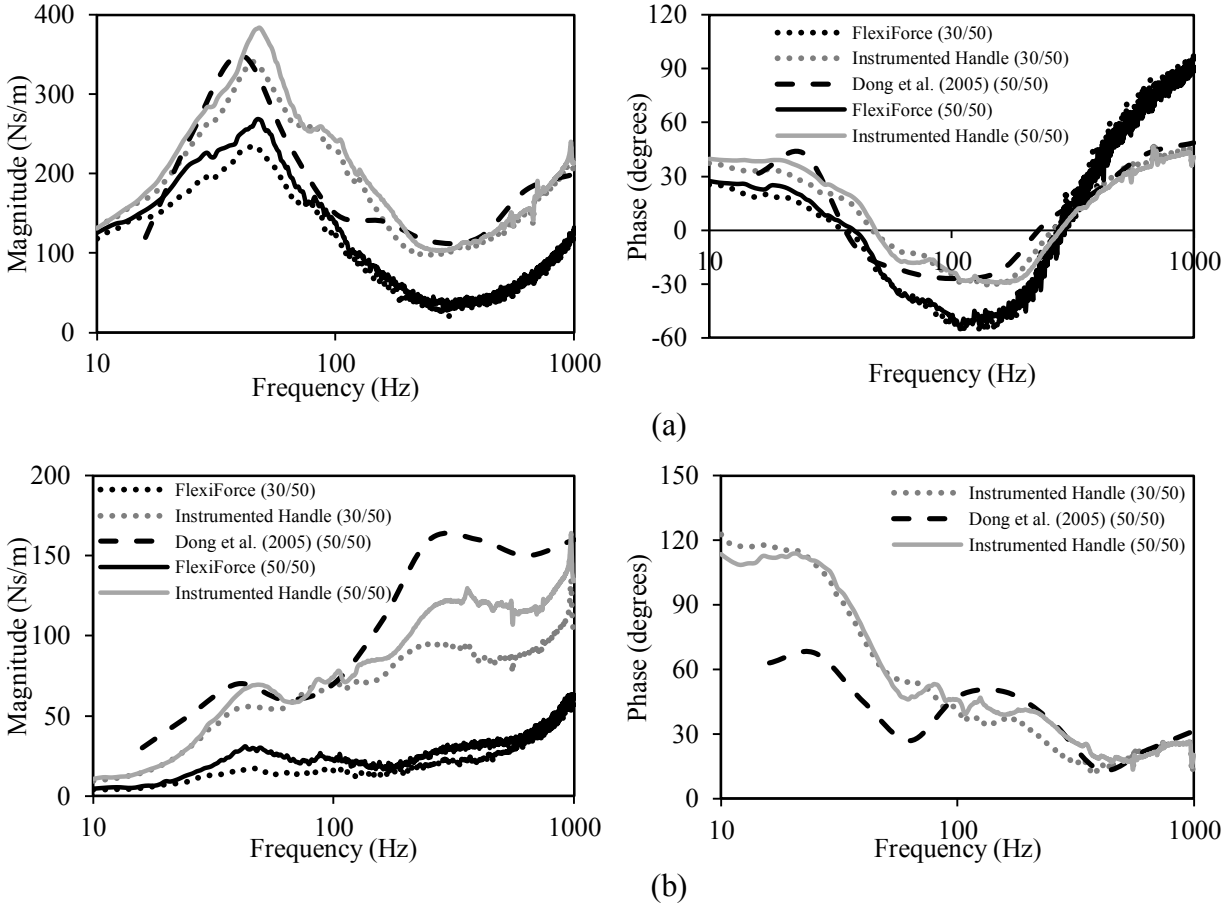

Figure 4.4: Comparisons of mean palm and finger impedance responses obtained from the instrumented handle and FlexiForce sensor with the reported data: (a) Palm; and (b) Fingers (1.5 m/s^2 excitation).

The comparisons between the responses obtained with the instrumented handle and the reported data show comparable trends. Some differences, however, are evident in the 63 to 160 Hz range where the reported magnitudes are lower than the measured magnitudes. The differences, however, are considerably smaller than those observed between the data reported in different studies on DPMI [21], and are likely attributed to a different set of subjects used in the two studies and the nature of vibration. The FlexiForce measurements also exhibit comparable trends, though the impedance magnitudes are substantially lower in the entire frequency range. The magnitude is nearly 117 Ns/m lower than that derived from the instrumented handle around the most conspicuous peak near 46 Hz. The palm impedance phase response of the FlexiForce sensor, however, is reasonably comparable with the reported phase response and that obtained from the instrumented handle, although some differences exist particularly in the 40 to 100 Hz frequency range.

The comparison of finger phase response, however, is limited to that derived from the instrumented handle alone. The measured responses exhibit trends similar to those of the reported responses, yet the magnitude and phase values differ notably. The finger impedance magnitude obtained from the instrumented handle compares reasonably well with the reported magnitudes up to 100 Hz. The measured magnitudes are slightly lower at higher frequencies. Considerable differences exist in the phase response at frequencies lower than 100 Hz. The finger impedance magnitudes obtained from the FlexiForce sensor are substantially lower than the reported values in the entire frequency range, as it was observed in case of the palm impedance magnitude.

4.3.3. Frequency response characteristics of the FlexiForce sensors

Lower impedance magnitude responses of the FlexiForce sensors were believed to be caused by the poor frequency response of the resistive sensors resulting in a limited bandwidth. A

recent study measured the biodynamic response of the seated body exposed to whole-body vibration using resistive pressure sensors for the measurement of the biodynamic force [59]. The study also reported substantially lower magnitudes of apparent mass measured from the resistive pressure sensors compared to a force plate, which was attributed to the limited frequency response of the resistive pressure sensors. The study also proposed a methodology to compensate for the limited frequency responses using the inverse frequency response function (FRF) of the pressure sensing system. In this study, the frequency response characteristics of the FlexiForce sensors are evaluated from the measured impedance responses, which could be applied as a correction for realizing better estimates for the hand-arm system impedance.

The FRF of the FlexiForce sensor was estimated from the ratio of the complex impedance response measured with the FlexiForce sensor to the reference response from the instrumented handle. The FRFs were computed for each subject, grip and push force combination, and excitation level. As an example, Fig. 4.5 illustrates the FRFs of the sensors obtained from the ratios of the palm and finger impedance responses corresponding to 1.5 m/s^2 excitation, and 30 N grip and 50 N push force combination. The figures show the FRFs obtained from the data acquired for all six subjects and the mean FRF. It should be noted that FRF phase response of the sensor is not presented for the finger side due to extreme variability. The results show comparable trends in the FRFs obtained for different subjects, although scatter is also evident especially at lower frequencies. This data scatter is caused by inter-subject variability of the measurements, which have also been reported to be significant in hand-arm impedance responses [11, 21, 31, 51].

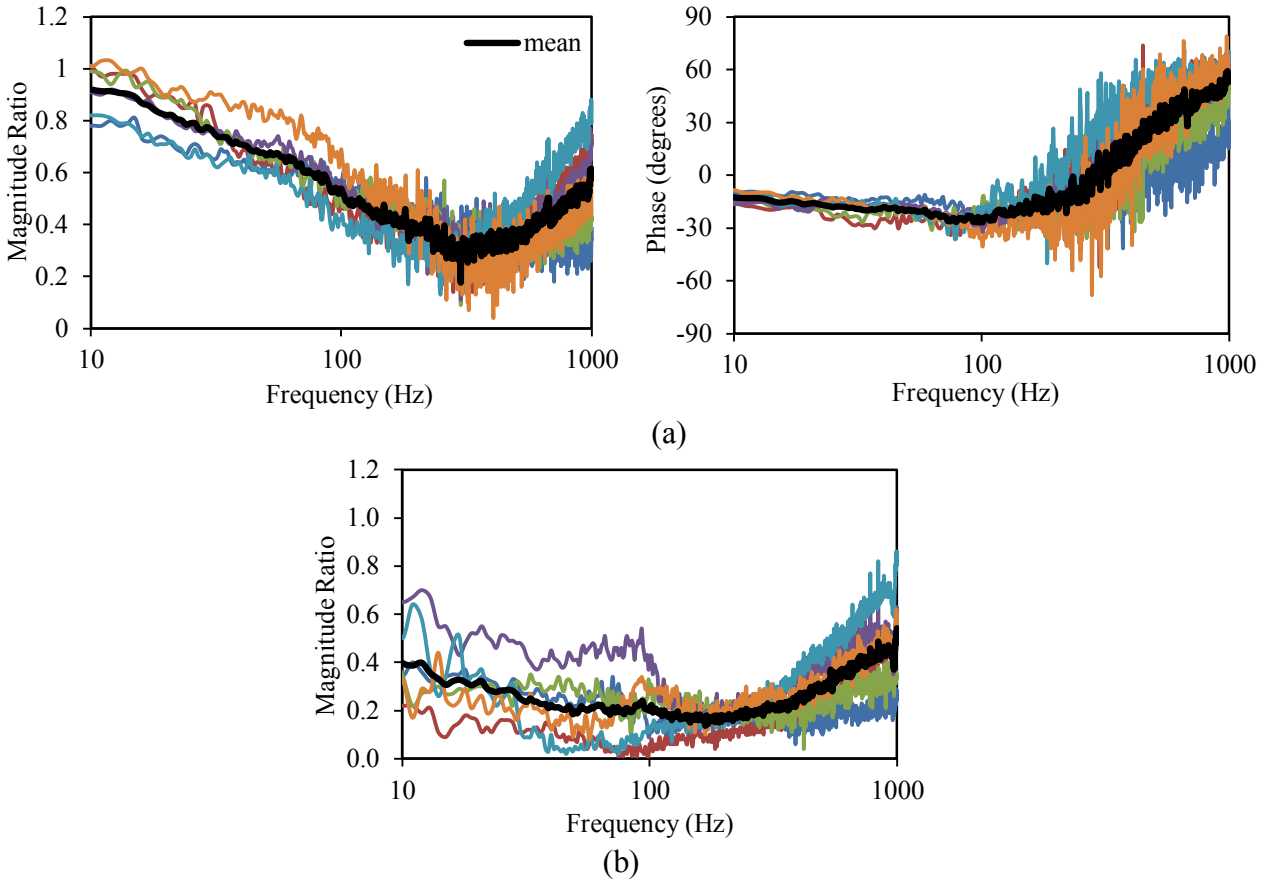

Figure 4.5: Frequency response characteristics of the FlexiForce sensors obtained from the palm and finger impedance responses of six subjects, together with the mean (FRF): (a) palm-side sensor; and (b) finger-side sensor (30 N grip, 50 N push and 1.5 m/s^2 excitation).

The results show a nearly unity ratio of the palm impedance magnitudes (FRF) at very low frequencies, which decreases to nearly 0.3 near 240 Hz and increases to about 0.5 at 1000 Hz. The mean ratio of the finger magnitude responses also shows a similar tendency. The palm sensor FRF phase is also observed to be very small at low frequencies but it decreases gradually to about –25^o near 90 Hz and then increases with an increase in frequency. The frequency response characteristics of the sensors obtained with different subjects, hand force and excitation level combinations revealed similar trends, while the magnitude ratio and the phase values differed considerably. These were attributed to variations in the hand dimensions, contact force distribution and the effective contact area. The influence of vibration level on the frequency response

characteristics of the sensors was observed to be small compared to that due to hand forces. As an example, Fig. 4.6 illustrates the variations in the FRF magnitude and phase responses of palm-side sensor for the nine hand force combinations, with palm force ranging from 35 to 125 N under 3 m/s^2 excitation. The results suggest substantial variations in the magnitude response, while the effect of hand force on the phase response is relatively smaller particularly at frequencies below 100 Hz. Similar variations were also observed for the finger-side sensor.

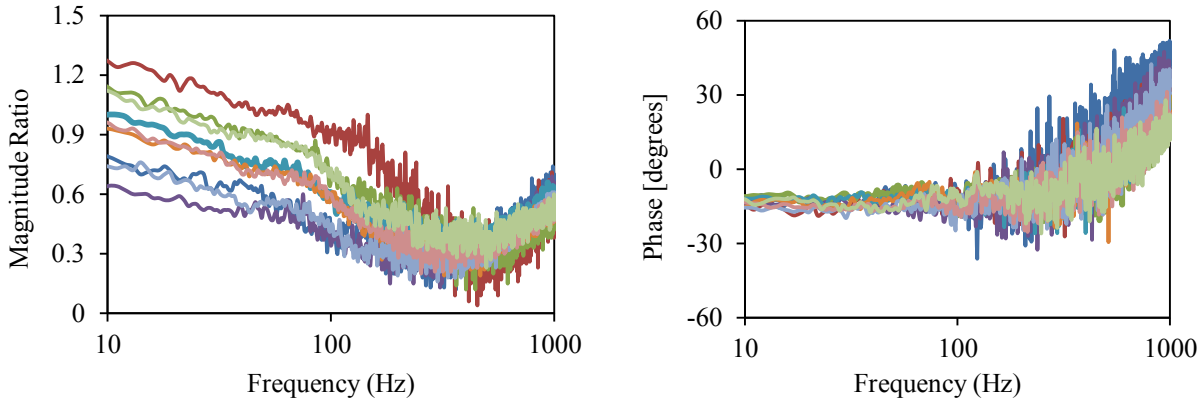

Figure 4.6: Influence of palm force on the frequency response characteristics of the FlexiForce sensor (3 m/s^2 excitation).

4.3.4. Application of the frequency response function of the FlexiForce sensor

The results in Fig. 4.6 suggest that application of the sensors' frequency response as a correction factor may thus necessitate characterization of the response for particular hand force combination. Alternatively, a mean FRF may be obtained for somewhat limited ranges of hand forces to obtain reasonable estimates of the DPMI responses. In this study, the inverse of the mean frequency functions of the FlexiForce sensors corresponding to different grip and push force combination are applied to the mean responses measured from the FlexiForce sensors, to obtain the corrected DPMI responses, as:

$$Z_c(j\omega) = FRF^{-1}(j\omega) * Z(j\omega) \tag{4.1}$$

Where Z_c is the corrected DPMI response and FRF^{-1} is the inverse of the mean transfer function.

Figures 4.7 and 4.8 illustrate comparisons of the corrected palm and finger impedance responses with the reference values corresponding to selected grip and push forces combinations for 1.5 and 3 m/s^2 rms acceleration excitations, respectively. The figures also show the uncorrected responses obtained directly from the FlexiForce sensor signals, while the reference responses are those derived from the instrumented handle.

The comparisons clearly show that the FlexiForce sensors could provide effective measurements of the palm and finger impedance responses in the entire frequency range, when the frequency response correction is applied. Such sensors could thus be applied for measurements of biodynamic responses and hand forces in tools handles in the field. The determination of FRFs of the sensors, however, would be quite challenging considering its nonlinear dependence on the hand forces. Considering that the hand-handle interface pressure distributions strongly depend upon the handle size and cross-section [30], it is very likely that the FRFs of the sensors would also depend upon the handle size. Further efforts to identify a generalized FRF would thus be worthy to facilitate measurements of the biodynamic responses under representative field conditions.

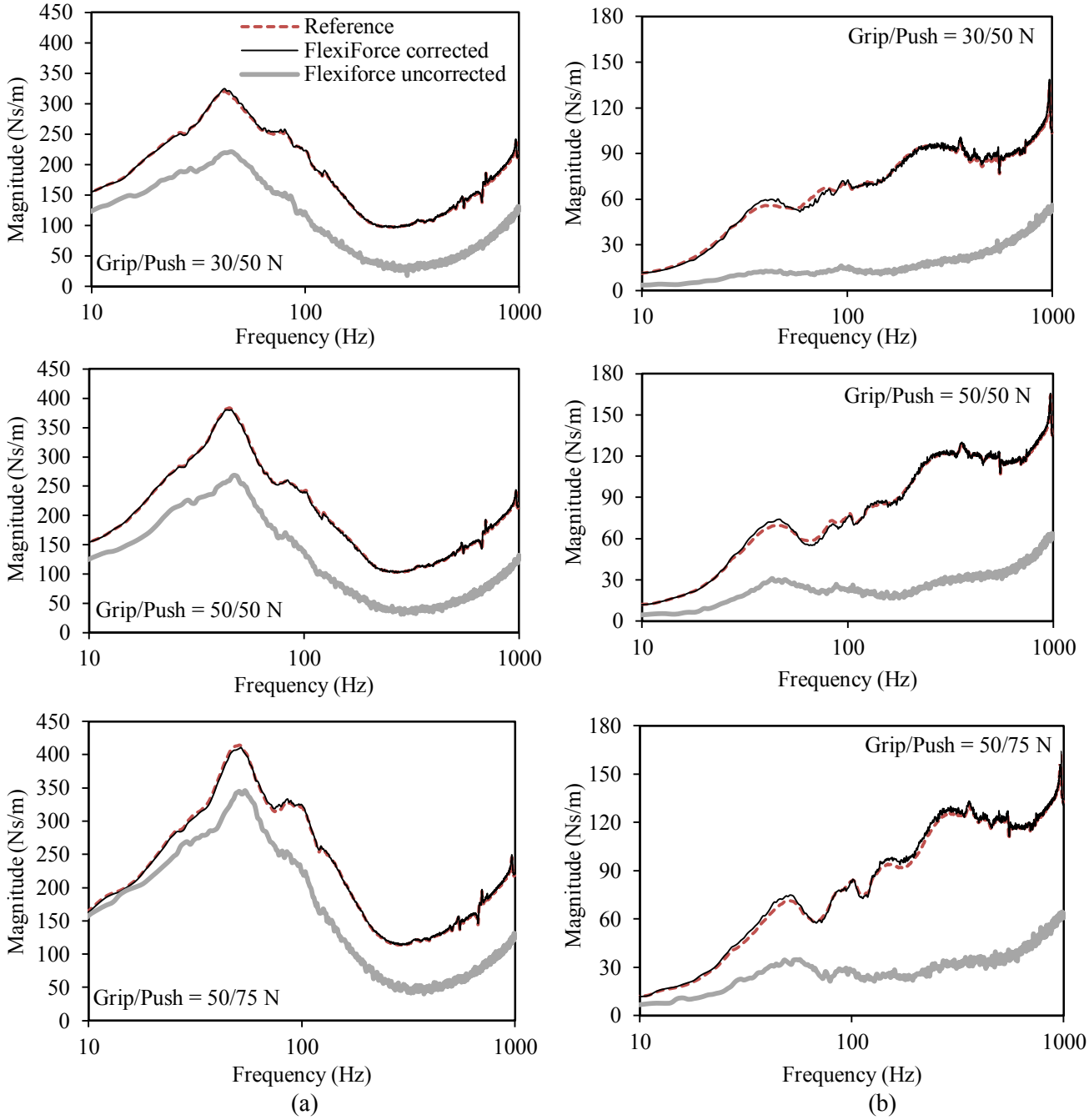

Figure 4.7: Comparisons of the corrected and uncorrected impedance responses obtained from the FlexiForce sensors with the reference response from the instrumented handle: (a) palm impedance; and (b) finger impedance (1.5 m/s^2 excitation).

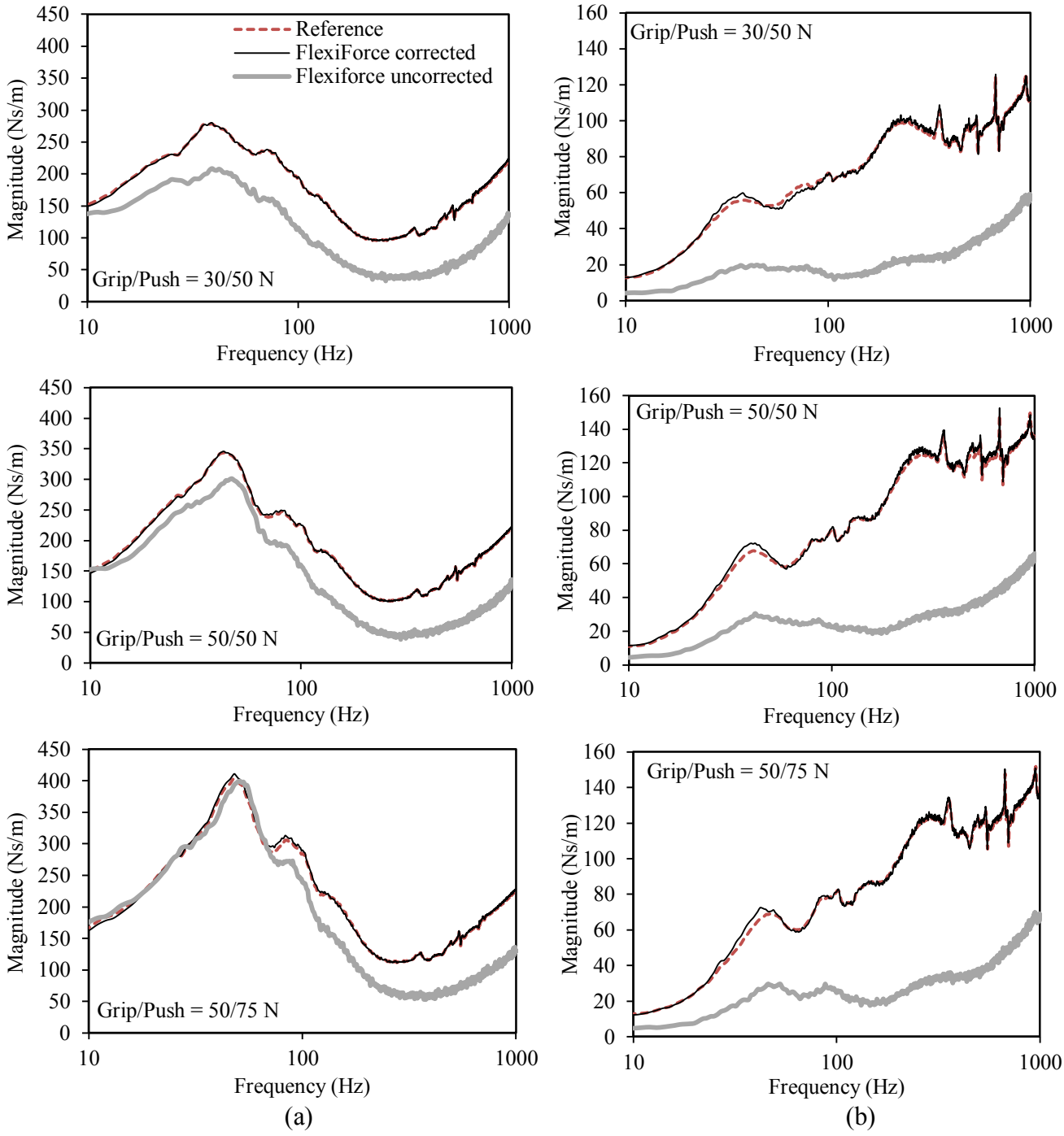

Figure 4.8: Comparisons of the corrected and uncorrected impedance responses obtained from the FlexiForce sensors with the reference response from the instrumented handle: (a) palm impedance; and (b) finger impedance (3 m/s^2 excitation).

Chapter 5
CONCLUSIONS AND RECOMMENDATIONS OF FUTURE WORK

5.1. Major Contributions

This dissertation's principal concern was the exploration of a low cost hand-handle interface force measurement system capable of accurately estimating the hand coupling forces at the tool handle interface. The major contributions are summarized as follows:

i. A low-cost measurement method is developed for acquiring hand grip and push forces imposed on real tool handles.

ii. The capabilities and major limitations of the FlexiForce sensors are illustrated through extensive measurements and analyses.

iii. The effectiveness and validity of the measurement system is presented by considering five different instrumented handles as well as a percussion tool handle.

iv. The distributions of the hand-handle interface force is estimated for the five different handles.

v. The applicability of the measurement system is illustrated for measurements of the hand-arm system biodynamic responses, where the potential errors associated with the handle inertia could be eliminated.

vi. A compensation function is proposed to account for sensors' limited frequency response.

5.2. Major Conclusions

i. Force sensing resistors (FSR) offer an effective, low-cost and attractive mean for measurement of hand-handle interface forces compared to capacitive sensors. The flexible, thin-film and trimable FlexiForce sensors can be conveniently applied to various tool handles.

ii. The in-depth static calibrations of the FlexiForce sensors under various conditions involving variations in applied load, load contact area, position and stiffness as well as the sensor length revealed good linearity and repeatability of the sensors. Although, the sensors were designed for only qualitative tactile feedback it was concluded from the calibration results the sensors could yield accurate quantitative measurements provided that each individual sensor is calibrated under the specific operating condition.

iii. The FlexiForce sensors applied to three cylindrical and two elliptical handles in addition to a percussion tool handle revealed good linearity and repeatability under stationary and vibrating conditions. The measured responses demonstrated the feasibility of the FlexiForce sensors for on-site field measurements.

iv. The hand-handle contact forces on the tool handles is mostly around the handle centerline along the direction of the forearm axis. It was thus concluded that sensor positions located symmetrically about the handle's vertical axis and offset by 5 mm in the counter-clockwise direction could yield accurate measurements of the hand grip and push forces. The results obtained with different handles showed superior sensor measurement performance when placed symmetrically about the vertical axis.

v. The biodynamic responses measured using the FlexiForce sensors showed comparable trends with the reference responses; albeit, with substantially lower magnitudes in the entire frequency range.

vi. The frequency response characteristics of the sensor revealed very limited bandwidth of the sensors. The application of the inverse frequency response function of the sensors could yield accurate measurements of the hand-arm system.

5.3. Recommendations for future work

The static and dynamic performance of the low-cost FlexiForce sensors as a hand-handle interface force measurement system implemented on various handles greatly exceeded the expectations by demonstrating high degrees of linearity and repeatability for all subjects. When transferred to a percussion tool handle the measurement system was able to once again provide linear and repeatable results and was able to accurately measure hand-handle forces at the tool interface, despite the sensors' inability to effectively encompass the handle surface due to an asymmetric cross-section. Furthermore, the measurement system could be effectively used to measure hand biodynamic responses given the implementation of a compensation function. This dissertation successfully contributed to developments in low cost devices for measurements of hand-handle coupling forces with hand-held power tools. Although, the need for additional efforts is recognized to facilitate further developments for field application to help increase the viability, performance and accuracy of the proposed measurement system, which are briefly described below:

i. Despite showing a high degree of linearity and repeatability further usage of the measurement system would benefit from improved sensor designs with greater consistency across the sensors in order to minimize the performance variabilities arising from changes in the contact force positioning and area.

ii. The development of a testing standard to calibrate each sensor during the manufacturing phase prior to its usage could greatly limit the need for individual sensor calibration prior to each test condition or subject, serve as a reference for laboratory/field experiments and help the sensors transition to a quantitative measurement method rather than simply qualitative.

iii. Improving the flexibility of the sensors for application to asymmetrical curved geometries would ensure improved contact on surfaces such as percussion tools to provide more dependable results.

iv. The limitation of the measurement system requires it to be in direct contact with the hand surface. Envisioning a design which can be easily manoeuvered inside gloves would significantly increase the versatility of the measurement system as an additional reference in laboratory settings or as the primary measurement method in field settings. This improvement would also permit the usage of antivibration gloves/materials on the hand forces imparted by the operator.

REFERENCES

[1] M. Bovenzi, L. Petronio, and F. Di Marino, "Epidemiological survey of shipyard workers exposed to hand-arm vibration," *International archives of occupational and environmental health,* vol. 46, pp. 251-266, 1980.

[2] M. Bovenzi, "Exposure-response relationship in the hand-arm vibration syndrome: an overview of current epidemiology research," *International archives of occupational and environmental health,* vol. 71, pp. 509-519, 1998.

[3] J. Malchaire, B. Maldague, J. Huberlant, and F. Croquet, "Bone and joint changes in the wrists and elbows and their association with hand and arm vibration exposure," *Annals of Occupational Hygiene,* vol. 30, pp. 461-468, 1986.

[4] M. J. Griffin, *Handbook of human vibration*: Academic press, 2012.

[5] ISO-5349-1, "Mechanical vibration and shock — Measurement and evaluation of human exposure to mechanical vibration — Part 1: General requirements," ed: International Organization for Standard, 2001.

[6] M. Bovenzi, "Epidemiological evidence for new frequency weightings of hand-transmitted vibration," *Industrial health,* vol. 50, pp. 377-387, 2012.

[7] M. J. Griffin, "Frequency-dependence of psychophysical and physiological responses to hand-transmitted vibration," *Industrial health,* vol. 50, pp. 354-369, 2012.

[8] E. Hartung, H. Dupuis, and M. Scheffer, "Effects of grip and push forces on the acute response of the hand-arm system under vibrating conditions," *International archives of occupational and environmental health,* vol. 64, pp. 463-467, 1993.

[9] ISO-15230, "Mechanical vibration and shock - Coupling forces at the man-machine interface for hand-transmitted vibration," ed: International Organization for Standard, 2007.

[10] S. Adewusi, S. Rakheja, P. Marcotte, and J. Boutin, "Vibration transmissibility characteristics of the human hand–arm system under different postures, hand forces and excitation levels," *Journal of sound and vibration,* vol. 329, pp. 2953-2971, 2010.

[11] P. Marcotte, Y. Aldien, P.-É. Boileau, S. Rakheja, and J. Boutin, "Effect of handle size and hand–handle contact force on the biodynamic response of the hand–arm system under z_h-axis vibration," *Journal of Sound and Vibration,* vol. 283, pp. 1071-1091, 2005.

[12] R. G. Radwin, T. J. Armstrong, and D. B. Chaffin, "Power hand tool vibration effects on grip exertions," *Ergonomics,* vol. 30, pp. 833-855, 1987.

[13] R. Gurram, S. Rakheja, and G. Gouw, "A study of hand grip pressure distribution and EMG of finger flexor muscles under dynamic loads," *Ergonomics,* vol. 38, pp. 684-699, 1995.

[14] U. Kaulbars, "Measurement and evaluation of coupling forces when using hand-held power tools," *Central European journal of public health,* vol. 4, pp. 57-58, 1996.

[15] U. Kaulbars and N. Raffler, "Study of vibration transmission on a paver's hand hammer," *Canadian Acoustics,* vol. 39, pp. 52-53, 2011.

[16] S. Riedel, "Consideration of grip and push forces for the assessment of vibration exposure," *Central European journal of public health,* vol. 3, pp. 139-141, 1994.

[17] P. Lemerle, A. Klinger, A. Cristalli, and M. Geuder, "Application of pressure mapping techniques to measure push and gripping forces with precision," *Ergonomics,* vol. 51, pp. 168-191, 2008.

[18] B. P. Kattel, T. K. Fredericks, J. E. Fernandez, and D. C. Lee, "The effect of upper-extremity posture on maximum grip strength," *International Journal of Industrial Ergonomics,* vol. 18, pp. 423-429, 1996.
[19] E. A. Kuzala and M. C. Vargo, "The relationship between elbow position and grip strength," *American Journal of Occupational Therapy,* vol. 46, pp. 509-512, 1992.
[20] R. J. Marley and R. R. Wehrman, "Grip strength as a function of forearm rotation and elbow posture," in *Proceedings of the Human Factors and Ergonomics Society Annual Meeting*, 1992, pp. 791-795.
[21] S. Adewusi, S. Rakheja, P. Marcotte, and P.-É. Boileau, "On the discrepancies in the reported human hand–arm impedance at higher frequencies," *International Journal of Industrial Ergonomics,* vol. 38, pp. 703-714, 2008.
[22] R. G. Dong, D. Welcome, T. W. McDowell, and J. Z. Wu, "Analysis of handle dynamics-induced errors in hand biodynamic measurements," *Journal of Sound and Vibration,* vol. 318, pp. 1313-1333, 2008.
[23] Y. Aldien, P. Marcotte, S. Rakheja, and P.-É. Boileau, "Mechanical impedance and absorbed power of hand-arm under xh-axis vibration and role of hand forces and posture," *Industrial health,* vol. 43, pp. 495-508, 2005.
[24] Y. Aldien, P. Marcotte, S. Rakheja, and P.-É. Boileau, "Influence of hand forces and handle size on power absorption of the human hand–arm exposed to z_h-axis vibration," *Journal of sound and vibration,* vol. 290, pp. 1015-1039, 2006.
[25] L. Burström, "Measurements of the impedance of the hand and arm," *International archives of occupational and environmental health,* vol. 62, pp. 431-439, 1990.
[26] E. Chadwick and A. Nicol, "A novel force transducer for the measurement of grip force," *Journal of biomechanics,* vol. 34, pp. 125-128, 2001.
[27] R. Lundström and L. Burström, "Mechanical impedance of the human hand-arm system," *International Journal of Industrial Ergonomics,* vol. 3, pp. 235-242, 1989.
[28] R. W. McGorry, "A system for the measurement of grip forces and applied moments during hand tool use," *Applied ergonomics,* vol. 32, pp. 271-279, 2001.
[29] B. Wimer, R. G. Dong, D. Welcome, C. Warren, and T. McDowell, "Development of a new dynamometer for measuring grip strength applied on a cylindrical handle," *Medical engineering & physics,* vol. 31, pp. 695-704, 2009.
[30] Y. Aldien, P. Marcotte, S. Rakheja, and P.-É. Boileau, "Influence of hand–arm posture on biodynamic response of the human hand–arm exposed to z_h-axis vibration," *International Journal of Industrial Ergonomics,* vol. 36, pp. 45-59, 2006.
[31] L. Burström, "The influence of biodynamic factors on the mechanical impedance of the hand and arm," *International archives of occupational and environmental health,* vol. 69, pp. 437-446, 1997.
[32] R. G. Dong, D. Welcome, T. McDowell, and J. Wu, "Measurement of biodynamic response of human hand–arm system," *Journal of Sound and Vibration,* vol. 294, pp. 807-827, 2006.
[33] ISO-10819, "Mechanical vibration and shock — Hand-arm vibration — Measurement and evaluation of the vibration transmissibility of gloves at the palm of the hand," ed: International Organization for Standard, 2013.
[34] Y. Aldien, "A study of hand-handle interactions and hand-arm biodynamic response to vibration," Concordia University, 2005.
[35] M. Van der Kamp, B. Conway, and A. Nicol, "A novel instrumented ring for the measurement of grip force adjustments during precision grip tasks," *Proceedings of the*

Institution of Mechanical Engineers, Part H: Journal of Engineering in Medicine, vol. 215, pp. 421-427, 2001.

[36] M. H. Yun, K. Kotani, and D. Ellis, "Using force sensitive resistors to evaluate hand tool grip design," in *Proceedings of the Human Factors and Ergonomics Society Annual Meeting*, 1992, pp. 806-810.

[37] Y. Aldien, D. Welcome, S. Rakheja, R. G. Dong, and P.-E. Boileau, "Contact pressure distribution at hand–handle interface: role of hand forces and handle size," *International Journal of Industrial Ergonomics,* vol. 35, pp. 267-286, 2005.

[38] D. Welcome, S. Rakheja, R. G. Dong, J. Wu, and A. Schopper, "An investigation on the relationship between grip, push and contact forces applied to a tool handle," *International Journal of Industrial Ergonomics,* vol. 34, pp. 507-518, 2004.

[39] J. G. Young, M. E. Sackllah, and T. J. Armstrong, "Force distribution at the hand/handle interface for grip and pull tasks," in *Proceedings of the Human Factors and Ergonomics Society Annual Meeting*, 2010, pp. 1159-1163.

[40] A. Calvo and R. Deboli, "The Use of a Capacitive Sensor Matrix to Determine the Grip Forces Applied to the Olive Hand Held Harvesters," *Agricultural Engineering International: CIGR Journal,* 2009.

[41] VIBTOOL, "Grip force mapping for characterization of hand-held vibrating tools," European Community Competitive and Sustainable Growth Program Report 2008.

[42] E. R. Komi, J. R. Roberts, and S. Rothberg, "Evaluation of thin, flexible sensors for time-resolved grip force measurement," *Proceedings of the Institution of Mechanical Engineers, Part C: Journal of Mechanical Engineering Science,* vol. 221, pp. 1687-1699, 2007.

[43] J. Rossi, E. Berton, L. Grélot, C. Barla, and L. Vigouroux, "Characterisation of forces exerted by the entire hand during the power grip: effect of the handle diameter," *Ergonomics,* vol. 55, pp. 682-692, 2012.

[44] B.-E. 420, "General requirements for gloves.," ed: British Standard, 1994.

[45] L. Cronjager and M. Hesse, "Hand-arm system's response to stochastic excitation," in *5th international conference on hand-arm vibration*, 1990, pp. 39-42.

[46] D. D. Reynolds and R. Falkenberg, "A study of hand vibration on chipping and grinding operators, Part II: Four-degree-of-freedom lumped parameter model of the vibration response of the human hand," *Journal of Sound and Vibration,* vol. 95, pp. 499-514, 1984.

[47] K. Dewangan, S. Rakheja, P. Marcotte, A. Shahmir, S. Patra. "An exploratory study of a measurement system for characterizing seated body apparent mass coupled with elastic seats under vertical vibration," IRSST2013.

[48] R. G. Dong, S. Rakheja, A. Schopper, B. Han, and W. Smutz, "Hand-transmitted vibration and biodynamic response of the human hand-arm: a critical review," *Critical Reviews™ in Biomedical Engineering,* vol. 29, 2001.

[49] ISO-10068, "Mechanical vibration and shock – Free mechanical impedance of the human hand-arm system at the driving-point," ed: International Organization for Standard, 1998.

[50] ISO-8662-2, "Hand-held portable power tools—measurement of vibrations at the handle—part 2: Chipping hammers and riveting hammers," ed: International Organization for Standard, 1992.

[51] R. G. Dong, J. Wu, T. McDowell, D. Welcome, and A. Schopper, "Distribution of mechanical impedance at the fingers and the palm of the human hand," *Journal of biomechanics,* vol. 38, pp. 1165-1175, 2005.

[52] I. Tekscan. (June). *Force v. Resistance/Conductance*. Available: http://www.tekscan.com/custom-OEM-force-sensors
[53] P. Marcotte, S. Adewusi, and S. Rakheja, "Development of a low-cost system to evaluate coupling forces on real power tool handles," *Canadian Acoustics,* vol. 39, pp. 36-37, 2011.
[54] F. O. Medola, D. C. Silva, C. A. Fortulan, V. M. C. Elui, and L. C. Paschoarelli, "The influence of handrim design on the contact forces on hands' surface: A preliminary study," *International Journal of Industrial Ergonomics,* 2014.
[55] J. Malinowska-Borowska, B. Harazin, and G. Zieliński, "The influence of wood hardness and logging operation on coupling forces exerted by lumberjacks during wood harvesting," *International Journal of Industrial Ergonomics,* vol. 41, pp. 546-550, 2011.
[56] A. Akgunduz, S. Rakheja, and A. Tarczay, "Distributed occupant–seat interactions as an objective measure of seating comfort," *International Journal of Vehicle Design,* vol. 65, pp. 293-313, 2014.
[57] C. Ashruf, "Thin flexible pressure sensors," *Sensor Review,* vol. 22, pp. 322-327, 2002.
[58] C. Hall, "External pressure at the hand during object handling and work with tools," *International Journal of Industrial Ergonomics,* vol. 20, pp. 191-206, 1997.
[59] K. Dewangan, S. Rakheja, P. Marcotte, A. Shahmir, and S. Patra, "Comparisons of apparent mass responses of human subjects seated on rigid and elastic seats under vertical vibration," *Ergonomics,* vol. 56, pp. 1806-1822, 2013.
[60] S. Rakheja, P. Marcotte, M. Kalra, S. Adewusi, K. Dewangan, "A laboratory study of a low-cost system for measurements of coupling forces at the vibrating handle-hand interface," IRSST2014.

APPENDIX A
FLEXIFORCE SENSOR CHARACTERISTICS

The initial measurements to characterize the sensor output were performed under various static conditions in order to understand several properties of the sensors as described in section 2.2.1. The following section presents more detailed static sensor calibration results than those presented in Chapter 3. A total of twenty-one sensors were used during the complete study. The sensors were numbered chronologically; however, due to sensor failure/damage some results are presented with sensor numbers placed out of order. The sensor nomenclature has no bearing on the sensor output. The following section details the static sensor calibration results performed on six sensors (labeled #1, 4, 5, 6, 7, 8).

A.1. HYSTERISIS

Initially, it was uncertain whether to load the sensors from 0 to 100 N or vice versa. Since the application of hand forces would not ideally be unidirectional since many subjects would be likely to unintentionally overshoot the target values, it was imperative to determine whether the output was affected by the applied load's directionality. As an example, fig A.1 illustrates the input-output characteristics of two different sensors acquired during gradual loading and unloading on a flat surface. The applied load increased from 0 to 120 N then was gradually unloaded in increments of 10 N. Due to the relaxation properties of the sensor output and applied force displayed considerable drift at each load increment; thus, the elastomer was allowed to relax for nearly one minute during each force level or until steady force and voltage values were retrieved.

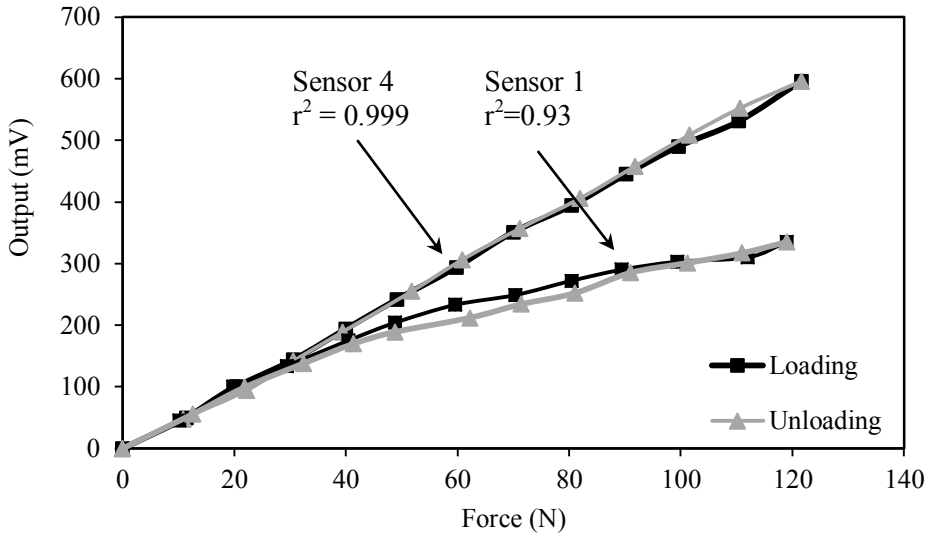

Figure A.1: Input-output properties of two sensors subject to gradual loading and unloading.

The drift was noticed to be higher when considering larger values of force. Both sensors show highly linear outputs, with sensor #4 displaying near perfect correlation and sensor #1 with an $r^2 = 0.93$. Sensor #1 shows a decreased in linearity after attaining 40 N however, considering the overall correlation this sensor is still considered acceptable for usage with hand force testing. Furthermore, the results yielded linearity well below 3% and very low hysteresis (below 3.5%)

A.2. Linearity and Consistency

Despite both sensors displaying highly linear behaviour there are considerable differences between the output voltages. Through discussions with the manufacturer it was realized that these sensors were designed solely for qualitative tactile sensing and would likely show poor repeatability of objective measurements across a sample of sensors. It would however be feasible to fabricate such sensors with enhanced consistency for repeatable objective measurements, which would involve a substantial setup cost. To determine whether this study could reliably use the FlexiForce sensors for repeated measurements multiple static loading trials were conducted on three untrimmed 'nominal' sensors with unidirectional loading applied from 0 to 100 N. Each

sensor was paired with the 'stiff' elastomer. Figures A.2a-c show the sensor voltage output recorded between forces of 0-100 N for three nominal sensors with twelve repeated trials.

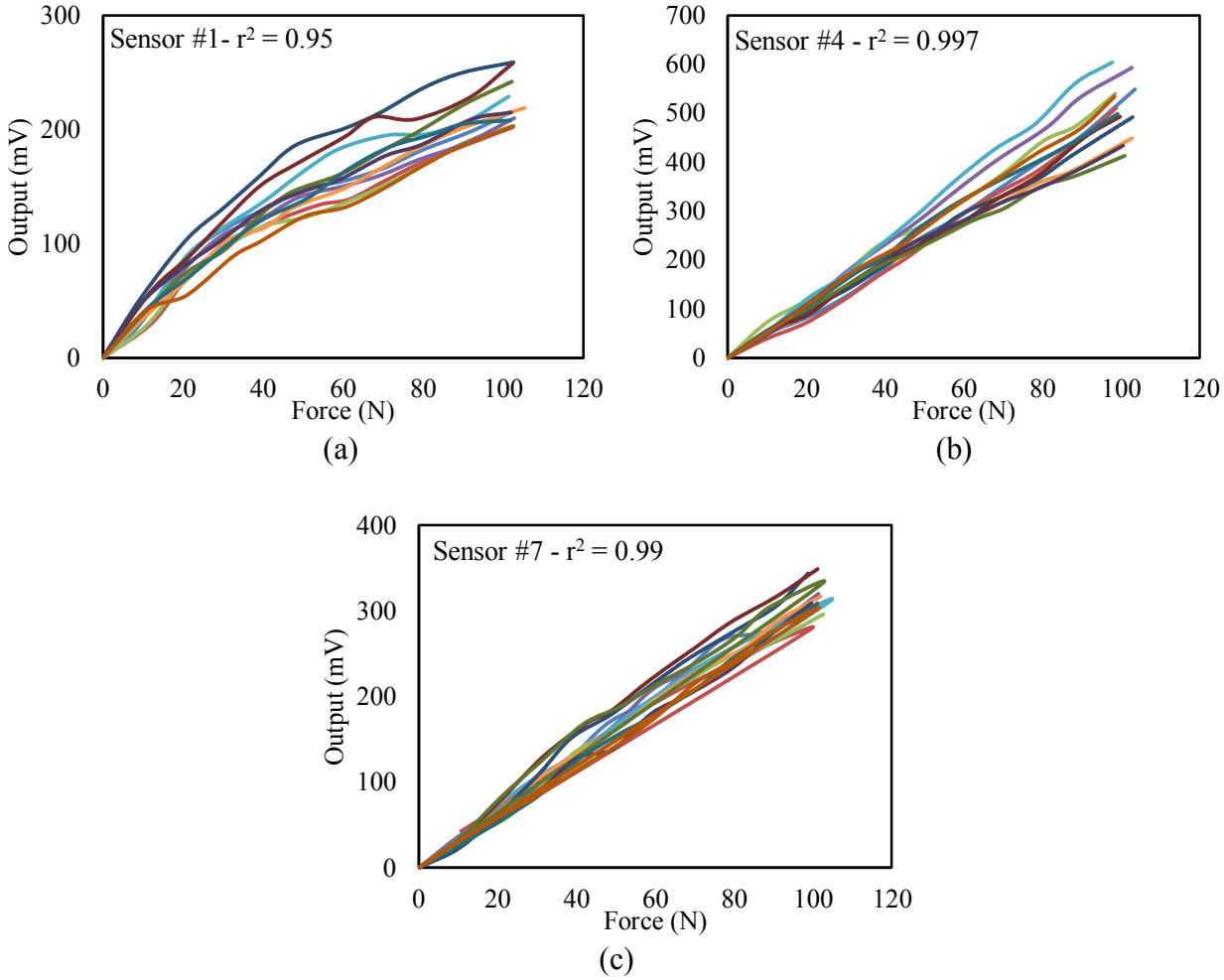

Figure A.2: Static sensor calibrations conducted on nominal sensors (a) Sensor # 1; (b) Sensor # 4; and (c) Sensor # 7.

Of the 36 trials from the three sensors the majority show linear trends. A few trials from sensor #1 have a slight curvature due to changes in the linearity during force application. This fluctuation was expected due to the output drift associated with the elastomer's relaxation time requirement. Each sensor shows intra-trial sensitivity differences; however, the linearity and consistency amongst the trials showed highly favourable results. These results are further reinforced based on the average r^2 values displayed in the upper left-hand corner of each graph.

Despite sensor #1 showing a few curved trials it resulted in an r^2 coefficient of 0.95. Sensors #4 and #7 display r^2 averages of 0.997 and 0.99, respectively.

A.3. Sensor Length

Since the length of the five handles is considerably shorter than the sensor each sensor would have to be trimmed to accommodate the hand-handle force measurements. Three sensors were trimmed to an approximate length of 117 mm and tested for linearity and consistency similarly with the three nominal sensors. A different trio of sensors were expected to exhibit different sensitivities; however, the intra-trial linearities were of greater concern than intra-trial sensitivities. Figures A.3a-c show the sensor voltage output recorded between forces of 0-100 N for three 'trimmed' sensors with twelve repeated trials, except for sensor #6 which was tested for nine trials due to incurred damage. The trends for all three cases again show highly linear behaviour as with the nominal sensors and demonstrate that with uniform loading over the entire sensor area any sensor behaves linearly and it's linearity is unaffected by reducing its size. With each sensor the linearity of the trials demonstrates strong intra-trial correlation since all three sensors demonstrate r^2 values of at least 0.99. It is thus established that trimming the sensors does not affect their precision. Comparing the sensitivities of all trials amongst the six nominal and trimmed sensors provides a measure of the accuracy of the FlexiForce sensors. The mean sensitivity, standard deviation (SD) and covariance (COV) of all trials are shown in table A.1. It is now evident there is a large inter-sensor discrepancy in the sensitivities. However, the intra-sensor sensitivities are largely consistent and considered favourable. Sensor #1 displays the highest intra-sensor variability with a COV value of 10.9 %; while, the other five sensors all have COV values below 10 %.

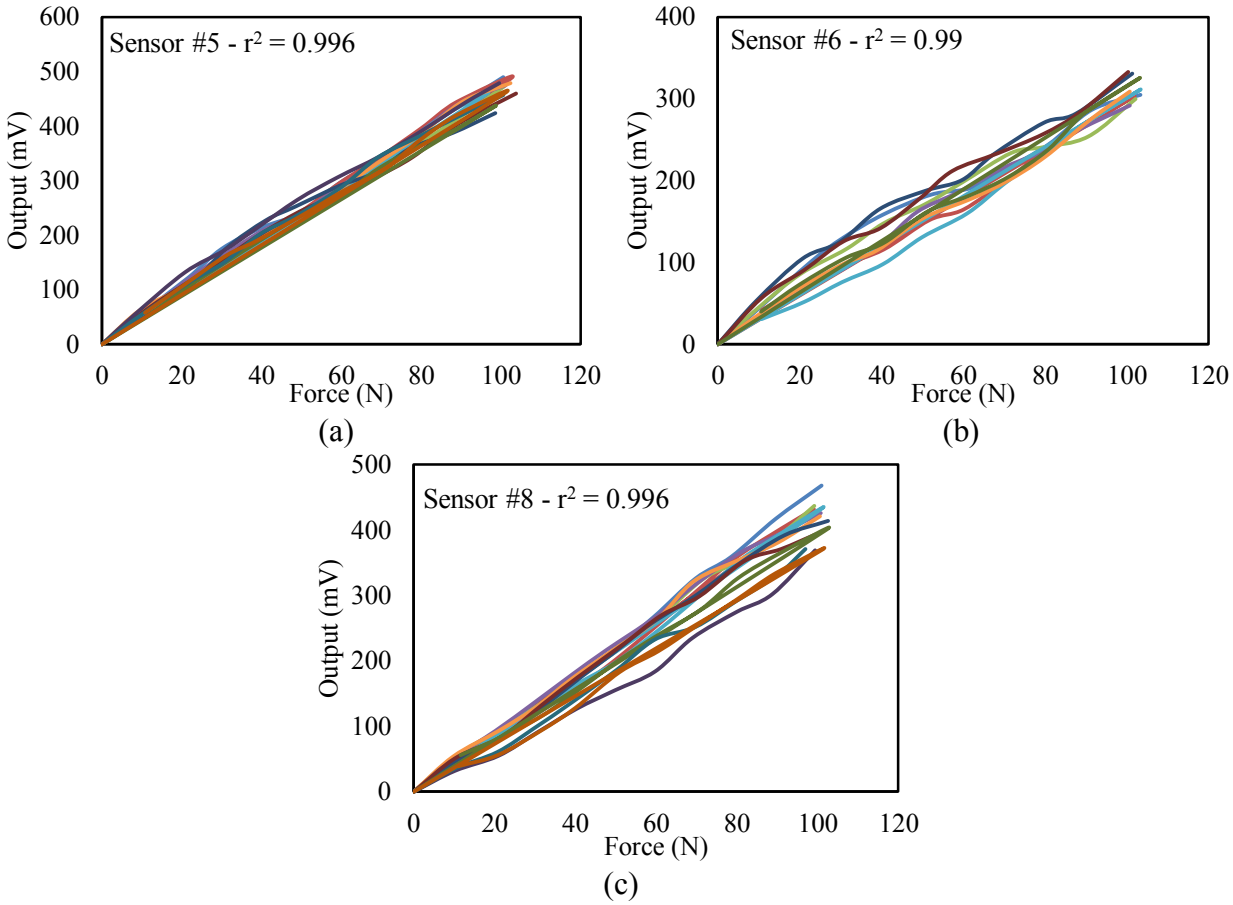

Figure A.3: Static sensor calibrations conducted on trimmed sensors (a) Sensor # 5; (b) Sensor # 6; and (c) Sensor # 8.

	Sensitivity mV/N					
Sensor #	**1**	**4**	**7**	**5**	**6**	**8**
T1	2.4	4.1	3.3	4.9	3.2	4.6
T2	2.2	4.2	3.0	4.9	2.9	4.3
T3	2.2	3.9	3.1	4.7	3.1	4.4
T4	2.3	4.0	3.2	4.9	3.0	4.4
T5	2.6	4.2	3.2	4.8	2.9	4.2
T6	2.3	4.1	3.2	4.8	3.0	4.3
T7	3.0	4.8	3.5	4.6	3.4	4.2
T8	2.8	4.6	3.6	4.5	3.4	4.2
T9	2.6	4.5	3.4	4.5	3.1	4.0
T10	2.4	4.2	3.0	5.0	-	3.4
T11	2.4	4.3	3.0	4.7	-	3.7
T12	2.1	4.2	3.0	4.7	-	3.6
Mean	2.5	4.3	3.2	4.8	3.1	4.1
SD[1]	0.27	0.24	0.21	0.15	0.19	0.36
COV[2]	10.9%	5.7%	6.4%	3.1%	6.2%	8.9%

SD[1] – standard deviation, COV[2] – covariance, T – Trial

Table A.1: FlexiForce sensor sensitivities for nominal (#1,4,7) and trimmed (#5,6,8) sensors.

From table A.1 as well as figures A.2 and A.3 it may be misconstrued that trimmed sensors are more linear or consistent than nominal sensors. This idea is invalid since sensors 6 and 8 show the similar degrees of variability compared to sensors 4 and 7. Sensor #1 simply contains a few trials with serve as anomalies. Based on the results obtained from the six aforementioned sensors it was thus concluded that these sensors would be feasible for quantitative measurements of static force, provided each sensor is calibrated individually on the flat surface prior to implementation on an instrumented handle or tool.

To compare the effect of sensor trimming on the sensitivity the output three trials are conducted with an unused nominal sensor with a standard length of 149 mm. Subsequently, the sensor is trimmed to approximately 117 mm to resemble the length of the cylindrical handle. Conducting the trimmed sensor tests with the elastomer used thus far resulted in the elastomer covering a larger area than the sensor. The default 'long' elastomer's length measured 141.7 mm and it was presumed this would not be an issue since as long as the majority of the sensor remained covered by an elastomer. A 'medium' length elastomer measuring 115.6 mm in length was shaped to confirm this presumption. Preliminary tests with both elastomers on a trimmed sensor revealed almost identical sensitivities sensor and it was not deemed necessary to record these results. To conform to the test methodology establish in previous calibrations the trimmed sensor was paired with the 'medium' elastomer since nominal sensors were also paired with slightly shorter elastomers. Figure A.4 illustrates the measured input-output properties of the nominal and trimmed sensors, obtained during three trials.

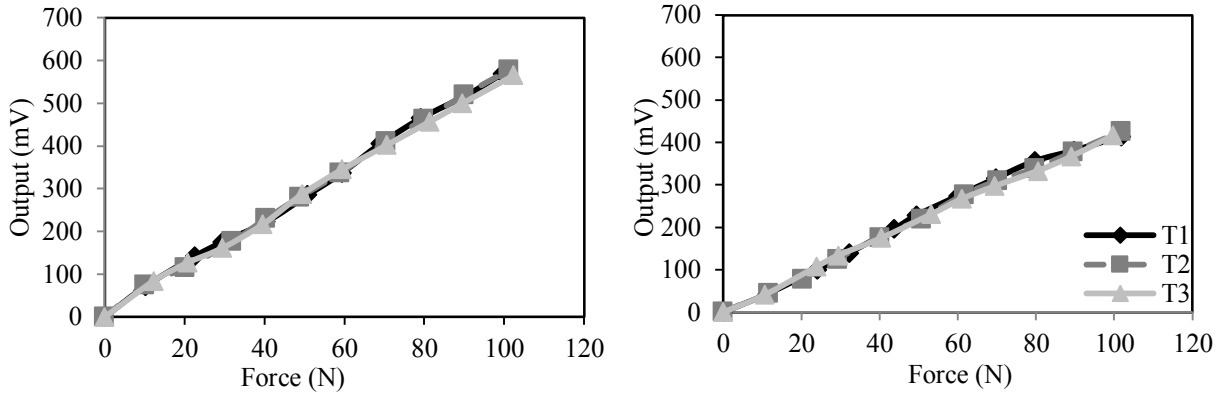

Figure A.4: Input-output characteristics of one sensor during three trials: (a) untrimmed - 149 (mm) and (b) trimmed – 117 (mm).

The results show reasonably good linearity (r^2>0.99) and good repeatability of measurements during the three trials. The trimmed sensor, however, showed higher sensitivity compared to the standard sensor, which was attributed to reduced contact area and thereby higher contact pressure under equivalent loads. The mean sensitivity of the nominal sensor was obtained as 4.28 mV/N with a SD of 0.06 mV/N, while that of the trimmed sensor increased to 5.71 mV/N with a corresponding of SD 0.07 mV/N. The results confirm that output of the FlexiForce sensor depends on both the applied force and the effective area. However, trimming the sensor does not affect the linearity or consistency of the output sensitivity, thus, it is expected the sensitivity results due to hand-handle forces on the instrumented handles will exhibit similar linear trends.

A.4. Elastomer contact area

As stated in the previous section the long and medium elastomers had profoundly similar results when placed on a trimmed sensor since both elastomers were able to encompass most or all of the sensor's length. Both elastomers left a portion of the sensor's width uncovered; yet, as explained in section 2.1 the sensor's construction does not require force to be applied over the entire surface. However, it was also established the sensors would yield more consistent results from surface loads covering a greater number of sensels due to their unpredictability with localized

applied forces. To observe the effects of loading area on sensor output three elastomer lengths were tested on a nominal sensor. The long full-length elastomer (141.7 x 33.3 mm), the 'medium' length elastomer (115.6 x 32.7 mm) and a 'short' length elastomer (60.7 x 30 mm) were tested on the same sensor whereby the 'medium' and short covered only a portion of the sensor's area. All three elastomers were the same material and were placed symmetrically about the sensor's midpoint. The effect of contact area was hypothesized to be negligible as observed with effects of the 'long' and 'medium' elastomers on the 'trimmed' sensor; yet, the results show a profound impact of loading area on the nominal sensor output. Figure A.5 shows the sensor output with two trials conducted for each of the three elastomer lengths.

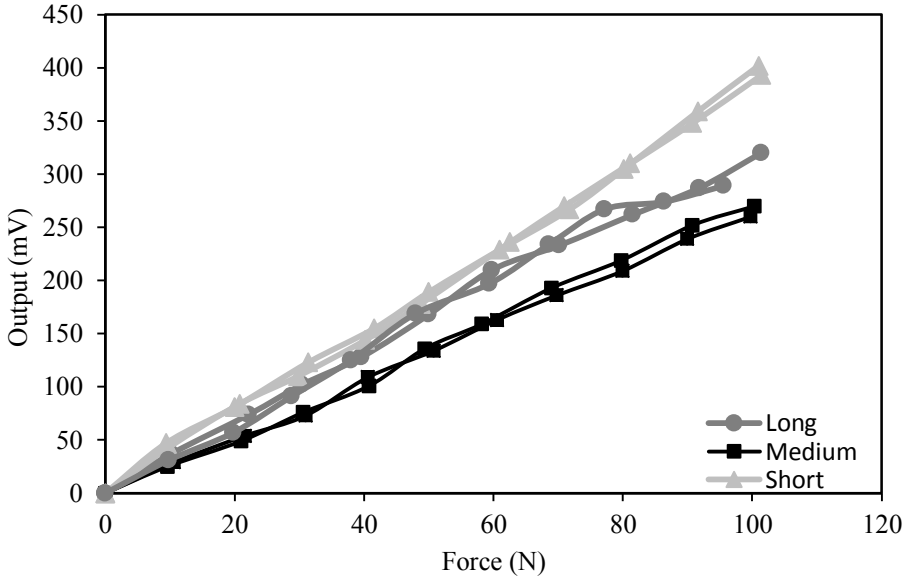

Figure A.5: Effect of elastomer contact area on sensor output.

The short and long elastomer pads exhibit comparable sensor output only up to 60 N force, while the long pad yields lower output compared to the short pad under higher forces. This is most likely due to higher concentrated contact pressure imposed by the short 'pad' on the sensor. The medium 'pad' resulted in considerably lower sensor output in the entire force range compared to

the other two lengths. The nature of the sensors causes them to conduct an output if the force is applied on an intersecting sensel located between the two polymer layers (as explained in section 2.1). The likely reason for the short pad resulting in the highest sensitivity is due to this pad contacting the highest amount of intersecting locations per unit area of elastomer; thus, resulting in higher concentration of contact pressure. The 'medium' pad likewise covered fewer intersecting locations per unit of its elastomer length thus resulting in a lower overall sensitivity. Logically, a smaller hand applying equivalent force over a more concentrated area results in higher pressure; therefore, it is expected for smaller hand sizes to yield higher sensitivities.

A.5. Elastomer location

The previous sub-section demonstrates the effect of load surface area on the effect of a nominal sensor's sensitivity. Due to varying grasping preference different users would have a tendency to grasp handles in different positions. To test the effect of location of the applied force on a nominal sensor the short elastomer is placed in four positions along the sensor's long axis while measuring the sensor's sensitivity. The effect of the elastomer location on the sensor was further investigated through repeated measurements with the short loading elastomer (60.7x30.0 mm) located at four different positions. A coordinate system was defined on the sensor to facilitate the shift in pad positioning. The width of the sensor is defined as the y-axis and the length as the x-axis. For each position the short elastomer was aligned with the bottom edge of the sensor and shifted along the x-axis; thus, ensuring the y-axis position would not change during each position. This results would therefore be entirely correlated to the shift along the x-axis. Positions 1 and 4 represent the elastomer located at either edge of the sensor, position 2 represents the elastomer located centrally and position 3 was arbitrarily chosen as x = 60 mm. Figure A.6 shows coordinate system as well as the location and average sensor sensitivities of one trial conducted for each

elastomer position and Figure A.7 shows a graphical illustration of the effect of elastomer position on sensor output.

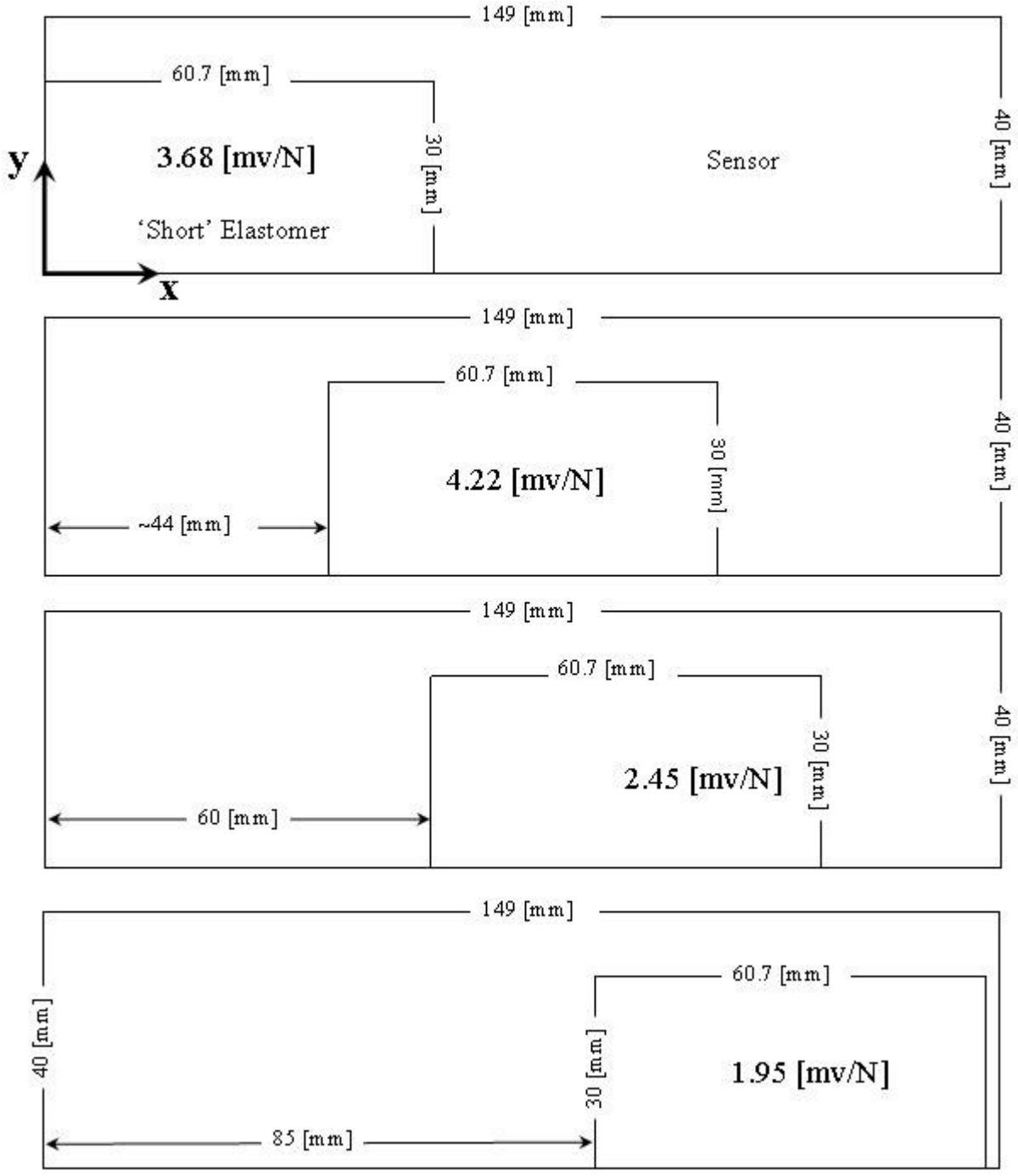

Figure A.6: Effect of nominal sensor sensitivity based on the short elastomer placed at four positions.

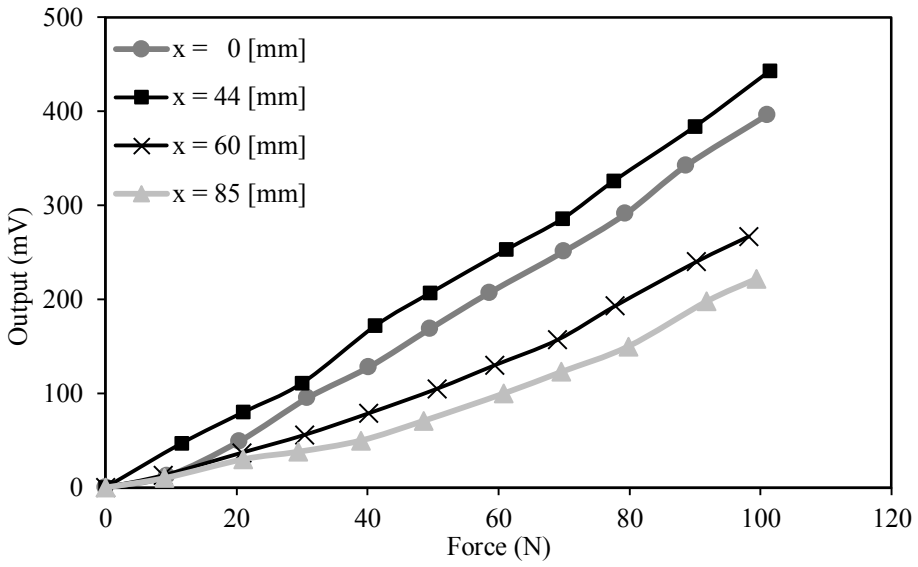

Figure A.7: Effect of elastomer position on sensor output.

The results clearly show substantial effect of position of the load on the sensor output. The sensor outputs corresponding to the four loading positions exhibit output sensitivity of 3.68, 4.22, 2.45 and 1.93 mV/N, respectively. The sensor exhibits the highest output, when the applied force is symmetric about the center of the sensor. The discrepancy is again likely due to differences in the amount of intersecting locations that each elastomer makes contact with. The sensor also yields a more nonlinear input-output relationship, when loading elastomer is located asymmetrically about the center of the sensor.

A.6. Plate surface curvature

Three nominal sensors (#1, #4 and #7) are tested on the curved surface platform to gauge the effect of curvature on sensitivity output. The applied force is identical to that applied on the flat surface. However, the elastomer used during the curved test is thin and flexible unlike the rigid one used for the flat surface. Initially, when the upper metal plate is placed upon the sensor the natural stiffness of the sensor resists the weight of the plate. Hence, in order for the plate to uniformly cover the sensor a preload of 7 N is applied. Every sensor has an identical stiffness

coefficient; thus, the same preload is applied across all sensors. Figures A.8a to c display the sensor outputs when placed on the curved surface.

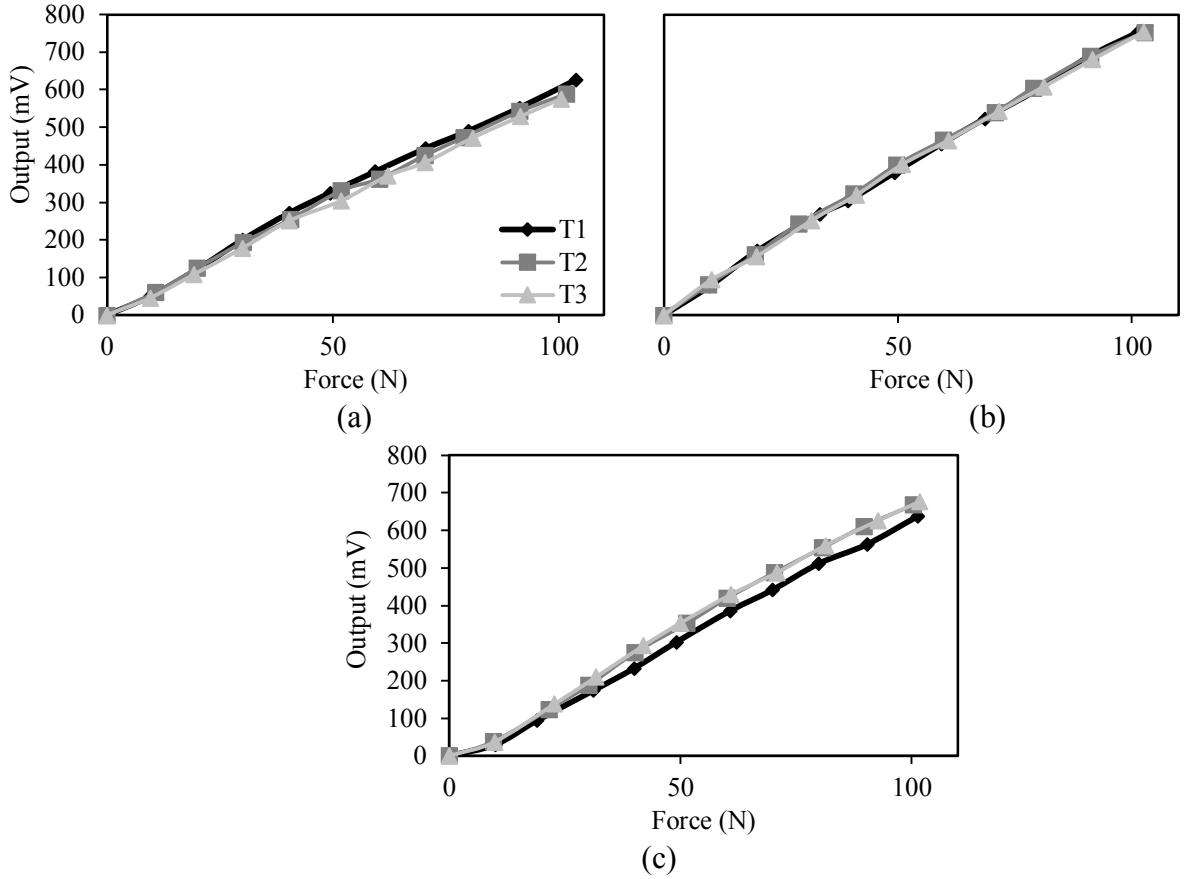

Figure A.8: Static input-output characteristics of two sensors subject to loading on the curved surface: (a) sensor #1; (b) sensor #4; and (c) sensor #7.

The 7 N applied to the curved surface is identical to a much higher value applied on a flat surface. As an example the 7 N preload on sensor #7 when placed on the curved surface is equivalent to a 20.8 N baseline force applied on the flat surface. The other two sensors similarly experience large baseline voltages. A potential reason to the baseline is the nature of deformation the sensor experiences. Bending a flat plate induces tensile and compressive stresses on the upper and lower surfaces. It is widely known that the stress is zero along the neutral axis (N.A.) and the sum of all stresses above and below the N.A. is also zero. The FlexiForce sensors have an upper

and lower substrate and it is feasible to presume the upper is under tensile stress and the lower under compressive; yet, since the substrates only measure changes in resistance and are unconcerned with the sign convention of the applied stresses/forces, the tension and compression effects are likely added resulting in a high baseline preload. Despite, the increased voltage outputs all three sensors still retain the same level of linearity and consistency comparative to the trials conducted on the flat plate. Table A.2 shows the differences in sensitivities, standard deviations and covariances for the nominal sensors 1,4 and 7 on the flat and curved surfaces.

	Sensor	**1**	**4**	**7**
Flat Surface	Mean S^1 (mv/N)	2.45	4.25	3.21
	SD^2	0.27	0.24	0.21
	COV^3 (%)	10.9	5.7	6.4
Curved Surface	Mean S^1 (mv/N)	6.00	7.57	6.60
	SD^2	0.19	0.05	0.32
	COV^3 (%)	3.2	0.6	4.8

S^1 – sensitivity, SD^2 – standard deviation, COV^3 – covariance

Table A.2: Comparison of sensor output on flat vs. curved surface.

A.7. ELASTOMER RIGIDITY

To be certain the increase in sensitivity on the curved surface is in fact due to curvature the final static sensor calibration involved testing nominal sensors 1,4 and 7 with the 'stiff' and 'soft' elastomer on a flat surface. Figures A.9a to c show the outputs of each sensor under the influence of the 'stiff' and 'soft' elastomer conducted with two trials for each elastomer.

Both elastomers require a certain relaxation time period once the control knob from the force indenter is released. The substantially lower sensor output with the 'soft' pad was partly attributed to larger elastomeric deformations, which could cause non-uniform pressure distribution on the contact surface due to its longer relaxation time requirement.

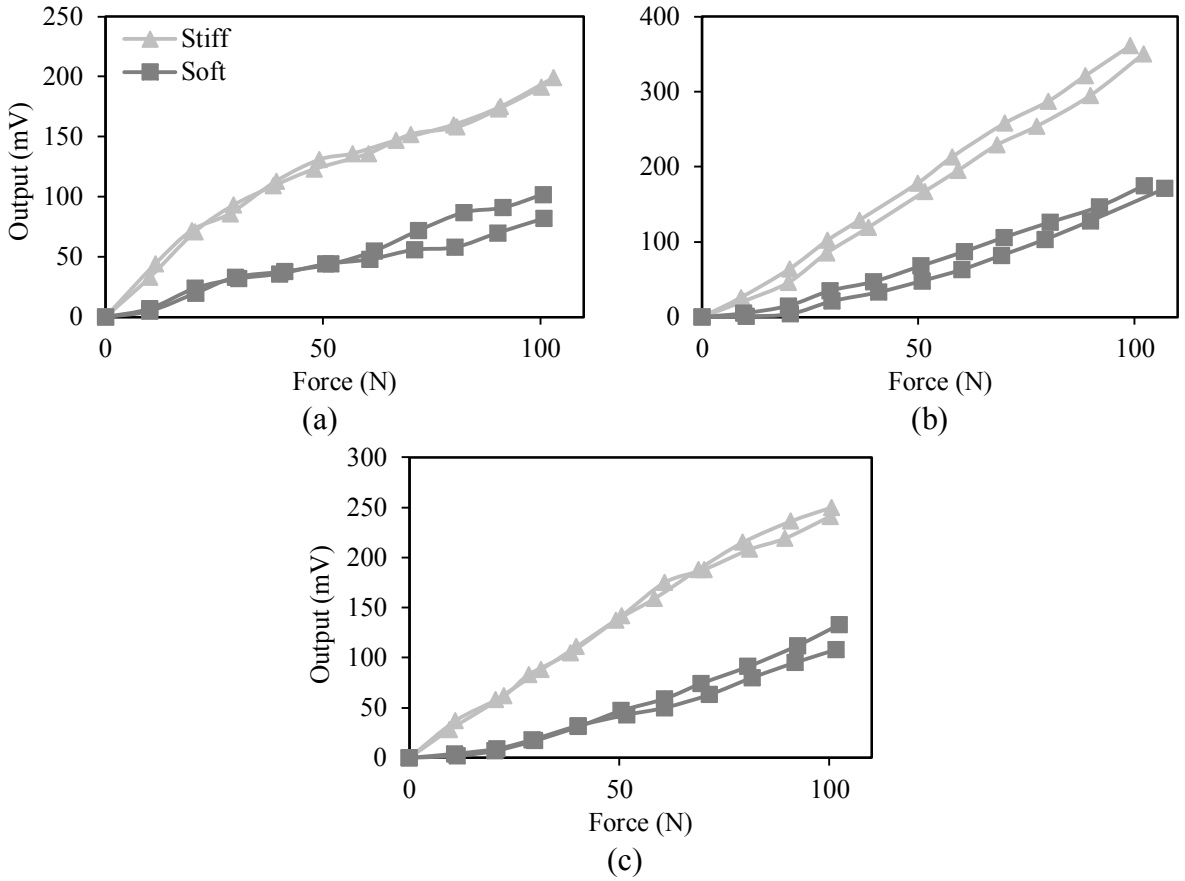

Figure A.9: Influence of elastomeric pad flexibility on the sensor output over two trials: (a) sensor 1; (b) sensor #4; and (c) sensor #7.

The increased flexibility of the 'soft' pad appears to attenuate more of the applied force as evident in the 0 to 30 N stages of force application for sensors #4 and #7. This attenuation is the cause of non-uniformity thus, resulting in decreased linearity. Since the 'soft' elastomer results in lower sensitivities on the flat surface versus the 'stiff' elastomer the higher sensitivities observed with the 'soft' pad from the curved surface calibration results can definitively be attributed to surface curvature rather than elastomer rigidity.

A.8. Sensor degradation

It has been reported that the FlexiForce sensors' outputs decrease with their usage [42]. Figure A.10 shows the sensor output for sensors #1, #4 and #7 over a period of eight weeks. Week 8 represents a verification of static sensitivity prior to trimming the sensors for static and dynamic

measurements of hand-handle forces and the sensors were not tested between weeks 2 and 8. The results indicate degradation is also possible over a period of time despite inactivity; however, the sample is insufficient to make a definite conclusion.

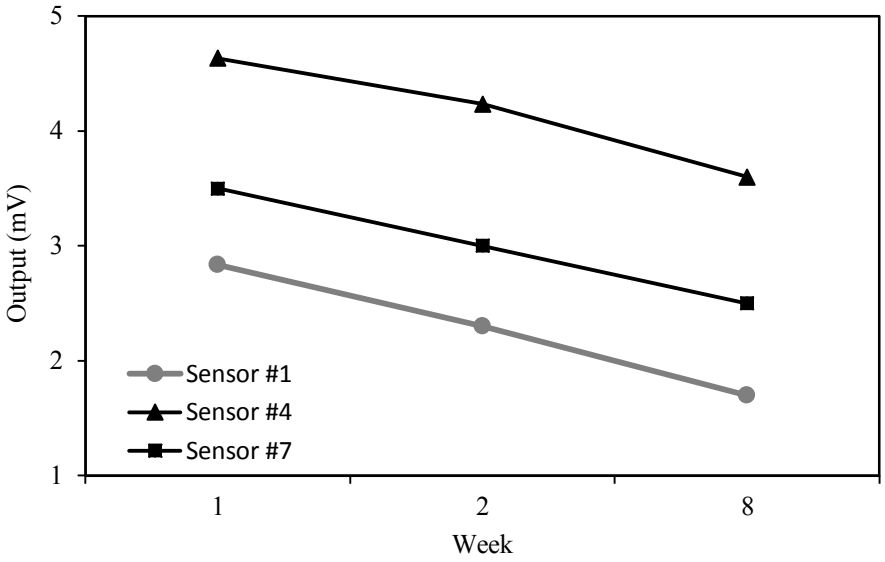

Figure A.10: Sensor sensitivity degradation based on usage for three sensors.

While the primary objective of this dissertation was not to study the effect of usage on the sensor output, the output was observed to decrease through typical sensor use for the majority of sensors, especially when used for measurements of hand-handle forces. It is important to distinguish decrease in sensitivity with decrease in linearity. In general, sensors that showed decreases in sensitivity at the onset of degradation still remained highly linear. However, continued usage of degraded sensors produced non-linear outputs as evident in Figure A.10. It was established the sensor required replacement when the r^2 value of the output sensitivity dropped to below 0.90. Moreover, if an unused sensor produced an output similar to that in Figure A.11 (as some occasionally did) due to manufacturing defect it would also be discarded.

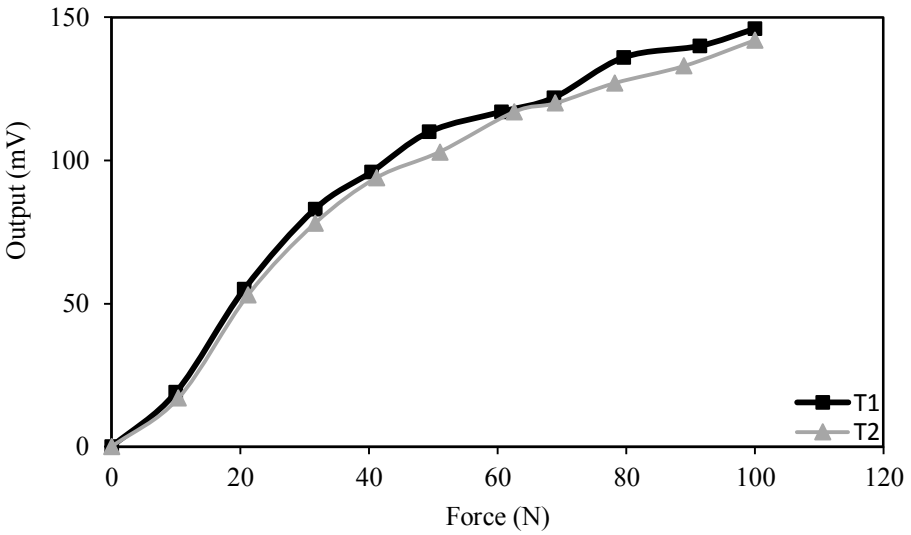

Figure A.11: An example of a sensor established as unfit for measurement ($r^2 = 0.86$).